Novel Approaches to Studying the Role of the Anterior Cingulate Cortex in Cognition and Parkinson's Disease

Alexander R. Weiss

Exeter College

University of Oxford

A dissertation submitted for the degree of

Doctor of Philosophy

Michaelmas 2017

NOVEL APPROACHES TO STUDYING THE ROLE OF THE ANTERIOR CINGULATE CORTEX IN COGNITION AND PARKINSON'S DISEASE

Alexander R. Weiss, Exeter College

Dissertation submitted for the degree of Doctor of Philosophy, Michaelmas 2017

The motor symptoms of Parkinson's disease (PD) have been linked to the emergence of exaggerated oscillatory activity in the 13 - 35 Hz beta range in recordings of the basal ganglia (BG) thalamocortical circuit of PD patients and animal models. PD patients and animal models also express dopamine-dependent cognitive impairments, implying effects of dopamine loss on the function of the anterior cingulate cortex (ACC). This thesis examines the electrophysiological behavior of the BG thalamocortical circuit in PD and dopamine-normal states during cognitive and motor activity. *In vivo* recordings in the BG of PD and dystonic patients were used to study the influence of dopamine during a test of executive function. Normal executive function was also investigated in the dopamine-healthy ACC of chronic pain patients. Both the BG and ACC exhibited lateralized electrophysiological responses to feedback valence. The BG also exhibited dopamine-sensitive event-related behavior. In additional experiments, chronically implanted recording electrodes in awake, behaving hemiparkinsonian rats were used to examine the transmission of synchronized oscillatory activity from the BG, through the ventral medial (VM) thalamus, to the ACC. Modulation of subthalamic nucleus, VM thalamus, and ACC activity during a simple cognitive/movement task was also investigated in hemiparkinsonian rats. Findings in the rat model suggest that ACC-mediated executive function is dopamine-sensitive and is reflected in the region's electrophysiology. These results may provide further insight into the significance of excessive oscillatory activity in PD and its influence on cognitive systems.

TABLE OF CONTENTS

I. Statement of Authorship

This thesis is all my own work with the following exceptions.

- Chapter 2 is composed of materials from the published article, *The Cognitive Role of the Globus Pallidus Interna; Insights from Disease States* (Gillies et al. 2017). As a co-author of this article, I contributed to designing the research, performing research and obtaining data, analyzing data, and writing the paper.
    - Figure 2.3.2 contains data which were collected and analyzed collaboratively with Dr. Gillies *et al*.
    - Figure 2.3.4 contains data which were collected by me and which were analyzed collaboratively with Dr. Gillies *et al*.
    - Figure 2.3.4 contains data which were collected and analyzed collaboratively with Dr. Gillies *et al.*
- Chapter 3 is composed of materials from a manuscript accepted for publication, *Anterior Cingulate Cortices Differentially Lateralize Decision Confidence and Error in a Visual Prediction Task.* As first author of this article, I contributed to designing the research, performing research and obtaining data, analyzing data, and writing the paper.
    - Figure 3.3.1 contains data which were obtained by Dr. Boccard and results which were collaboratively analyzed with Dr. Boccard.
    - Figure 3.3.3 contains analysis performed by Dr. Philiastides.
- Chapter 4 features materials from an *in-preparation* scientific review "Characterizing movement related oscillatory activity throughout basal ganglia-thalamocortical circuits in Parkinson's disease rats." As first author of this review, I contributed through the creation of figures and writing the paper. Chapter 4 also features a figure (4.3.5) adapted from the work of Delaville *et al*. and Brazhnik *et al*. (Brazhnik et al. 2016; Delaville et al. 2015).
    - Figure 4.1B contains data which were obtained by Avila *et al.*, Brazhnik *et al.*, and Delaville *et al*. (Avila et al. 2010; Brazhnik et al. 2012; Brazhnik et al. 2016; Delaville et al. 2015).
    - Figure 4.3.5C contains data which were obtained by Brazhnik *et al*. and Delaville *et al*. (Brazhnik et al. 2016; Delaville et al. 2015).

Peer-Reviewed Published Manuscript

Gillies M.J., Hyam J.A., **Weiss A.R.**, Antoniades C.A., Bogacz R., FitzGerald J.J., Aziz T.Z., Whittington M.A., Green A.L. The cognitive role of the globus pallidus interna; insights from disease states. Exp. Brain Res. (2017) 235:1455-1465.

Accepted for Publication

Weiss A.R., Gillies M.J., Philiastides M.G., Apps M.A., Whittington M.A., FitzGerald J.J., Boccard S.G., Aziz T.Z., Green A.L. (2018). Anterior cingulate cortices differentially lateralize decision confidence and error in a visual prediction task. Frontiers in Human Neuroscience. (2018) doi: 10.3389/fnhum.2018.00203.

In Preparation

Weiss A.R. *et al*. Characterizing movement related oscillatory activity throughout basal ganglia-thalamocortical circuits in Parkinson's disease rats. *In preparation.*

II. Acknowledgements

I would like to express my gratitude to my supervisors, Prof. Tipu Aziz of the University of Oxford and Dr. Judith Walters of the National Institutes of Health. Their combined expertise, patience, kindness, and vast knowledge have helped me immensely. This thesis and the work I have completed in the last few years would not have been possible without them, and for that I thank them. I would like to thank Prof. John Stein and Prof. Dipankar Nandi for taking time out from their busy schedules to serve as my assessors.

In the Oxford Functional Neurosurgery and Experimental Neurology Group, I would like to thank Alex Green, Martin Gillies, Sandra Boccard, Dali Wu, and Faizal Bahuri for their guidance and friendship when I was a stranger in a strange land. It was with their help that I focused on the anterior cingulate in the first place, avoided killing any patients, contributed to my first published article, and discovered the joys of the White Hart. In the Neurophysiological Pharmacology Section, I would like to thank Kristin Dupre, Claire Delaville, Heysol Bermudez-Cabrera, Michael Preston, Alex McCoy, Nikolai Novikov, and Elena Brazhnik. Through their help, I've learned a million different skills including surgery, electrophysiological recording, histology, and how to be a better lab mate. Additional thanks go to the world's best interns, Selena Gonzalez, Angela Yim, and Yiqiu Yang, without whom I'd never have finished my analyses on time. Thanks also go to Yarimar Carasquillo for her help with pain experiments and Michael Sheridan for keeping me sane.

I would like to thank the clinical DBS patients who volunteered for my Oxford experiments for their patience in working with a bumbling young researcher. You all are inspirational in your bravery, and I wish you the best. Some very special thanks go to the 60 plus rats that gave their lives for the NIH work I performed here. Because of the life each was born into, they were stuck with a life-or-death existence. Their lives are decided at our whim, and it is important that we remember their sacrifices and be thankful for them.

I would like to thank my parents, Jack and Wendy, and my sister, Hayley, for the support and love (and more recently editing assistance!) that they have provided me with every day of my life. Additional thanks go to a myriad of friends and family too numerous to name from Syracuse, Oxford, and everywhere in between for making the moments outside of work worth living. In particular, I must thank Fang Hsiao Yu. Without her love and encouragement, I would not have finished this thesis. I'm a pretty lucky guy.

In conclusion, I recognize that this research would not have been possible without the financial assistance of the NIH, NINDS, the University of Oxford, Exeter College, and the NIH Oxford-Cambridge Scholars Program. I express my gratitude to these groups for making this thesis happen.

Alexander Weiss

III. Abbreviations

6-OHDA	6-hydroxydopamine
ACC	Anterior cingulate cortex
BG	Basal ganglia
CT	Computed tomography scan
D1	D1 striatal dopamine receptor
D2	D2 striatal dopamine receptor
dACC	Dorsal anterior cingulate cortex
DBS	Deep brain stimulation
DTI	Diffusor tensor imaging
ERP	Event-related potential
ERSP	Event-related spectral perturbation
FDR	False discovery rate
FFT	Fast Fourier transform
fMRI	Functional magnetic resonance imaging
GP	Globus pallidus
GPe	External segment of the globus pallidus
GPi	Internal segment of the globus pallidus
Hz	Hertz
IED	Intra- extra-dimensional set shift task
ILC	Infralimbic cortex
i.p.	Intraperitoneal
L-DOPA	Levodopa
LFP	Local field potential
MCx	Primary motor cortex
MFB	Medial forebrain bundle
mPFC	Medial prefrontal cortex
MRI	Magnetic Resonance Imaging
MSN	Medium-spiny neurons
mL	Milliliter(s)

mm	Millimeter(s)
NHP	Non-human primate
PBS	Phosphate-buffered saline
PD	Parkinson’s disease
PFC	Prefrontal cortex
PLC	Prelimbic cortex
RT	Reaction time
SEM	Standard error of the mean
SN	Substantia nigra
SNpc	Substantia nigra pars compacta
SNpr	Substantia nigra pars reticulata
STWA	Spike-triggered waveform average
SRD	Medullary subnucleus reticularis dorsalis
STN	Subthalamic nucleus
TH	Tyrosine hydroxylase
VM	Ventral medial thalamus

1. Introduction

Excessive synchronization in the beta frequency range has been consistently observed in the basal ganglia (BG)-thalamocortical circuit in Parkinson's disease (PD) patients and parkinsonian animal models and is thought to be related to the motor symptoms associated with this disorder. PD patients and animal models are also known to express a wide variety of dopamine-dependent non-motor symptoms, including cognitive and executive dysfunction. Such symptomology suggests that in PD, dopamine depletion influences the prefrontal cortex (PFC), and in particular the anterior cingulate cortex (ACC) – a cortical region known for executive function processing. While PD's motor symptomology, and by extension its electrophysiological underpinnings, holds the general public's attention and PD clinical research's focus, PD non-motor symptoms and their electrophysiological correlates are not as well understood. The presence of electrophysiological abnormalities associated with cognitive function in the BG and ACC of PD patients could be used as biomarkers to advance the early diagnosis of PD, the development of PD treatments, and the overall understanding of this increasingly common disease. To better understand the rationale behind this thinking, the functional anatomy of the ACC and BG-thalamocortical circuit, PD symptomology, PD electrophysiology, and the effects of PD on the activity of this circuit's components are summarized in this section.

1.1 Anatomy of the Basal Ganglia Thalamocortical Circuit

The pathological synchronization of the high beta band observed in the BG thalamocortical circuit is believed to play a crucial role in the pathophysiology of PD. To understand this electrophysiological activity, one must first gain an understanding of the sources of excitation or disinhibition within the circuit. Knowledge of the anatomical and functional organization of the circuit can also provide insight into how motor and cognitive functions operate in both the healthy and pathological brain. While any explanation for the origin of PD-induced excessively synchronized beta activity remains both speculative and controversial, through the lens of anatomy one can postulate experiments to gain further insights. A basic schematic of the BG thalamocortical circuit in the normal and Parkinsonian states is presented in Figure 1.1.

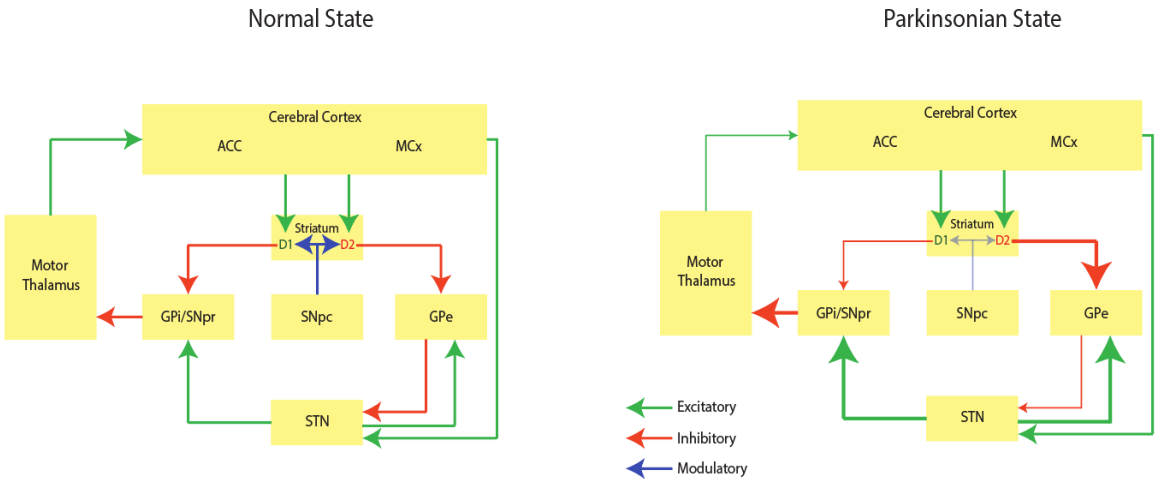

Figure 1.1 Basic schematic summary of the basal ganglia thalamocortical circuit.
The motor circuit is composed of a cortico-striatal projection, a cortico-subthalamic projection (hyperdirect pathway), two striatal systems giving rise to direct and indirect pathways, and the pallido-thalamo-MCx projection. The cognitive circuit replaces the MCx with the PFC and its subregion, the ACC. The thickness of arrows represents the functional state of a given circuit, wherein thicker arrows suggest hyperactivity while thinner arrows suggest hypoactivity.

1.1.1 Basal Ganglia

The “basal ganglia” is a group of subcortical nuclei known primarily for its role in motor control. More recently, the BG has been identified as also playing a role in motor learning, emotions, and executive function processing (P. Brown and Marsden 1998; Desmurget and Turner 2008, 2010; Falkenstein et al. 2001; Grillner et al. 2013; Lanciego et al. 2012; R. S. Turner and Desmurget 2010). Models of BG anatomy categorize the circuit into input, intrinsic, and output nuclei. Input nuclei receive information from external sources and include the caudate nucleus, putamen, and nucleus accumbens of the striatum. Intrinsic nuclei classically refer to the external segment of the globus pallidus (GPe), the substantia nigra pars compacta (SNpc), and the subthalamic nucleus (STN). More recent work has demonstrated that the STN also receives cortical afferents and so also acts as an input nuclei (Nambu et al. 2002). The output nuclei are structures that project outwards to the thalamus and consist of the internal segment of the globus pallidus (GPi) and the substantia nigra pars reticulata (SNpr).

1.1.1.1 Striatum

The striatum, one of the largest subcortical structures in the mammalian brain, is a heterogeneous structure that receives input from cortical and subcortical structures and projects throughout the BG (Lanciego et al. 2012; Schroder et al. 1975). The striatum is made up of three anatomical regions; the caudate, putamen, and nucleus accumbens, together composed of approximately 90 % projection neurons and 10 % interneurons (Carpenter 1976). While the striatum appears homogenous when viewed through cytoarchitectural techniques, immunohistochemical markers have revealed two subdivisions: striosomes and matrix components (Graybiel and Ragsdale 1978). These two regions maintain independent striatal afferent and efferent systems in that striosomal dendrites do not enter the matrix and vice versa

(Kawaguchi et al. 1989; Lanciego et al. 2012; Penny et al. 1988). Almost the entire cerebral cortex has been found to project to the striatum as do the thalamus and the amygdala. Dopaminergic afferents project to the striatum from the SNpc. Afferent connections are heterogeneously distributed throughout both strisome and matrix components, with motor and sensory cortical regions, thalamostriatal projections, and dopaminergic SNpc afferents mainly innervating the matrices while cortical limbic areas, the amygdala, and ventral SNpc preferentially target striosomeal regions (Donoghue and Herkenham 1986; Gerfen 1992; Graybiel 1984). There are two main routes for striatal output: D_1R-expressing mediospinal neurons (MSN) that project to the GPi and SNpr (known as the direct pathway) and D_2R-expressing MSN that project to the GPe (known as the indirect pathway) (Beckstead and Cruz 1986; Bertran-Gonzalez et al. 2010; Parent et al. 2000).

1.1.1.2 Globus Pallidus

The globus pallidus (GP) consists of an internal component, the GPi, and an external component, the GPe. Both the GPi and GPe receive excitatory glutamatergic input from the STN, and inhibitory GABAergic input from the caudate and putamen of the striatum (Chang et al. 1995; Hazrati and Parent 1991b). The GPi and GPe differ in their respective outputs. The GPi acts as a major BG output nucleus sending its inhibitory GABAergic efferents throughout the thalamus (Hazrati and Parent 1991a). The GPe sends its inhibitory GABAergic output to the striatum, STN, SNPr, and the GPi (Hazrati and Parent 1991a, 1991b; Joel and Weiner 1997).

1.1.1.3 Subthalamic Nucleus

The STN, a small subcortical nucleus located ventral to the zona incerta and rostral to the substantia nigra (SN), receives excitatory glutamatergic projections from multiple cortical areas and inhibitory GABAergic projects from the GPe (Nambu et al. 2002). The STN has also been found to receive glutamatergic innervation from the ipsilateral thalamic caudal intralaminar nuclei, the contralateral caudal intralaminar nuclei, and a small dopamine projection from the SNpc. The cerebral cortex directly innervates the STN, which in turn projects to BG output nuclei. This provides a means for motor-related cortical areas to access BG output nuclei directly (the "hyperdirect pathway"), thus exerting powerful excitation onto BG output (Levy et al. 1997; Martinez-Fernandez et al. 2014; Nambu et al. 1997; Nambu et al. 2002). The glutamatergic efferent axons of the STN project to a wide array of areas including the GPi, GPe, SNpr, and even to regions of the cortex such as the sensory-motor areas and the prefontal cortex (PFC) (Castle et al. 2005; Degos et al. 2008; Gerfen et al. 1982; Rommelfanger and Wichmann 2010; Sugimoto and Hattori 1983; Sugimoto et al. 1983). The STN is recognized as one of the best surgical targets for electrode placement during deep brain stimulation (DBS) (Albin et al. 1989; DeLong 1990).

1.1.1.4 Substantia Nigra

The SN is composed of two substructures: the SNpr and the SNpc. The SNpr (like the GPi) is an inhibitory GABAergic output of the BG. The SNpr receives excitatory glutamatergic input from the STN and inhibitory GABAergic inputs from the striatum and the GPe. The SNpr has inhibitory GABAergic outputs that project primarily to the ventroanterior, ventrolateral, and ventromedial parts of the thalamus (Herkenham 1979; Kuramoto et al. 2011; Kuramoto et al. 2015). The SNpc, meanwhile, deep in the ventral midbrain, contains tyrosine hydroxylase

(TH)-positive neurons that supply the BG with dopamine (Dahlstrom and Fuxe 1964). These dopaminergic neurons in the SNpc are the cells that degenerate progressively in PD, leading to dopamine deficiency and thus the appearance of the cardinal features of the disease (Lanciego et al. 2012).

1.1.2 Ventral Medial Thalamus

The rat ventral medial (VM) thalamus, roughly corresponding to the human magnocellular division of the ventral anterior motor thalamus, is characterized by its extensive neocortical projections and its complex afferentation (Herkenham 1979). The VM thalamus projects primarily to the outer half of layer I of the neocortex (including the ACC and the motor cortex (MCx)) and, in turn, receives reciprocal projections from layer VI of the cortex (Herkenham 1979; Klockgether et al. 1986). The VM thalamus's major input comes from the output of the BG, in particular the SNpr.

1.1.3 Anterior Cingulate Cortex

The PFC, a part of the mammalian cerebral cortex, is a major component of the frontal lobe. Implicated in a who's who of cognitive behaviors, the most generalized description of PFC function would be executive function (Alvarez and Emory 2006; Funahashi and Andreau 2013; Miller and Cohen 2001; Passingham and Wise 2012). For our purposes, the anatomy of the PFC can be subdivided between what are known in the cerebral cortex as granular and agranular parts (Fuster 2008). The whole cerebral cortex can, in fact, be broken down into these two categories according to the state of neuronal cell bodies in its internal granular layer IV. Granular areas of the cortex have a distinct, obvious 4th layer while agranular areas have fewer cell bodies between the 3rd and 5th layers. In humans and non-human primates (NHP), the

largest part of the PFC is granular (Warren et al. 1964). While all mammals possess a PFC, only the agranular parts of the PFC are shared amongst all mammals (Passingham and Wise 2012). This thesis focuses on the agranular PFC.

The agranular PFC can be further divided into two subregions: the medial and lateral agranular areas (Passingham and Wise 2012). These areas correspond to the primate medial PFC (mPFC) and orbital PFC. Herein, when we discuss the broader agranular areas of the PFC, we will be referring to the mPFC. The mPFC consists of the anterior cingulate cortex (ACC), the infralimbic cortex (IFC), and the prelimbic cortex (PLC) (Ongur and Price 2000; Ongur et al. 2003). The mPFC makes up some of the most evolutionarily ancient parts of the PFC, and as mentioned above are shared amongst all mammals including rodents and primates.

The ACC is inconsistently defined in the literature. Herein, when we discuss the ACC, we exclude the PLC, ILC, and the cingulate motor areas from the ACC. Thus, the ACC, as discussed herein, aligns only to a part of Brodmann area 24 (Allman et al. 2001). The ACC lies dorsal to the corpus callosum in the human, and stretches rostrally to the frontopolar cortex and caudally to its borders with the posterior cingulate cortex (PCC) (Passingham and Wise 2012). The distinction between the ACC and PCC is clear cytoarchitectonically due to the latter's granular nature. The ACC has connections to a broad array of brain systems, including those associated with cognition and executive function (dorsal PFC, ventrolateral PFC, frontal pole, and parietal cortex), emotion (amygdala, hypothalamus, insula, ventral striatum, and ventrolateral PFC), and motor control (MCx, pre-MCx, and spinal cord) (Barbas and Pandya 1989; Heilbronner and Hayden 2016; Morecraft and Van Hoesen 1998; Vogt et al. 1987; Vogt and Pandya 1987). The aforementioned ACC connections, in conjunction with the cortical pain network, serve as foundations for theories of ACC function (Morecraft and Van Hoesen 1998; Paus 2001; Price 2000; Rushworth et al. 2011).

A major theory of ACC function characterizes the ACC as a monitor (Heilbronner and Hayden 2016; Schall et al. 2002). According to this theory, the ACC monitors both external and internal environments, makes predictions, observes outcomes, and provides a summary report of outcomes to downstream circuits. While ACC monitoring signals are usually observed after decisions and feedback, in some cases ACC signaling can occur throughout the decision-making process allowing for real-time updating of performance (Blanchard and Hayden 2014; Carter et al. 1998; Holroyd and Coles 2002). The ACC's role as a monitor includes processing conflict (Botvinick et al. 2001) and error (Holroyd and Coles 2002). While there is no question that ACC neurons are sensitive to error commission, as evidenced by error-related negativity signals in event-related potential (ERP) studies, the strict view of the ACC as exclusively an error detector has been generally rejected (Amiez et al. 2005). Most likely, the ACC reacts to error as one of a series of stimuli that drive the region. For example, the ACC has been shown to increase in activity in contexts where errors are likely but do not actually occur (J. W. Brown and Braver 2005). Conflict monitoring, on the other hand, proposes that ongoing levels of conflict or competition are tracked by the ACC and signaled as additional cognitive resources are required (Botvinick et al. 2001). While this is an appealing idea often suggested in neuroimaging studies, there is scant supporting evidence in electrophysiological recordings (Cai and Padoa-Schioppa 2012; Nakamura et al. 2005; Sheth et al. 2012). Unfortunately, electrophysiological studies of human ACC are rare, as there are few clinical justifications to warrant placing recording electrodes in or near the ACC. As a result, much of the research into ACC function has been performed by computer modelers. Such research proposes that error and conflict signals in the ACC may simply be a by-product of ACC function. This line of reasoning suggests that the ACC primarily concerns itself with context and action. Conflict and error are merely factors that modulate the activity of context and action neurons (Alexander

and Brown 2011). At present, the primary role of the ACC remains the subject of much debate and scientific attention (Marzullo 2008).

1.2 Electrophysiology

Human brain activity is dominated by synchronized oscillatory signals amongst populations of neurons. These oscillations appear in the brain as rhythmic fluctuations in local field potential (LFP) and electroencephalographic (EEG) recordings. While they have been used extensively to study the mechanisms of neural function, there is surprisingly little consensus regarding the underlying biophysical processes that generate these signals (Berens et al. 2008).

Oscillatory signals are a function of fluctuations in neuronal spiking and therefore are suggested to reflect important functions in both the developing and mature brain (Buzsaki and Draguhn 2004; Engel et al. 1992; Engel et al. 2001; Engel and Fries 2010; Fries 2005; Varela et al. 2001). EEGs, as recorded from surface EEG or MEG, and LFPs, as recorded from depth electrodes, are believed to reflect either net input to neurons nearby or surrounding the recording electrode (especially in the case of multi-unit recordings) (Delaville et al. 2015; Logothetis et al. 2001). They may also be associated with the weighted average of synchronized dendro-somatic spiking components. Oscillations in these forms are said to provide an effective means of controlling the timing of neuronal firing (Engel and Fries 2010). Oscillations are thus believed to temporally coordinate the transfer of information across regions of the brain and support spike-timing dependent plasticity (Buzsaki and Draguhn 2004; Engel et al. 2001; Fries 2005; Varela et al. 2001). Ongoing and event-related oscillations found in neuronal populations are traditionally categorized (with varying degrees of arbitrariness) according to the frequency band at which they occur (the following specifically in humans): delta (0.5 – 3.5 Hz), theta (4 – 7 Hz), alpha (8 – 12 Hz), beta (13 – 30 Hz), and gamma (> 30 Hz). Each type of oscillation is generally considered to be generated by a particular set of intrinsic neuronal activity,

interactions at the synaptic level, and other extracellular factors. One should keep in mind that precise boundaries between distinct LFP frequency bands are not well defined, and would benefit from increased attention (Watson et al. 2017). Important but still unanswered questions in neuroscience exist regarding these bands. Do these frequency bands have distinct functional significance? Can clear cognitive, perceptual, or sensorimotor operations be assigned to unique bands? Are they instead epiphenomenal or do they reflect compensatory plasticity?

The past few decades have seen great advances in the study of different neuronal frequency bands, relating them to a variety of functions and diverse brain states. Delta band frequency activity has been associated with learning, the brain's reward system, and motivation processes (Basar et al. 2013; Basar-Eroglu et al. 1992; Guntekin and Basar 2015). Delta is the predominant frequency active during sleep (Knyazev 2007; Steriade et al. 1993). Theta band frequency activity has been linked to emotional arousal, fear conditioning, and working memory (Jensen and Lisman 2005; Steriade et al. 1993). Alpha band activity has been suggested to play a role in working memory and short term memory functions (Palva and Palva 2007). Gamma band activity has been implicated in a range of processes including attention, conscious awareness, feature integration, multisensory and sensorimotor integration, preparation of movement, and stimulus selection (Engel et al. 1992; Engel et al. 2001; Engel and Fries 2010; Fries 2005; Jensen and Lisman 2005; Knyazev 2007). There is growing interest in the oscillations occurring in the beta band, which has classically been associated with sensorimotor functions (Pfurtscheller et al. 1996). Beta oscillations are prominent in the human motor system, having been recorded in the BG, cerebellar system, and somatomotor cortex (P. Brown 2007). The functional role of beta band activity remains unclear, but particular attention has been directed to beta activity in the BG, given observations of exaggerated beta activity in the BG of patients with PD that may play a role in PD motor impairment (P. Brown 2007; Hammond et al. 2007; Kringelbach et al. 2007; Uhlhaas and Singer 2006).

1.2.1 Interactions Across Frequencies

The wide variety of brain-related processes in which multiple frequency bands simultaneously appear suggest that it may not be possible to associate complex cognitive functions in unique and direct ways with the oscillatory activity of any single frequency band. Similarly, it is unlikely that a single frequency band is uniquely responsible for any particular cognitive function in the brain. While a unifying theory regarding the physiological origins and the functional relevance of the different frequency bands remains elusive, several hypotheses have been proposed (Engel and Fries 2010). It is well accepted that oscillations of different frequencies represent global changes of state in the brain. Higher frequencies may indicate states of enhanced arousal distinguished by spatially fine-grained and specific interaction patterns, while states of low arousal are characterized by the spatially less specific, global synchronization seen in slower oscillations (Alkire et al. 2008; Steriade et al. 1993). It has also been suggested that differences found in oscillation frequencies may reflect variations in cellular and local circuit properties, which may give rise to different frequency tuning properties of the given microcircuits (Alkire et al. 2008). Yet another hypothesis suggests that oscillations in different frequency ranges may allow for dynamic interactions across neural populations at different spatial scales. Slower oscillations, such as theta and beta, may support the functional coupling of neurons over larger distances than fast gamma oscillations, because the maximal conduction delays compatible with synchrony are directly related to the length of the cycle of an oscillation (Kopell et al. 2000; Solomon et al. 2017; Traub et al. 1996). It has been established that spectral coherence between LFPs from distant locations decrease with increasing distance between recording sites with higher frequency bands exhibiting steeper decreases (Destexhe et al. 1999; Leopold and Logothetis 2003). Oscillations at different bands may also have influence as a matter of relative power, e.g. a power spectra showing significantly greater power in the gamma band compared to the beta band. One should keep in

mind that a characteristic of LFP signals is that signal power generally declines as a function of its frequency, a phenomenon known as the inverse power law (Bedard et al. 2006; Bhattacharya and Petsche 2001; Dehghani et al. 2010; Pritchard 1992). Thus, while power spectra from biological sources will have much higher relative power in lower frequency bands, meaningful peaks can still emerge, as we have seen, in higher frequency bands.

There exist several theories as to how neural oscillations interact across different frequency bands. Nesting of slower theta and faster beta and gamma bands may provide a mechanism through which retrieval from long-term memory and sequential encoding of processed items into working memory can occur (Jensen and Lisman 2005; Kopell et al. 2000). It has also been proposed that the nesting of slow and fast oscillations, such as the phase-amplitude coupling in PD between beta band and gamma band, may enable cross-modal interaction between sensory channels to allow information to be processed across different time scales (Schroeder et al. 2008; Starr et al. 2005; Swann et al. 2016). Despite such evidence, we do not have a clear understanding as to why the brain oscillates at different frequency ranges nor how these oscillatory processes functionally interact with each other.

Remarkably, due to the architectural scalability of the vertebrate brain, the hierarchy of brain oscillations remains evolutionarily preserved across species (Buzsaki et al. 2013). Essential features of brain organization, such as activity-information retention and local-global integration are maintained by different frequency bands regardless of brain size. Rats, monkeys, and humans express the same oscillatory activity maintained by the same fundamental mechanisms (Buzsaki et al. 2013; Buzsáki 2006; Dehaene et al. 1998; Engel et al. 2001; Tononi et al. 1998; Varela et al. 2001). Oscillations are robust phenotypes across species, allowing them to be valuable targets for research into neuronal mechanisms and therapeutics.

1.2.2 How is Local Field Potential Activity Generated?

In the cerebral cortex, it has been shown that the elongated morphology and asymmetric representation of synapses found on pyramidal neurons generate a dipole, wherein their parallel orientation and the cortex's laminar architecture facilitate the summation of currents (P. Brown and Williams 2005). Oscillatory activity seen in cortical EEG, therefore, implies the synchronous fluctuation of current in large numbers of pyramidal neurons (Gloor 1985; Mitzdorf 1985). Although the BG does not share the laminar architecture of the cerebral cortex, studies in rodent and primate model STN have shown that the BG, despite minor interspecies variations in arborization, contains tightly packed principal neurons with elliptic dendritic fields, typically aligned along a primary axis (Chang et al. 1983; Hammond and Yelnik 1983). Some degree of synchronously activated LFP generation may still be expected; however, open or closed morphological arrangements do not define the absence or presence of LFP so much as their extent (P. Brown and Williams 2005). Indeed, BG-recorded LFPs may, like cerebral cortex LFPs, reflect the synchronous change of large populations of neurons (Goto and O'Donnell 2001; Magill et al. 2004). The relative extent to which pre- and post-synaptic components contribute to the LFP of individual nuclei remains to be clarified (P. Brown and Williams 2005). Oscillations can be imposed or generated locally, but their presence does not necessarily imply one over the other.

Although the overall function of beta oscillatory activity remains controversial, in this thesis we accept the hypothesis that in motor contexts the healthy brain either uses synchronization in the beta frequency band as a status quo preservation mechanism, or epiphenomenally represents the underlying mechanisms that achieve this processing (Engel and Fries 2010).

1.2.3 Beta Oscillations in Motor Processes and Control

Historical observations of beta frequency band activity have linked this band to functions related to motor control. This may be due to the many studies demonstrating that beta activity is attenuated by voluntary movements (particularly during holding periods preceding a movement) and increased during steady contractions (Baker 2007; Klostermann et al. 2007; Sanes and Donoghue 1993). The beta frequency band is also found to be replaced by faster frequencies in the gamma band during the preparation and execution of movements (Donner et al. 2009). These distinctive relationships between beta and steady-state contractions can be observed in most parts of the motor system, from the BG to the motor and premotor cortexes, as well as in the peripheral motor units (Baker 2007; Waldert et al. 2008).

One suggested role of beta activity in the motor system is that of an idling rhythm (Pfurtscheller et al. 1996). However, more recent work suggests that, rather than beta oscillations simply supporting a lack of movement, they may be evidence of an active process that promotes an existing motor set while attempting to prevent the neuronal processing of a new movement (Pogosyan et al. 2009). Gilbertson *et al.* demonstrated that increases in beta activity are associated with deficiency of movement performances, suggesting that during periods of enhanced beta band activity voluntary movements are slowed (Gilbertson et al. 2005). Pogosyan *et al.* used transcranial alternating current stimulation to entrain the MCx to a beta band frequency while patients attempted visuomotor tracking tasks (Pogosyan et al. 2009). These patients displayed a decrease in velocity during voluntary movements. Such data suggest that beta band activity may promote the propensity of the sensorimotor system to maintain the status quo (Engel and Fries 2010). This may further suggest that beta reflects the processing of proprioceptive signals acting as feedback that are required for monitoring the maintenance of status quo and the recalibration of the sensorimotor system (Baker 2007). Beta activity in the motor system also appears to reflect anticipatory processes. Beta activity may

also change depending on the expectancy of an oncoming event, as Donner *et al.* were able to show lateralized changes in the beta band in premotor and MCx that reflected, several seconds in advance, a decision about a forthcoming action before it occurred (Donner et al. 2009). It is also possible that the beta band activity may accompany similar underlying mechanisms in cognitive processes beyond motor control.

Another hypothesis regarding beta activity suggests that the notion of status quo is merely epiphenomenal in nature with limited heuristic value. This proposes that beta activity in the cortical-BG system might represent an internal index of the likelihood of the need for a voluntary action as a consequence of net dopamine levels (Jenkinson and Brown 2011). Thus, within the cortical-BG system, the level of beta band activity would be inversely proportional to the likelihood that a new voluntary movement must be processed and performed (Leventhal et al. 2012). Beta activity, by this reckoning, is a predictive element, determining motor readiness (Jenkinson and Brown 2011). A reduction in beta activity in the BG-cortical system indicates the need for a novel voluntary action as suggested in studies indicating that imperative cues demanding voluntary movement suppress beta activity (Hammond et al. 2007). Several studies have also shown, in healthy and dopamine-depleted PD subjects during warning-go paradigms, that beta activity in both the cortex and BG is suppressed by warning cues with a correlation between degree of suppression and the degree to which cues predict a required action (Doyle et al. 2005; Tzagarakis et al. 2010; Williams et al. 2003). As such, the latency of this beta suppression correlates with reaction time (RT) both across and within subjects (Doyle et al. 2005; Williams et al. 2003; Williams et al. 2005). Meanwhile, in the MCx, beta band activity is also suppressed as evidence accumulates in anticipation of a response in a perceptual detection task (Donner et al. 2009). Importantly, as shown by Androulidakis *et al.*, the relationship between beta activity and the evidence in favor of action and motor readiness may not simply be limited to external cues (Androulidakis et al. 2007). Beta suppression may be

seen prior to internally generated voluntary movements, which may possibly reflect the salience of internal cues with respect to action commands. There also exists a large body of work supporting the theory that changes in beta activity are underpinned by net dopamine levels. Several studies show that the prevalent level of beta band oscillations in the BG can be altered through pharmacological methods that manipulate dopamine and its receptors (Hammond et al. 2007; Kuhn et al. 2008a). Dopaminergic neurons within the SN in the BG have been shown to respond with bursts of action potentials at beta frequencies to salient auditory, olfactory somatosensory, and visual stimuli – all without necessarily requiring primary or conditioned aversion or reward mechanisms (Horvitz 2000; Schultz 2010). These dopamine transients may be precipitated by novel cues, or may appear spontaneously during exposure to novel situations and environments, implying that they may be related to salient cues in the environment (Robinson and Wightman 2007). These salient events may cause the release of dopamine in motor regions of the BG's striatum and STN, and this adds to the dopamine released in other phasic bursts and with the preexisting background dopamine levels (Jenkinson and Brown 2011). As salient events in the environment occur, so in turn would dopamine release, in which case the level of dopamine could act as an index of the likelihood of motor action being provoked. In this way, net dopamine levels would predict a suppression of beta band synchrony, which might mediate dopamine's involvement in behavioral determination. Implicit in this notion is some degree of spatiotemporal integration of dopamine release (Jenkinson and Brown 2011).

1.2.4 Beta Band Activity and Cognitive Processes

If beta band activity were to play a similar role in non-motor-related functions as it does in motor circuits, one might predict that beta would remain constant if no changes were made

in the cognitive status quo. An elevated beta signal might signify the active attempt to maintain the current cognitive set while a decrease might indicate the disruption of the current state of affairs due to novel input. If this was the case, tasks requiring a strong endogenous, top-down response would be associated with high beta activity, while a decrease of beta band activity would be observed in situations where a behavioral response was determined by exogenous, bottom-up factors (Engel and Fries 2010). There is evidence supporting these predictions. Studies of sensory processing have shown that the appearance of new sensory stimuli causes a decrease in beta and an increase in gamma band power during stimulus-driven, top-down task settings (Engel et al. 2001; Fries 2009). Interestingly, a recent study in awake, active monkeys demonstrated that endogenously driven choices during a search task are accompanied by higher beta band activity as compared to stimulus-driven decisions (Pesaran et al. 2008). Similarly, several studies in humans have shown beta activity in association with endogenously triggered perceptual changes (Iversen et al. 2009; Okazaki et al. 2008).

Recent studies have observed a connection between beta band activity and attentional top-down processing (Engel and Fries 2010). Analysis of coherence between frontal and parietal signals in monkeys trained to detect targets among distractors revealed activity that occurred primarily in the beta band during the top-down, processing-heavy searching component of the test, while gamma was active during bottom-up attentional searches (Buschman and Miller 2007, 2009). These studies were some of the first to directly compare the effects on oscillatory response of top-down and bottom-up attention tasks in monkey subjects. The results displayed evidence that beta band coherency dominated top-down attention processing, while gamma was stronger in the reverse condition. Such studies suggest that endogenously driven, top-down attention is associated with communications between large populations of neurons at the lower frequency band of beta, while higher gamma frequencies occur during the conveyance of bottom-up signals.

1.3 Parkinson's Disease

Parkinson's disease (PD) was first characterized as a neurological condition by James Parkinson in 1817 (Parkinson 1817). PD is the second most common neurodegenerative disorder in industrialized countries after Alzheimer's disease, affecting approximately 0.3 % of the population and about 1 % of individuals over the age of 60 (de Lau and Breteler 2006; Nussbaum and Ellis 2003). As the average age of the population increases, PD is expected to exact an increasing economic and social burden on society. Scientific interest in PD research has grown in recent years in part due to the discovery of several potentially causative implicated gene mutations. However, major gene mutations are considered to cause less than 10 % of all incidences, with the remainder arising sporadically. As such, the neurogenesis of PD is still largely unknown. Since the pioneering work of Brissaud, PD as a neurodegenerative disease has been associated with selective dopamine cell loss in the SNpc and the subsequent dopamine depletion of the striatum of the BG (Brissaud and Meige 1895; Carlsson et al. 1958; Deuschl et al. 2001; Foix and Nicolesco 1925; Sano et al. 1959). The exact pathogenic mechanisms underlying dopamine-depletion are not well understood. Several theories exist that attempt to explain dopaminergic cell loss including influences from non-genetic oxidative stress, protein mishandling, and mitochondrial dysfunction, to environmental causes such as cell death through pesticide poisoning, together with potential interaction with susceptibility genes (de Lau and Breteler 2006; Greenamyre and Hastings 2004). There is presently no easy or reliable predictive diagnostic test for PD.

Treatment of PD was based on ineffective 19th century practices until the work of Birkmayer, Cotzias, Hornykiewicz and others heralded the use of the dopamine precursor levodopa (L-DOPA) as an anti-akinetic pharmaceutical (Barbeau 1969; Birkmayer and

Hornykiewicz 1961; Cotzias et al. 1969; Ehringer and Hornykiewicz 1960; Yahr et al. 1969). L-DOPA remains the flagship agent for the treatment of PD symptoms and signs. As L-DOPA can cross the blood-brain barrier, it is used to increase dopamine concentrations in the central nervous system (CNS) where it is converted to dopamine by the enzyme dopa decarboxylase (Brogden et al. 1971). PD symptoms generally respond well to treatment with L-DOPA, although it is not possible to accurately predict its specific effectiveness in individual patients. While the cardinal motor and non-motor symptoms of PD respond well to treatment with L-DOPA, the activity of dopa decarboxylase is higher in the periphery than in the CNS, resulting in much of the administered L-DOPA converting to dopamine outside of the CNS. This requires the co-administration of dopa decarboxylase inhibitors, to allow greater quantities of administered L-DOPA to reach the brain. Chronic administration of L-DOPA and plasticity associated with declining dopamine levels result in subjects developing a variety of adverse side-effects, most prominently abnormal involuntary movements called dyskinesias (Brogden et al. 1971; Dupre et al. 2016; Rascol et al. 1998). The delayed development of unpredictable drug therapy responses and L-DOPA-induced dyskinesias have led to the popularity of DBS as a treatment for advanced PD (P. Brown 2007). Developed through the work of Benabid and DeLong, DBS electrodes are implanted into the STN, GPi, or the thalamus and chronically stimulated at high frequencies (> 100 Hz) to therapeutic effect. Although not fully understood, there exist several hypotheses that attempt to explain the therapeutic effects of DBS. These include antidromic cortical activation of MCx (Ashby et al. 2001; Gradinaru et al. 2009), depolarization block (Beurrier et al. 2001), synaptic depression and inhibition (J. O. Dostrovsky et al. 2002), and the normalization of pathological network oscillations (P. Brown and Eusebio 2008).

1.3.1 Parkinson's Disease Motor Symptomology

PD diagnoses are primarily based on clinical motor-deficit symptoms, as the disease is most visible for its motor symptoms. There are four characteristic motor features of PD that can be grouped using the acronym TRAP: tremor, rigidity, akinesia (also known as bradykinesia), and postural instability (Jankovic 2008). Other motor symptoms include flexed posture and freezing. Bradykinesia, recognized as a cardinal feature of PD since Charcot, is a slowness of movement impairing the planning, initiating, and executing of movement (Charcot and Bourneville 1872; Cooper et al. 1994). Bradykinesia is easily recognizable and is often apparent to examiners before formal neurological evaluations are conducted. While the pathophysiology of bradykinesia is poorly understood, bradykinesia, of all the PD motor symptoms, appears most highly correlated with dopamine deficiency and is observed in all dopamine-lesion animal models of PD (Vingerhoets et al. 1997). Tremor is also one of the most common and recognizable symptoms of PD, occurring at frequencies between 4 and 6 Hz in the distal parts of extremities (Shahed and Jankovic 2007). Rigidity is characterized by increased resistance to movement in limbs affecting flexion, extension, and rotation around joints and can cause flexed postures through stiffness in the neck and trunk (Jankovic 2008). Increased spinal interneuron excitability is thought to be responsible for PD rigidity, but the exact mechanisms of this symptom are not well understood (Le Cavorzin et al. 2003). Postural instability is generally a late-stage PD symptom where a loss of postural reflexes occurs, and is unfortunately one of the few symptoms that does not respond well to dopamine therapy, pallidotomy, or DBS (Maurer et al. 2003). Freezing is a loss of movement affecting the legs during walking (Giladi 2001).

1.3.2 Parkinson's Disease Non-Motor Symptomology

PD is typically considered a motor disorder. This focus on motor deficits, however, consigns the disease's many non-motor symptoms to relative neglect. This is regrettable, as non-motor symptoms are highly prevalent in PD patients and a source of debilitating consequences (Schaeffer and Berg 2017; Zesiewicz et al. 2006). Studies have shown that more than 95 % of PD patients exhibit at least one non-motor symptom of the disease (Erro et al. 2013; Witjas et al. 2002; Q. Zhang et al. 2014). There are a wide range of non-motor symptoms including autonomic dysfunction, sleep and sensory deficits, and cognitive deficits (Jankovic 2008). Autonomic failure is one of the more common presenting features of PD, with symptoms including orthostatic hypotension, sweating, and erectile and sphincter dysfunction (Senard et al. 1997; Swinn et al. 2003). Sleep disturbances, including both excessive sleepiness (Gjerstad et al. 2006) and insomnia (Gjerstad et al. 2007) are now considered integral parts of PD. Sensory abnormalities vary widely, and include symptoms such as olfactory dysfunction (hyposmia) and pain (Djaldetti et al. 2004; Stern et al. 1994; Tinazzi et al. 2006). Hyposmia may act as an early biomarker of PD, as it is correlated with a 10 % increased risk for PD onset within 2 years of diagnosis (Ponsen et al. 2004). Pain is estimated to occur in approximately 40 % of PD patients, but its nature and origins are not well characterized (Ford 1998b; Goetz et al. 1986; Goetz et al. 1987). Interestingly, studies on experimentally induced pain in PD patients reported increased pain sensitivity in "off phase" (off-medication) that was normalized after L-DOPA medication (Brefel-Courbon et al. 2005a; Djaldetti et al. 2004; Gerdelat-Mas et al. 2007).

Cognitive, neurobehavioral, and neuropsychiatric disturbances are found in approximately 85 % of PD patients, and nearly 50 % of PD patients meet the diagnostic standards for dementia after 15 years of follow-up (Hely et al. 2005). Cognitive deficits are, in some cases, also apparent in early-stage PD (Dubois and Pillon 1997; Owen 2004; Zgaljardic

et al. 2004). Executive dysfunction is perhaps the best defined non-motor symptom of PD. Studies have shown that relative to healthy, age-matched control subjects, PD patients exhibit deficits on executive tests such as the Wisconsin Card-Sorting Task (Cooper et al. 1992; Gotham et al. 1988; Lees and Smith 1983). PD patients exhibit executive function impairment, including declines in working memory, planning, problem solving, and set-shifting (Dimitrov et al. 1999; Farina et al. 2000; McKinlay et al. 2010; Muslimovic et al. 2005; Tamaru 1997). Traditionally, medical treatment of motor symptoms with dopamine-medication has been shown to have variable effects on executive deficits.

The non-motor symptoms of PD are of particular interest and relevance to the progression of research due to the potential of non-motor symptoms as biomarkers to identify pre-symptomatic PD (A. H. Schapira 2013; A. H. Schapira et al. 2014; A. H. V. Schapira et al. 2017). The diagnosis of PD most commonly depends on the identification of the familiar motor deficits of the disease. The very visible appearance of tremor, bradykinesia, rigidity, and a good response to dopaminergic medication make for an effectivemethod of diagnosis. However, these motor symptoms are often preceded by non-motor symptoms, such as executive dysfunction, and such symptoms may be present years before the eventual emergence of the familiar motor deficits (Schrag et al. 2015). While none of the parkinsonian non-motor symptoms are exclusively characteristic of PD, the combination of multiple non-motor symptoms in conjunction with other PD symptomology, such as the correlation of non-motor symptoms with the preclinical loss of dopamine observed through imaging, could improve the sensitivity of PD diagnoses or the monitoring of patients from pre- to post-symptomatic disease states (Berg et al. 2013; A. H. V. Schapira et al. 2017). Biomarkers that proceed or evolve in parallel with clinical features and pathology would help in evaluating treatments or prescribing medication designed to slow the development of PD.

1.3.3 Parkinson's Disease Pathophysiology and the Beta Frequency Band

PD is not a homogenous disease, in that it expresses differently across patients or even within a single patient's disease progression. PD tremor, for example, is not necessarily a consistent feature of the disease, but rather occurs episodically (Rivlin-Etzion et al. 2006). Unlike with rigidity and akinesia, there is no correlation between the clinical severity of PD tremor and the extent of striatal dopaminergic deficit or the clinical progression of the disease as a whole (Deuschl et al. 2000).

An improved understanding of PD-related changes in the architecture of functional networks is essential for a better understanding of the pathophysiology of the disorder and may lead to the development of novel therapeutic strategies (Eckert et al. 2007; Eidelberg 2009; Rosin et al. 2007). Indeed, how BG dysfunction leads to PD, or even how the BG control movement is not yet clear.

The role that neuronal oscillations play in the pathophysiology of PD remains the subject of debate. Depth recordings in patients with PD have shown the existence of synchronization within neural populations in the BG in several different frequency bands, particularly in the STN (Kuhn et al. 2004; Levy et al. 2002). This synchronization tends to prevail in the beta band, and it has been suggested that excessive beta band synchronization may contribute to PD symptoms (P. Brown 2003; Kuhn et al. 2006). Supporting this theory, decreases in beta power occur before and during movement (Kuhn et al. 2004; Levy et al. 2002). Oscillations in the STN have been shown to be coherent with oscillations in cortical areas (P. Brown 2003; Fogelson et al. 2006; Hirschmann et al. 2011; Marsden et al. 2001). Coherence between the STN and the premotor and ipsilateral sensorimotor cortex has been identified, but further investigation is warranted to interpret these findings and determine the exact topography of STN-cortical coherence (Hirschmann et al. 2011).

It is likely that the coupling between BG LFPs and BG neuronal discharges is evidence of Parkinsonian beta LFPs having been locally generated, although neuronal activity may be synchronized across multiple levels, especially in the PD individual (P. Brown et al. 2001; Goldberg et al. 2004). A clear demonstration of LFP activity can be shown during intra-operative recording using microelectrodes, as seen by the clear step increase in beta band power on electrode entry to the STN (Kuhn et al. 2005). This may suggest that LFP oscillations recorded using microelectrodes are focally generated. This does not, however, necessarily mean that such synchronization is brought about by processes intrinsic to the STN (P. Brown and Williams 2005).

One would hypothesize that if beta band activity promoted a low likelihood of change in sensorimotor circuits, one would expect that pathologically high beta activity or coherency would result in abnormal inhibition of behavioral and cognitive changes. This can be seen in studies of PD patients and those with other movement disorders (P. Brown 2003, 2007). Evidence for beta activity prohibiting movement can be seen in recordings in human subcortex during stereotactic operations for PD treatment (Limousin et al. 1995). Such surgeries allow researchers unprecedented ability to record neural signals from target structures, allowing studies of oscillatory activity and its coherency with EEG and EMG during motor tasks. A series of studies by Brown *et al.* (P. Brown et al. 2001; Cassidy et al. 2002; Kuhn et al. 2004; Lalo et al. 2008) investigating dopamine-dependent changes on coherence between the cortex and the BG have furthered our understanding of PD mechanisms during “on” and “off” medication states. Measurements taken without medication showed that for PD subjects in the “off” and akinetic state, beta band frequency oscillations and tremor frequencies dominate coherence measurements, while the introduction of L-DOPA to the system acted to reduce beta activity and promote coherency in the gamma frequency of 70 Hz (P. Brown et al. 2001). Oscillatory activity was also investigated by observing the modulation of coherence before and

during voluntary movements; beta coherence was decreased during movement preparation and execution in the “off” state, while after L-DOPA treatment gamma was boosted during movement (Cassidy et al. 2002).

Observing the effects of electrical stimulation through surgically implanted DBS electrodes has also resulted in advances in our understanding of pathological beta activity. Physiological studies in monkeys have shown that the use of DBS entrains the stimulated region to the characteristics of the electrical stimulation (Vitek 2008). Analysis of which regions exhibit excessively synchronized beta oscillations in PD patients can help to predict the clinical effects of DBS; stimulation at the sites where beta activity coherence is highest with EEG yields the best results when improving PD symptoms (Marsden et al. 2001). Kuhn *et al.* (Kuhn et al. 2008b) were the first to show that high frequency DBS leads to a suppression of beta band activity in patients with PD with a resulting improvement of motor performance. Importantly, the opposite is shown in that bradykinesia in PD patients is worsened when DBS is set to stimulate in the beta band, while it is improved at high stimulation frequencies (Chen et al. 2007).

The beta frequency band appears to be the least understood of the different frequency bands in terms of functional significance. Recent studies in the motor system, cognitive processing, and pathophysiology have suggested that beta frequency activity acts by maintaining the current set of neural affairs. In motor systems, beta appears to uphold the current motor set. Beta in cognitive processing may relate to the dominance of top-down processing that act to supersede the effect of novel or unexpected external stimuli. The studies discussed show support for the notion that abnormal increases in the beta band resulting from a decrease in dopamine production act to disrupt normal motor function. Gamma band activity, on the other hand, seems to be required for the preparation and control of normal voluntary movements. Supposing that beta activity does stimulate the maintenance of the current motor

set in normal individuals, beta activity in pathological settings may be manifesting as an inability to modify the existing motor conditions.

1.4 **Research Question and Experiment Summaries**

Movement-related excessive synchronization in the beta frequency range has been consistently observed in the BG thalamocortical circuit in PD patients and parkinsonian animal models. PD subjects are also known to express dopamine-dependent cognitive dysfunction. While the electrophysiological underpinnings of PD motor symptomology are characterized, PD non-motor symptoms, their electrophysiological correlates, and the extent to which the oscillatory activity that is observed throughout the BG thalamocortical circuit following dopamine cell loss is transmitted to limbic and cognitive components of the circuit are poorly understood. The presence of electrophysiological abnormalities associated with cognitive function in the BG and ACC of PD patients could be used as biomarkers to help advance the early diagnosis of PD, the development of PD treatments, and the overall understanding of this increasingly common disease.

To better understand the relationship between the ACC and the BG thalamocortical circuit in the normal and parkinsonian brain, activity in these regions was studied in PD, dystonia, and chronic pain patients (at the University of Oxford, Oxford, UK) and in the hemiparkinsonian rat model of PD (at the National Institutes of Health, Bethesda, MD, USA). In humans, 2 studies were performed. Electrodes were localized to regions of both clinical and scientific importance: GPi implantation for the treatment of PD and dystonia and dorsal ACC (dACC) implantation for the treatment of chronic pain. No other regions were investigated in humans as we were limited to only DBS subjects with either GPi or ACC implants. In the first human study, the electrophysiological output of the BG in PD subjects and dystonic subjects (the latter representing “healthy” dopaminergic function) performing a forced-choice decision-making task with sensory feedback was compared to investigate PD-associated executive dysfunction.

In the second human study, chronic pain subjects were examined using the same decision-making task to explore dopamine "healthy" ACC executive function. In rats, two further studies were conducted to expand on the human findings. To investigate ACC activity in the dopamine-depleted condition, chronically implanted, awake, and behaving hemiparkinsonian rats performing treadmill walking were recorded simultaneously from the STN, VM, and ACC. Chronically implanted, hemiparkinsonian rats also performed a cognitive/movement paradigm, wherein the electrophysiological correlates of cognitive function and dysfunction in the parkinsonian state could be examined.

2. Executive Function in the Human Basal Ganglia

The motor symptoms of both PD and focal dystonia arise from dysfunction of the BG, and are improved by pallidotomy or DBS of the GPi. However, PD is associated with a greater degree of BG-dependent learning impairment than dystonia. We attempt to understand this observation in terms of a comparison of the electrophysiology of the output of the BG between the two conditions. We use the natural experiment offered by DBS to compare GPi LFP responses in subjects with PD compared to subjects with dystonia performing a forced-choice decision-making task with sensory feedback.

2.1 Introduction and Rationale

The BG are a network of subcortical nuclei extensively interconnected with the overlying neocortex, which play an essential role in the control of voluntary movement (P. Brown 2003; Smith et al. 1998). The nature of this control is still to be fully elucidated and several hypotheses, not necessarily mutually exclusive, have been proposed. A consistent theme is that the BG optimize motor response to environmental cues to gain maximal sensory reward, or in other words, to minimize the cost/benefit ratio of motor behavior within the current environment (Bogacz and Gurney 2007). This is a multi-faceted process and a variety of studies suggest different nuclei may play different roles in this process, including learning of action-outcome associations in striatum (Balleine et al. 2009), signaling the receipt of sensory reward in the mesolimbic and nigro-striatal dopamine pathways (Gan et al. 2010; Zaghloul et al. 2009), reducing the probability of motor error in the context of conflict in the STN (Zavala et al. 2013), and error monitoring (Herrojo Ruiz et al. 2014) and the appropriate scaling of ongoing voluntary movements (minimization of movement cost) in relation to movement goal (predicted reward) in the GPi (R. S. Turner and Anderson 2005). The introduction of DBS for movement disorders such as PD and dystonia have allowed some of these theories to be tested in humans, both by recording the electrophysiology of BG nuclei whilst subjects perform tasks (Jenkinson and Brown 2011) and by testing the psychophysical effects of DBS therapy (Antoniades et al. 2014). With regards to learning, one hypothesis is that the BG performs fast, directed formation of action-reward associations that, with repetition of the task, train slower Hebbian thalamocortical circuits such that the BG acts as a ‘tutor’ to the cortex (R. S. Turner and Desmurget 2010). Supporting this view, lesioning or inactivation of the GPi, the main output nucleus of the BG, is associated with impairment of new motor skill acquisition but not the retention or recall of already-learned skills (Desmurget and Turner

2008). Learning can still take place in PD subjects despite degeneration of nigro-striatal pathways critical in the signaling of the receipt of reward feedback upon motor action; PD subjects are still able to perform implicit memory tasks with a reduced motor component (Sage et al. 2003). This suggests some BG-dependent learning functions are dopamine or striatum independent. Pallidotomyablation of the GPi is associated with a mild impairment of this faculty despite improved motor symptoms (Sage et al. 2003). In contrast, primary focal dystonic sufferers do not appear to suffer from significant cognitive deficits compared to control subjects despite the manifest motor symptoms of the disease and amelioration by pallidotomy (Jahanshahi et al. 2003). These observations prompt two questions. First, what is the difference between dystonic and PD GPi 'tutor' signals that largely preserves BG cognitive function in dystonic subjects? The comparison of neural activity in BG in these two patient groups is particularly interesting as PD patients have a much greater loss of dopamine neurons, which are thought to encode information about feedback (Schultz et al. 1997), thus feedback related activity present in dystonic but not PD patients may be related to dopaminergic modulation. Second, what are the similarities in dystonic and PD GPi outputs during learning that allow for PD subjects to still have BG-dependent learning capacity despite degeneration of the nigro-striatal pathway? We use a unique natural experiment offered by functional neurosurgery to attempt to answer these questions. Eight patients undergoing DBS of the GPi were studied; 5 with dystonia and 3 with PD. Two of the 3 PD patients were tested 'on' and 'off' dopamine medication. LFP electrical activity was recorded from their indwelling brain electrodes during an onscreen version of the Wisconsin Card Sorting Test called Intra-extradimensional (IED) set shifting (CANTAB®). During this task, subjects have to make a forced choice between 2 objects and are provided with feedback indicating a positive (correct choice) or negative (incorrect choice) outcome. 'Correct' or 'incorrect' depends on a series of rules learned across trials during the task. We analyzed evoked potentials related to the sensory

feedback component of the task (consisting of an auditory tone specific to correct/incorrect and also visual feedback). We further analyzed these changes in the frequency domain and show results from dystonic and PD patients ('on' and 'off' medication) as well as dominant and non-dominant GPi.

Attentional set shifting, as presented in our chosen cognitive task, IED, is a measure of cognitive flexibility and executive function referring to the ability to switch between arbitrary internal rules (Keeler and Robbins 2011; Scheggia et al. 2014). IED, and its physical variation Wisconsin Card Sorting, is the most widely used neuropsychological task for the evaluation of this function in humans (Barnett et al. 2010; Eling et al. 2008). Such tasks have been used to identify executive function abnormalities in a wide range of mental disorders including attentional deficit disorders, obsessive-compulsive disorders, and PD (Chamberlain et al. 2011; Head et al. 1989; Owen et al. 1993). Attentional set shifting tasks, such as IED, are important because they allow for the selective measurement of the processes underlying discriminative learning, reversal learning behavior, and the switching of attention within both the same dimension (the intradimensional shift) and an alternative dimension (extradimensional shift) in a tested subject. Such a distinction is relevant, as a functional specialization governs these two shifts. This has been demonstrated between the orbital regions and the lateral (in NHP) and medial (in rodents) regions in the PFC, respectively (Scheggia et al. 2014). Orbitofrontal cortex has been shown to be selectively involved in reversal shifts, while the lateral/medial PFC has been shown to be involved in the extradimensional shift (Dias et al. 1996; Hampshire and Owen 2006; Keeler and Robbins 2011).

2.2 Methods

Patients gave informed written consent; the study was approved by Oxfordshire Research Ethics Committee A (Ref 08/H0604/58 & 11/SC/0229) and the study conformed to the Declaration of Helsinki.

2.2.1 Patient Group

The patient group is described in detail in table 2.2. Eight patients (4 female and 4 male) were studied: 4 with focal dystonia (ages at time of testing 21, 53, 59 and 66 years), 1 with spasmodic torticollis (aged 65 years), 3 with idiopathic PD (ages 44, 55, and 66 years). Seven patients were habitually right handed, 1 left-handed. At the time of testing, no dystonic patients were on anti-dystonic medication, as a failure to benefit from medication is a major indication for DBS in dystonic patients (Yianni et al. 2011). Intellectual indicators were generally comparable to population averages. All 3 PD patients continued their normal anti-PD dosing regimen during testing to prevent akinesia interfering with their ability to perform the task. Two of the 3 PD patients were tested both ‘on’ and ‘off’ dopamine medication.

Patient	Sex	Diagnosis	Age at surgery	Age at 1st reported symptoms	Handedness	NART IQ	AMIPB (delayed)	SDMT written/oral
1	m	Focal dystonia (neck)	53	15	Right	100	100 (108)	98/110
2	f	Focal dystonia (L foot)	21	7	Left	90	94 (100)	96/99
3	f	Focal dystonia (cervical)	59	35	Right	n/a	n/a	n/a
4	m	Spasmodic torticollis	65	59	Right	95	98 (84)	72 (82)
5	f	Focal dystonia (cervical)	66	56	Right	102	114 (117)	91 (102)
6	f	Parkinson's disease	66	52	Right	116	Passed (15)	n/a / 0.00
7	m	Parkinson's disease	44	34	Right	102	Passed (11)	-0.06/0.49
8	m	Parkinson's disease	55	47	Right	103	Passed (9)	n/a

Table 2.2 Participants' characteristics
All scores have a mean 100 and SD 15 unless otherwise stated. Performance is classified as: impaired (< 69), borderline (70 - 79), low average (80 - 89), average (90 - 109), high average (110 - 119), superior (120 - 129), very superior (> 130).
Abbreviations: NART IQ, National adult reading test intelligence quotient; AMIPB, adult memory and information processing battery; SDMT, symbol digit modalities test.

2.2.2 Electrode Implantation and Electrode Placement Confirmation

All 8 patients underwent bilateral implantation of GP DBS (Yianni et al. 2011). In summary, GPi targets were selected on preoperative magnetic resonance imaging (MRI) scans (Figure 2.2.2). Subjects underwent general anesthesia, and Cartesian coordinates were generated for preselected targets using the Brown-Roberts-Wells stereotactic localizer frame, preoperative computed tomography (CT) head scan performed under anaesthesia, and Radionics® (Burlington, MA) or NeuroInspire® (Renishaw plc, Wotton-under-edge, UK) image fusion software. Cartesian coordinates were configured on the Cosman-Roberts-Wells frame attached to the subject's head. A 2.7 mm twist drill craniostomy was made and Medtronic 3387® (Medtronic Neurological Division, Minneapolis, MN, USA) DBS leads were passed to target coordinates, with extension leads attached and externalized. Each DBS lead has 4 platinum-iridium cylindrical circumferential 1.5 mm electrodes separated by a 1.5 mm gap. A CT head scan was performed, before recovery from anaesthesia, to confirm lead position and was verified by image fusion with the pre-operative MRI. The internalization of DBS leads and

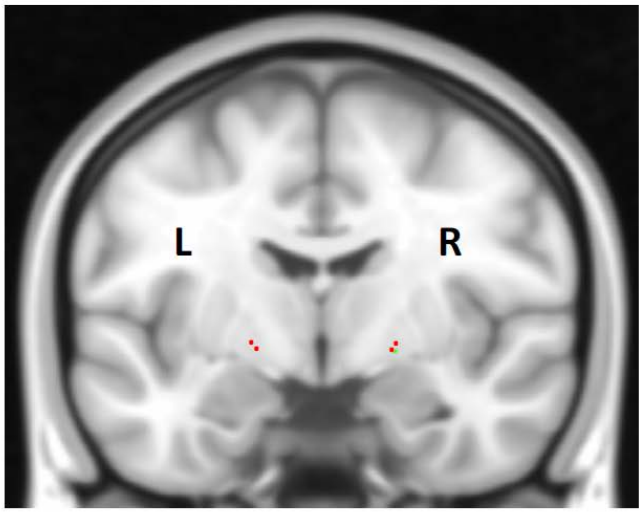

Figure 2.2.2 Representative GPi electrode location
Representative MRI scan of bilateral DBS electrode location. GP electrode positions in each patient were normalized in MNI space from postoperative radiological imaging to identify contacts occupying (or lying closest to) left and right GPi and GPe.

the implantation of the internal pulse generators generally took place a week later following clinical testing for efficacy.

2.2.3 Intra- Extradimensional Set Shifting Task

Subjects performed an on-screen variation of the Wisconsin card sorting test called the IED set shifting task. See figure 2.2.3 for an illustration of IED rule order and a schematic of a single trial. This test was utilized because it is widely used in clinical practice and also has the basic form of object-presentation-motor action-outcome/feedback-repeat. Subjects learn a series of 9 2-alternative forced-choice discrimination rules between 2 visual objects presented on screen based on feedback provided automatically by computer.

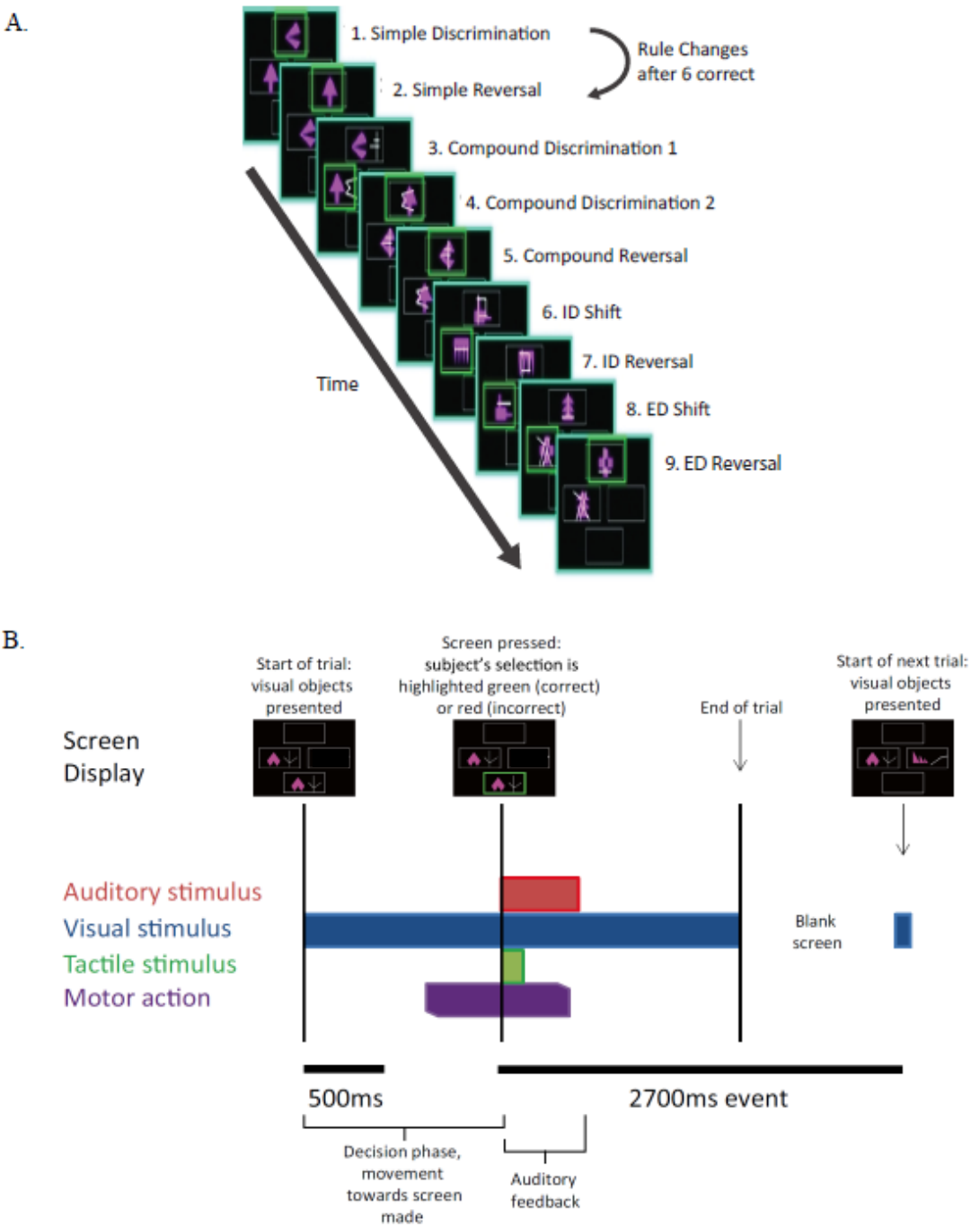

Figure 2.2.3 Intra- Extradimensional Set Shift Task (IED)

A. Schematic of the IED task from the Cambridge Neurophysiological Test Automated Battery (CANTAB) displaying rule order during a given recording. Green rectangles indicate the correct choice. Rule progresses after 6 consecutive correct choices. Test will terminate if 6 consecutive correct choices cannot be made in 50 attempts. Copy right 2008 Cambridge Cognition, Ltd. All rights reserved.

B. Schematic representation of IED sensory and motor events within a given trial. The trial begins with presentation of the two visual objects. After a variable decision-making phase, the subject then makes a movement to touch the screen. Screen press elicits auditory and visual feedback indicating whether the subject has chosen the correct or incorrect figure for the current rule. After an interval of 1.5 s, the screen becomes blank before the start of the next trial.

The task begins with the presentation of 2 abstract objects. Each of the 2 visual objects are composed of a single solid abstract shape initially (the internal dimension), which may only occupy 1 of 4 on-screen rubrics. The spatial relationship between the 2 visual objects varies randomly as a distractor during a sequence of trials governed by the same rule. As the task progresses, the visual objects acquire an additional abstract element in the form of white lines (the external dimension) after the successful completion of trials governed by the first 2 rules (simple discrimination and reversal). The white line dimension acts as a distractor during rules 3 to 5 (compound discrimination 1, compound discrimination 2, and reversal), as the rule at this point is based on the solid shape dimension only. During sequences governed by rules 3 to 5, the white line dimension is randomly associated with each solid shape dimension, with a small variable range of configurations relative to the solid shape dimension. Upon transition to rule 6 (intra-dimensional shift), the solid shapes change to 2 new visual objects composed of new solid shape and white line images, but the rule governing correct object choice remains determined by the solid shape dimension only (i.e. intra-dimensional component). The white line dimension acts as the stimulus dimension governing correct object choice during the extra-dimensional phase of the task during rule 8 (extra-dimensional shift) and rule 9 (reversal). A script is read to the subjects before the task begins, informing them to pick one of two on-screen visual objects. They are informed one object will be “correct” and the other “incorrect.” They are informed that there is no stimulus characteristic which indicates which object is correct or incorrect on the first trial, but that the computer will give feedback after selection to inform them whether they selected the “correct” or “incorrect” object. Subjects were informed that the rules would change over the course of the test, but that these rules would not change often, and would only change after the preceding rule had been learned. They were not informed how many times the rules would change or how many correct trials in a sequence they would have to achieve before the rule would change. Selection of an object on-screen by

touch caused an audible tone (pure tone for correct, low frequency modulated pure tone for incorrect) and simultaneous presentation of a colored box around the edge of the screen (green for correct and red for incorrect) with the word “correct” or “incorrect” lasting 0.5 s, all acting as feedback to inform the subject whether their choice was “correct” or “incorrect” per the rule governing object selection. The next trial would begin automatically 2.7 s after the start of object selection auditory feedback. Subjects were invited to use their dominant hand for object selection. Through trial and error over time the subject interacts with the test, receives feedback, and learns the rule. The rule was defined as “learned” when the subject achieved 6 correct object selections in a row. After a 6^{th} correct selection, the rule criteria would then be changed. At this point, the subject would likely unexpectedly get the next choice wrong and must, again, by trial and error, learn the new rule. On some rules, this was not associated with a change in the stimulus pair displayed on screen (reversal rules i.e. the “correct” object becomes “incorrect” or vice versa). Other rules are associated with a novel pair of objects, either solid shapes alone or solid shapes with white line objects superimposed. As the IED test progresses, rules become more complicated (for example, intradimensional shifts occur where rules change in the same category, e.g. solid shapes, or extradimensional shifts occur where a new dimension becomes pertinent, e.g. solid shapes being the relevant “correct” component to white lines becoming the “correct” component). During transition to reversal rule trials (rules 2, 5, 7, and 9), the visual objects do not change compared to the last trial of the previous rule. During transition to discrimination and dimensional shift rule trials (rules 3, 4, 6, and 8), the on-screen visual objects change (although some component elements of the objects may not) compared to the last trial of the previous rule. To complete the IED task, the subject must learn 9 rules, with a maximum of 50 attempts allowed per rule before a subject failed and the test aborts. In this study, we were primarily concerned with whether a response was “correct” or “incorrect” or if object pairs were “familiar” or “novel.”

The dystonic patients each performed 1 IED task. Four of the 5 dystonic patients passed the test, the subject who failed learned 7 rules successfully. Two PD patients performed 1 IED task “off” medication and 1 task “on” medication. While “off” medication, 1 subject passed the IED task and 1 subject failed. While “on” medication, both subjects passed. One subject performed 3 IED tasks in succession and passed on the 1st and 3rd attempts and failed on the 2nd attempt. The PD patients also performed the IED task as part of a neuropsychological investigation several months prior to DBS surgery.

2.2.4 Electrophysiology and Analysis

Differential recordings were made from adjacent circumferential 1.5 mm contacts on each deep brain macroelectrode. A bipolar configuration was utilized to limit the effects of volume conduction and limit the spatial resolution of recordings to a few mm of adjacent tissue (Lempka and McIntyre 2013). Signals were high pass filtered at 0.5 Hz, amplified (10,000x) using isolated CED 1902 amplifiers and digitized using CED 1401 Mark II at a rate of 2.5 kHz (Cambridge Electronic Design, Cambridge, UK), or recorded via a Porti system (Twente Medical Systems International, B.V., Netherlands) and recorded onto disc using Spike2 software. Raw data was notch filtered at 50 Hz, 100 Hz and 150 Hz as required using Spike2 infinite impulse response Bessel filters, Q value adjusted to avoid unwanted filtering of adjacent frequencies as much as possible.

Preprocessing and analysis of LFPs was performed offline using MATLAB software (Mathworks Inc., Natick, MA, USA) and EEGLab (Brunner et al. 2013; Delorme and Makeig 2004; Delorme et al. 2011). Spike2 data were imported into EEGLab in MATLAB. Raw data were resampled at 300 Hz. 5 s epochs beginning 2000 ms prior to the start of auditory feedback and continuing to +3000 ms post-feedback were extracted from both left and right electrode

contacts and divided into correct and incorrect trials. Trials were divided into correct trials and incorrect trials only; there were insufficient trials to analyze differences between responses to specific rules. Baseline prior to feedback (-2000 ms – 0 ms) was subtracted and then data were normalized by individual mean and sample standard deviation using MATLAB z-score commands to allow for comparison between different disease states. EEGLAB commands were used to generate ERP, power spectra, and event-related spectral perturbations (ERSP).

2.2.5 Statistical Analysis

EEGlab non-parametric statistics with False Discovery Rate (FDR) correction were used to compare LFP data between trials and between study groups. Non-parametric Rank Sum and Kruskal-Wallis tests were used to analyze RT data since RT data were not normally distributed. RT data are therefore expressed as median: 25 – 75 % interquartile range. RTs were normalized to compare RTs between subjects and conditions in novel trials (rules 3, 4, 6, 8), reversal trials (2, 5, 7, 9) and 1^{st} correct vs. 6^{th} correct RTs.

Instantaneous power measurement of high gamma activity for figure 2.3.5 was achieved by bandpass filtering raw data between 100 Hz and 200 Hz, and averaging the raw data for a given subject to the start of auditory feedback, from 1.5 s before feedback to 1.5 s after (3 s window). Sliding time fast Fourier transform (FFT) windowed to encompass at least 4 periods of the high gamma oscillation, advancing by one data point per FFT (MATLAB spectrogram function) were used to generate a spectral power density matrix from the averaged response. For a given epoch in the high gamma band, peak power was extracted for each subject for each GPi (left and right) and each condition (correct and incorrect). GPi were grouped as left and right rather than dominant and non-dominant since the high gamma signal was detected in all 4 right handed dystonic subjects in the right GPi (non-dominant), but only in 2 out of 4 in the

left (dominant), and was of higher amplitude and greater trial to trial consistency in the right (dominant) GPi of the left handed dystonic subject. Correct trial vs. incorrect trial high gamma peak power was then compared. Peak power was first normalized by the first 200 data points (out of approximately 8000) in each subject to allow comparison across all 5 subjects. A bootstrap procedure was used to generate surrogate data for the null hypothesis (no difference between correct and incorrect trials) (Di Nocera and Ferlazzo 2000). We then compared, per time point, the empirical difference (between correct and incorrect responses) to the distribution of differences at that time point from the surrogate data, corrected for multiple comparisons using FDR. When concurrent differential recordings from GPi and GPe were possible, mean cross-correlograms per unit time of the tone-averaged high gamma oscillations between each layer were computed. The peak coherence value (range 1 to -1) was plotted against time to investigate any rhythmicity in interaction between these areas and quantify their relative states at the onset of response selection.

2.3 Results

2.3.1 Task performance

330 correct trials and 108 incorrect trials in 5 dystonic subjects were available for analysis, compared to 357 correct trials and 118 incorrect trials in 3 PD subjects on medication, and 139 correct and 40 incorrect trials in 2 PD subjects off medication. Detailed RT data were available from all 8 subjects. The RT between dystonic and PD subjects were not directly comparable, especially in the on-medication situation, since the PD subjects had performed the task on one or more occasions prior to recording, in contrast to dystonic subjects. RT were not significantly different between correct and incorrect trials in dystonic subjects (correct mean 1484 ms (1202 ms – 1966 ms) vs. incorrect 1493 ms (1099.75 ms - 2326.25 ms)). PD subjects on medication demonstrated significantly slower RT in incorrect trials compared to correct trials (correct 1181 ms (858 ms - 1960.5 ms) vs. incorrect 2112 ms (1355.75 ms – 2917.5 ms), $p < 0.01$). Two PD subjects tested off medication did not demonstrate this difference (correct 1009 ms (859.5 ms - 1210 ms) vs. incorrect 1065.5 ms (809.75 ms – 1160 ms), $p = 0.98$). Off medication, PD subjects performed the task significantly faster than on medication ($p < 0.01$), despite having performed the IED task off medication prior to performing the task on medication. Dystonic subjects performed the majority (54 %) of incorrect trials during extra-dimensional shift rule 8. Dystonic subjects made significantly fewer errors during intradimensional shift rule 6 compared to extradimensional shift rule 8 ($p < 0.01$). Incorrect trials were more evenly distributed across rules, with no statistical differences between error rates in the intradimensional and extradimensional shift rules ($p < 0.01$). Dystonic and PD subjects demonstrated similar prolonged RT responses to novel stimuli (rule 3, 4, 6, 8) trials ($p < 0.01$) but were not significantly different from each other in their responses to novel stimuli.

Post error (incorrect) trial RT was not significantly prolonged in either group ($p < 0.05$), and neither were RTs during the first or second attempts of a reversal rule trial sequence. RT did not change significantly between the 1st and 6th correct trials of a sequence of 6 correct trials.

2.3.2 Electrophysiology

A subject's movement to the screen was associated with a slow negative going ERP in the GPi, peaking and subsequently inverting prior to the commencement of auditory feedback in both dystonic and PD subjects (Figure 2.3.2). Dominant GPi in PD subjects on medication demonstrated a significantly smaller deflection from the baseline potential than was seen in dystonic subjects ($p < 0.05$). These subjects also had a shorter positive phase post-feedback. No significant differences were observed between the non-dominant GPi responses in the dystonic or PD subjects on medication.

LFP ERPs from dominant and non-dominant GPi were compared between correct and incorrect trials and between PD and dystonic subjects. In all 3 PD subjects, the dominant GPi was in the left hemisphere as they were right-handed. Four dystonic subjects were right handed (left hemisphere GPi dominant) while the last dystonic subject was left handed (right hemisphere GPi dominant). ERP and ERSP demonstrated distinct responses to sensory feedback between PD and dystonic subjects (Figure 2.3.2). Dystonic subjects displayed a phasic high gamma ERSP (125 – 135 Hz) upon the receipt of sensory feedback that lasted approximately 100 – 200 ms. Such a phasic high gamma signal was not observed in the PD subjects. Both dystonic and PD subjects exhibited a greater theta band frequency (3 – 8 Hz) ERSP response to the receipt of incorrect feedback as compared to the receipt of correct feedback in the subject's respective dominant GPi, but not in their non-dominant GPi. This theta band ERSP occurred at a lower peak-frequency in the dystonic subjects as compared to the PD subjects.

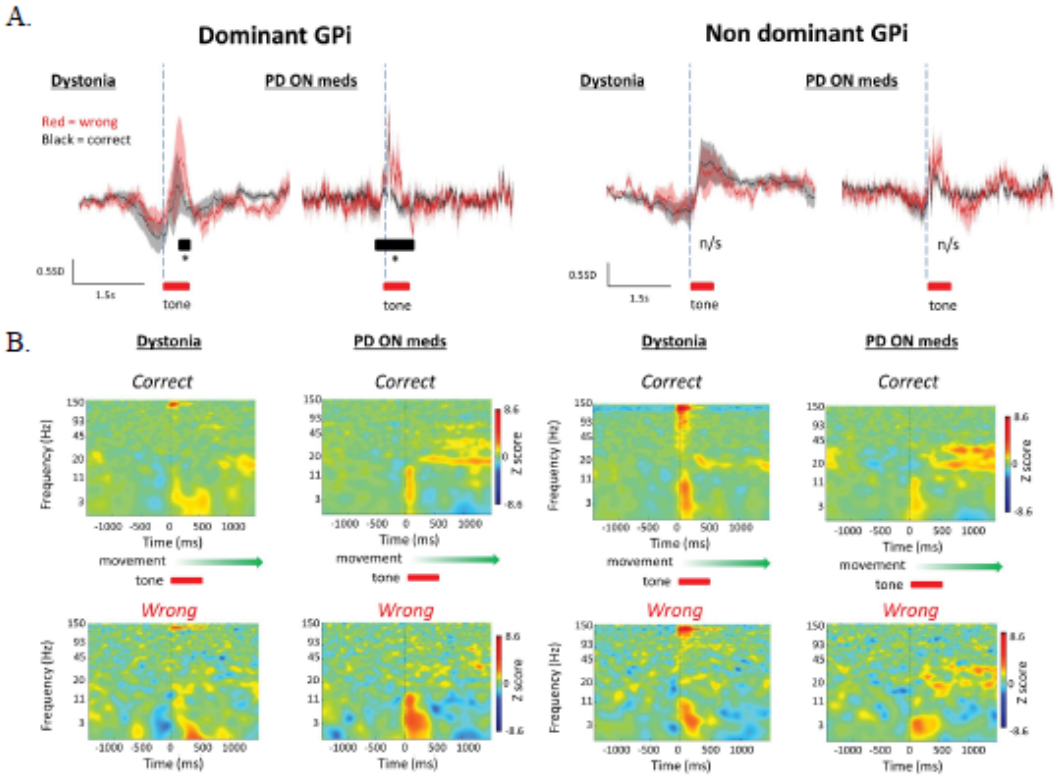

Figure 2.3.2 Event-related potentials (ERP) are elicited in GPi during a forced decision-making task requiring motor output.

A. Coherently averaged, normalized ERPs from 5 dystonic subjects and 3 PD subjects on medication averaged relative to the onset of auditory feedback and grouped according to correct (black line) versus incorrect (red line) trial performance, and dominant vs. non-dominant hemisphere GPi response (mean ± SEM). Movement was associated with a slow negative-going potential in dystonic subjects' GPi, peaking and subsequently inverting prior to the commencement of auditory feedback (hatched vertical line). Post-feedback positive ERP response had significantly greater power in the lower frequency range (< 5 Hz) during incorrect trials post-feedback, as compared to correct trials in dystonic subjects in the dominant GPi ($p < 0.05$). This was not observed in non-dominant hemisphere GPi. The dominant hemisphere GPi of PD subjects on medication during both correct and incorrect trials demonstrated both a significantly smaller deflection from baseline potential than dystonic subjects and a shorter positive phase post-feedback ($p < 0.05$). No significant differences were observed in the non-dominant hemisphere GPi responses in dystonic or PD subjects on medication. Post-feedback ERP in PD subjects on medication exhibited significantly greater power in the theta band (3 - 8 Hz) during incorrect trials compared to correct trials in the dominant hemisphere GPi but not in the non-dominant hemisphere GPi. Post-feedback ERP in dystonic subjects demonstrated significantly greater power in the low theta range (< 5 Hz) during incorrect trials compared to correct trials ($p < 0.05$).

B. Averaged event-related spectral perturbation (ERSP) was analyzed to further define the reponse to feedback. The receipt of feedback (correct vs. incorrect via tone and on-screen information) was accompanied by a transient burst of high gamma oscillations (100 - 150 Hz) in dystonic subjects in both correct and incorrect trials in both the dominant and non-dominant hemipsheres' GPi. PD subjects did not exhibit this response. Post-feedback gamma (30 - 100 Hz) and beta (15 - 30 Hz) oscillations had significantly greater power in PD subjects on medication as compared to dystonic subjects, but were not significantly different in either group between correct and incorrect trials.

2.3.3 Theta Findings

The GPi in both PD and dystonic subjects had a robust increase in ERP after both correct and incorrect feedback during the IED task (Figure 2.3.2A). This response, when viewing the time-frequency analysis (Figure 2.3.2B), appears to be localized in the theta frequency (3 – 8 Hz in humans) band across all disease and feedback states. The robust theta response merited inspection, so theta frequency power was compared between correct and incorrect trials in PD subjects. This revealed a significantly greater power response upon receipt of sensory feedback, occurring -190 ms prior to the start of sensory feedback to +500 ms, during trials resulting in incorrect feedback in the dominant hemisphere GPi but not in the non-dominant hemisphere GPi ($p < 0.05$). There was also a significant difference in LFP theta power in dystonic subjects in the dominant hemisphere GPi, occurring between +250 ms and +450 ms after the onset of sensory feedback ($p < 0.05$). In PD subjects off medication, the theta frequency ERP had a significantly longer duration (lasting a further 500 ms) during incorrect trials as compared to those subjects in the medicated state. During correct trials, there was no significant different in theta frequency activity across medication state.

2.3.4 Beta and Low Gamma Findings

Beta (13 – 30 Hz) and low gamma frequency (30 – 45 Hz) bands were examined and, consistent with the literature, PD subjects exhibited significantly greater power in both frequency bands in both dominant and non-dominant hemisphere GPi during both correct and incorrect trials as compared to dystonic subjects ($p < 0.05$) (Ramadan et al. 2009). There were no statistical differences in either frequency band during feedback receipt (0 ms - 1500 ms) in both dystonic subjects and PD subjects (Figure 2.3.4). The analysis of trial-by-trial ERP responses across individuals demonstrated that beta and low gamma frequency bands had a high variability across both correct and incorrect trials.

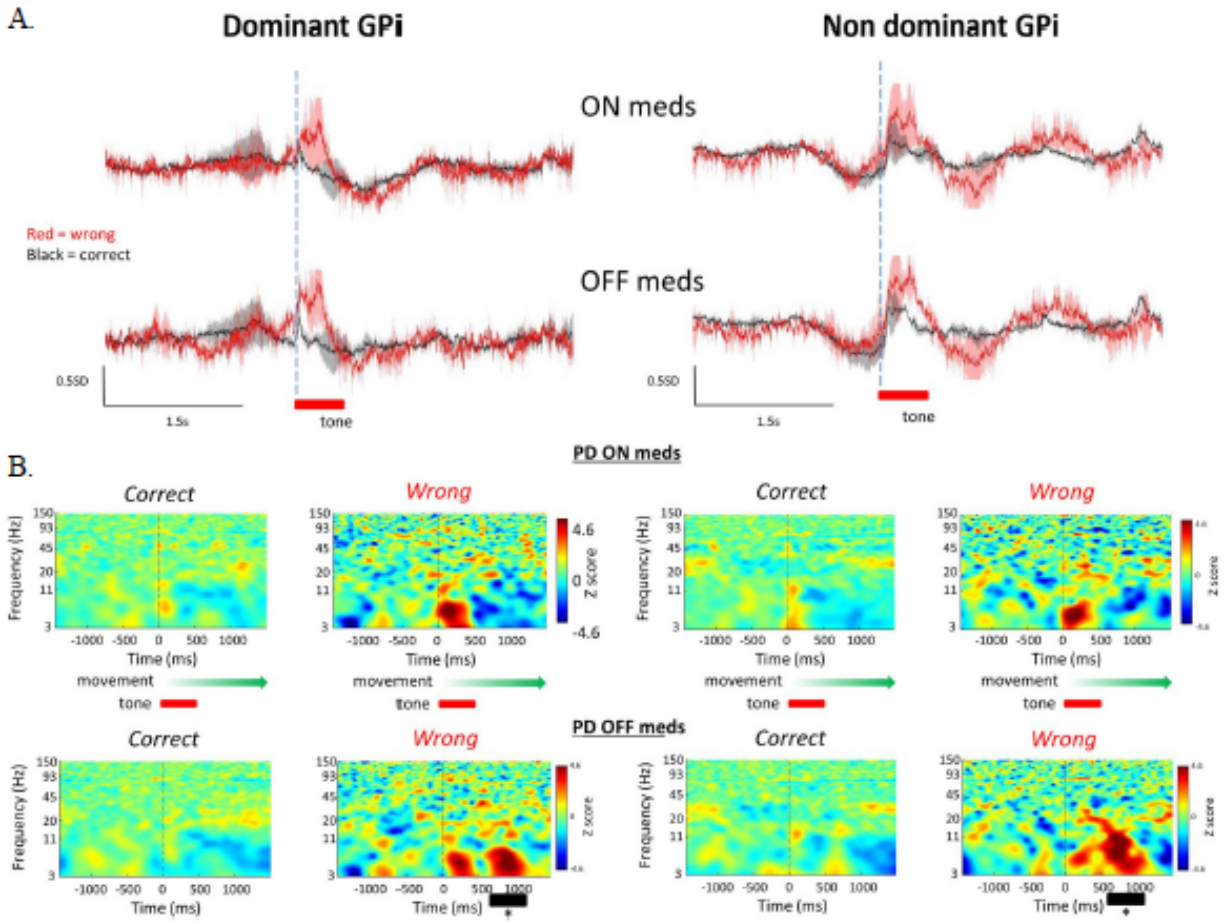

Figure 2.3.4 Comparison of ERPs between on medication and off medication conditions in two PD subjects.
A. Analysis of ERPs.
B. Analysis of ERSPs in two subjects on and off dopaminergic medication. On medication correct (n = 118) vs. incorrect (n = 23). Off medication correct (n = 139) vs. incorrect (n = 40). Incorrect trials were associated with significantly increased power in the theta band (3 - 8 Hz) post-feedback compared to correct trials both on and off medication. High gamma bursts were not observed in PD subjects on or off medication in dominant or non-dominant hemisphere GPi.

2.3.5 High Gamma Findings

After analyzing ERSP images, the high gamma band (90 - 150 Hz) was examined in higher detail (Figure 2.3.5). Average ERSPs from dominant and non-dominant hemisphere GPi in dystonic subjects revealed a significant increase in high gamma activity (125 - 135 Hz) upon receipt of feedback between 0 ms and 500 ms that was not observed in the GPi of PD subjects. While PD subjects had no distinct peak frequency in this frequency range, dystonic subjects had a distinct peak at approximately 130 – 132 Hz in both the dominant and non-dominant hemisphere GPi (Figure 2.3.5.C). Individual high gamma activity responses in GPi were studied in each dystonic patient. ERSPs performed upon individual patients demonstrated a statistically significant increase in power in the high gamma range ($p < 0.05$) associated with sensory feedback in all 5 non-dominant GPi of dystonic subjects and in 3 of 5 dominant GPi. The duration of this phenomenon was variable from individual to individual but ERP reveal the response was consistent from trial to trial. In PD subjects, there were no statistically significant changes in high gamma band power related to sensory feedback in any of the 3 subjects in either GPi.

High gamma oscillations in dystonic subjects occurred nestled on brief negative deflections during the movement-related ERP (Figure 2.3.5.A). ERSPs of correct and incorrect trials from dominant and non-dominant GPi of dystonic subjects were compared. The time to peak spectral perturbance was significantly longer in dominant GPi of dystonic subjects during incorrect trials than during correct trials (correct 20 ms vs. incorrect 70 ms) (Figure 2.3.5.B). This effect was not observed in ERSPs from non-dominant GPi. In the left-handed subject, it was noted that high gamma power was greater, and showed greater trial-to-trial consistency in the dominant (right) GPi, whereas in the right-handed subjects, high gamma activity was greater in the non-dominant (right) GPi. Also, it was noted that the peak frequency of the high gamma power varied from patient to patient within the range 125 to 135 Hz. We therefore

compared the peak power of the coherently averaged high gamma response to sensory feedback across the 5 dystonic subjects. This approach demonstrated a similar phenomenon to that observed with ERSP (non-coherently averaged) data in dominant GPi. In the non-dominant hemisphere GPi of dystonic subjects, the time to peak power was longer in incorrect trials as compared to correct trials (82 ms, $p < 0.05$). Peak high gamma power was also significantly greater in incorrect trials as compared with correct trials ($p < 0.05$). Although a maximum in the peak power of coherently averaged high gamma activity was observed at 100 ms after the start of auditory feedback, this was not significantly different between correct and incorrect trials.

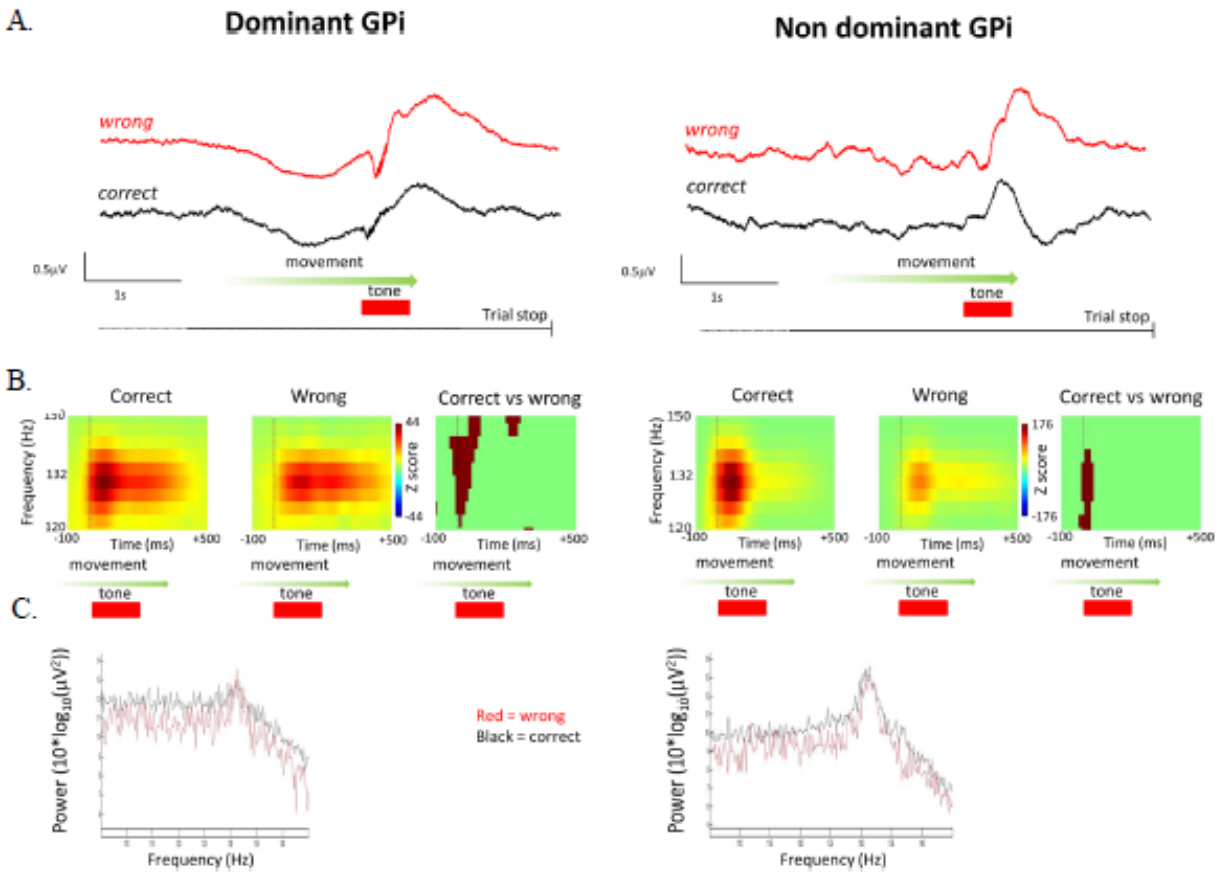

Figure 2.3.5 The high gamma signal contains trial performance information in dystonic subjects only.
A. Representative smoothed ERP from a single subject (subject 2, therefore, GPi is in dominant hemisphere). The onset of auditory feedback is associated with a transient negative deflection nesting a burst of high gamma activity with a peak frequency of 132 Hz.
B. ERSPs -100 ms prior to the start of auditory feedback to +500 ms after indicate that the time to peak high gamma power is longer post-feedback in incorrect trials as compared to correct trials. The time to peak power in correct trials occurs +20 ms, and during incorrect trials at +70 ms ($p < 0.05$) in both dominant and non-dominant hemipshere GPi ($n = 330$ correct trials, 108 incorrect trials).
C. There were no significant differences in high gamma band power between correct and incorrect trials, or between high gamma band power recorded in dominant and non-dominant hemisphere GPi.

2.4 Discussion

We present data from the BG of 5 patients with dystonia, a movement disorder not associated with neurodegeneration or dopaminergic depletion in the BG, and compare their electrophysiological data with data obtained from 3 patients with idiopathic PD. These patients performed a cognitive test sensitive to fronto-striatal disorders to offer further elucidation of the physiological role of BG neural networks.

Neural network rhythmic field potential oscillations are a ubiquitous feature of biological nervous systems. Oscillation signal parameters (e.g. frequency, amplitude, phase relationship to simultaneously recorded single cell activity) relate directly in a predictable way to the single cell physiology and microanatomy of the network from which they are recorded. With detailed knowledge of the single cell physiology and network anatomy of the region of interest, LFP recordings allow inferences to be made about the functions of neural networks in the vicinity of the recording electrode during behavioral tasks.

In this chapter, we show potential electrophysiological biomarkers for executive dysfunction in the BG of dystonic subjects (dopamine “normal”) and PD subjects (dopamine deficit).

2.4.1 Low Frequency Findings

Theta oscillations are ubiquitous in mammalian neural systems and are readily detectable in human scalp EEG particularly during tasks involving the detection of error or conflict (Cohen 2014; Fouragnan et al. 2015; Ruiz et al. 2011; van Driel et al. 2012; Womelsdorf et al. 2010). Our findings concerning the theta (3 – 8 Hz) frequency band suggest

that error detection mechanisms may be partially conserved in PD subjects and are dopamine-independent. Theta LFP activity has been reported previously in the human BG in the STN and the GPi, in a cognitive test called the Flanker task (Herrojo Ruiz et al. 2014; Zavala et al. 2013). In the STN, theta has been proposed to reflect status quo inertia in situations of cue conflict. By increasing the threshold for movement in the presence of conflicting cues, an animal can reduce the possibility of making dangerous movement errors. In the GPi, theta has been associated with the detection of upcoming and actual performance of motor error. This error signal even precedes the occurrence of cortical error-related negativity, suggesting that BG output may drive or contribute to the processing of motor error evaluation by the PFC. Our task, the IED, differed from the Flanker task in that sensory feedback was presented to a subject based on the actual outcome of movement. Our results support the view that the BG participates in some manner in the early stages of error detection. The GPi of subjects, regardless of disease state, exhibits a robust theta frequency response visible in both ERP and ERSP in the first 500 ms after feedback-receipt (Figure 2.3.2). This response varies in magnitude depending on outcome valence – whether a subject receives correct or incorrect feedback, and is greatest in magnitude following incorrect feedback. That this function of the BG occurs in PD subjects on and off medication may suggest that this function is dopamine-independent.

This data set raises the possibility that functions of this mechanism are abnormal in dystonia. Theta oscillations did not preempt incorrect feedback as they did in PD subjects' GPi. The frequency of theta oscillations in dystonic subjects was also lower compared to that in PD subjects. Additionally, dystonic subjects RT on incorrect trials were not significantly prolonged compared to correct trials, in contrast with what was observed in PD subjects. This may suggest that the status quo inertia of the BG in conflicting situations may be disordered in dystonia. One should remember, however, that the power of theta oscillatory activity was significantly higher in the GPi of PD subjects off medication than on medication. Dystonia is also not

generally considered to be a cognitive disorder. In addition, it should be noted that both the PD subjects and the dystonic subjects were able to successfully pass the IED test. IED performance did appear to be impaired in that most incorrect trials occurred in the extra-dimensional shift rule 8 of the task, but 4 of 5 subjects passed the task on the first attempt. The possibility that the BG of dystonic subjects may be disrupted during attentional set-shifting tasks thus may merit further investigation.

In Chapter 3, we further address the question of theta band oscillatory activity and its role in human cognition in the ACC, a region of the brain upstream (via the hyperdirect pathway through the STN) of the GPi. We use a method called multivariate analysis.to separate trial activity in the ACC into spatiotemporal components that most align with correct and incorrect trials (Fouragnan et al. 2015). In brief, we uncovered two separate but interacting temporal components in ACC activity after feedback receipt: an early component related to error detection and a later component related to reward learning (Figure 3.3.3). This activity was focused to the theta frequency band. It is unclear whether or not we would find these early and late components of theta activity in the GPi, without performing additional multivariate analysis, which may theoretically not be possible with the number of correct and incorrect responses yielded by our GPi subjects. In retrospect, when viewing ERSP results from Figure 2.3.4B, one may view the significant theta increases in PD subjects off-medication following incorrect feedback as the activation of the late temporal component seen in Chapter 3. That this activity only appears in the PD non-medicated state may reflect both levodopa medication-related deficits in reward processing and a dystonia-related deficit. This finding deserves additional attention in future studies.

2.4.2 Beta Frequency Findings

Synchronization of the beta frequency band is a prominent feature of network activity recorded from the PD motor system in primates, detectable in the MCx (Delaville et al. 2014; Saleh et al. 2010), BG (J. Dostrovsky and Bergman 2004; Jenkinson and Brown 2011; Weinberger et al. 2006; Weinberger et al. 2012), thalamus (Brazhnik et al. 2016; Malekmohammadi et al. 2015), cerebellum (Courtemanche et al. 2013), and spinal cord (Kozelj and Baker 2014). Beta oscillations are generated in cortico-thalamo-BG loops. *In-vivo* human recordings suggest beta oscillations are generated intrinsically within specific nuclei of the BG such as in the mutual innervation of the STN and GPe (Bergman and Deuschl 2002; Holgado et al. 2010). Work in primates suggests abnormal PD STN oscillations are driven by glutamatergic cortical inputs and reciprocal GABAergic inputs from GPe, generating and amplifying intrinsic oscillations in GP and STN. Beta frequency oscillatory parameters relate to movement parameters in a predictable, quantitative manner in some movement experiment paradigms in humans. Excessive beta oscillations are a feature of advanced PD, and can be related to the features of rigidity and bradykinesia experienced by sufferers of this condition. A proposed physiological role of BG beta frequency oscillations, therefore, is to suppress unwanted movement or maintain the status quo, in ways similar to theta frequency activity's function in error (Engel and Fries 2010; Herrojo Ruiz et al. 2014). In relation to the learning, memory, and reward encoding functions of the BG, dopamine levels recorded by microdialysis in rodent BG correlate to obtaining reward and appear to be independent of task features such as the effort required to gain reward or the probability of reward during a task. The excessive beta oscillations associated with the dopamine-depleted state of PD may therefore indicate that movement is overly suppressed in PD patients because the reward value of movement is not adequately signaled. Therefore, movement is inhibited because the reward value of movement is underestimated by the BG (or effort in relation to reward is over estimated) favoring no

movement. If this is the case, beta oscillations may still maintain “normal” physiological roles even in PD patients, with the excess oscillations resulting from reduced reward signaling. Our data potentially support this view since we did not find statistical differences in beta oscillations between correct and incorrect trials in PD patients in dominant or non-dominant GPi, despite observing a response to error in the theta frequency range. Equally, in the GPi of dystonic subjects, we did not observe statistical differences in beta frequency oscillations between correct and incorrect trials in dominant or non-dominant GPi despite our observations concerning high gamma. Analysis demonstrated that beta power was variable from trial-to-trial and from patient-to-patient. Since subjects were not restricted in terms of their motor response during this task, except by being restricted to using their dominant hand to touch the screen, movement metrics would vary from trial-to-trial in a subject, accounting for the absence of a consistent response in the task. Nonetheless, in 2 dystonic subjects we did observe a significant suppression of beta activity in dominant and non-dominant GPi (subjects 2 and 4) upon sensory feedback. This beta activity rebounded approximately 1 s afterwards to levels significantly greater than pre-feedback. This mirrors results identified in PD subjects performing a task where movement metrics were controlled and measured (Tan et al. 2014), suggesting that beta frequency oscillations, while exhibiting greater power in PD patients, may not necessarily reflect PD pathology but may yet reflect some aspect of physiological functioning in PD subjects. Therefore, studies of beta oscillations in PD subjects may potentially be applicable to non-PD subjects.

2.4.3 High Gamma Frequency Findings

We detected a phasic increase in high gamma oscillations in GPi upon receipt of feedback in dystonic subjects but not in PD subjects. This was more prominent on the right

side than the left. To our knowledge, this is the first description of high gamma oscillatory activity in the human GPi. High gamma oscillations, also known as very fast oscillations or "ripples", have been studied in the rodent hippocampus, human hippocampus, and human rhinal cortex (Ramadan et al. 2009). They are thought to be the result of axonal plexus activity amongst gap junction-connected axons of pyramidal cells in conjunction with interneuronal activity (Klausberger and Somogyi 2008; Traub et al. 2002). Sharp wave-ripple complexes, also similar in morphology to the high gamma activity that we demonstrate here, have been associated with long-term memory formation in the neocortex from transient hippocampal-based memory. This is also seen in the rodent hippocampus where long-term potentiation, a neurophysiological correlate of memory at the synaptic level, is associated with the generation of sharp wave-ripple complexes (C. J. Behrens et al. 2005).

High gamma oscillations have been detected in the nucleus accumbens and ventral striatum of human subjects undergoing DBS for depression during a motor task with feedback consisting of reward, neutral, or adverse visual stimuli dependent on motor performance, and during performance of motor actions that require enhanced cognitive control (Durschmid et al. 2013; Lega et al. 2011). Our findings echo these previous findings in that the nature of the feedback appeared to modify the temporal properties of the high gamma oscillation. In the nucleus accumbens, high gamma LFPs occurred at an earlier time in response to the receipt of positive sensory feedback as compared to negative feedback, and this activity was locked to the peaks of on-going alpha activity occurring during positive feedback and at the trough of alpha activity during negative feedback. We propose that the action-outcome information represented in the striatum in the work of Lega *et al.* may thus be not necessarily transmitted downstream but may influence activity in the GPi in the presence of normal nigro-striatal pathway function (Lega et al. 2011). The relative timing differences between high gamma oscillations in correct and incorrect trials further raises the possibility that high gamma LFPs

are a representation of axonal discharge via the direct and indirect pathways, respectively, but this is not verifiable at this time. This is supported by our observation that a high gamma burst in response to sensory feedback was entirely absent in PD subjects both on and off medication. This again suggests that such a signal relies upon intact nigro-striatal function and is compatible with the theory that such signals originate from the striatum. High gamma oscillations do, however, occur rapidly after the onset of auditory feedback before the peak of human nigro-striatal cell firing during the receipt of positive feedback, which would contradict this hypothesis (Zaghloul et al. 2009). Certainly, this deserves more study.

PD subjects were still able to pass the test albeit with significantly slower RTs (400 ms on average), which may suggest that the high gamma signal is either not a dopamine-dependent/reward signal or may be a pathological feature of dystonia but not PD. As LFP recordings from GPi of healthy human subjects are not available and the neuropathology of dystonia is not completely understood, it is impossible to distinguish between these possibilities. Although there is a severe degeneration of nigro-striatal dopaminergic neurons in PD patients, reward processing is still possible in PD patients as mesolimbic dopaminergic neurons are largely preserved. In some cases of PD patients given dopaminergic medications, the relative preservation of mesolimbic reward processing can lead to impulse control disorders with detrimental consequences for the sufferer and their family. Incorrect trials in the dominant GPi were also associated with a statistically robust low frequency theta response compared to correct trials (this was not seen in non-dominant GPi), which could indicate that sensory feedback indicating reward value may still be able to modify GPi output despite nigro-striatal pathway degeneration. Another possibility is that other neural mechanisms are able to compensate for BG neurodegeneration in this test leading to successful completion of the task at a slower rate.

2.4.4 Applicability of Dystonia Results to Normal Basal Ganglia Function

We propose that our dystonic subject group act as a stand-in for normal GPi function, as primary dystonia is not generally associated with dopamine-depletion, neurodegeneration, or cognitive decline. This suggestion, however, would require additional study as dystonic subjects have been shown to achieve a higher failure rate during IED tasks compared to healthy controls (dystonic 50 % failure rate vs. healthy control 5 % failure rate), suggesting that dystonia may be associated with attentional-executive deficits (Scott et al. 2003). In this study, 4 out of the 5 dystonic subjects did pass the IED test, although the group did have difficulty passing the extra-dimensional shift during rule 8 of the task. Difficulty with extra-dimensional shift changes have been reported in the PD population, which may suggest that BG function may be impaired to some extent in dystonic subjects as well. One should note, however, that Scott *et al.*'s study treated multiple forms of dystonia (including generalized, genetic, and focal) as one monolithic group. The comparison groups, meanwhile, were relatively small so it is possible the magnitude of the difference between the groups may be overestimated, and the findings may be accounted for by factors such as dystonia-associated pain or depression which could also have impaired subjects' performance. Other studies have not found significant deficits in dystonic subjects (Jahanshahi et al. 2003).

2.4.5 Laterality Differences

The data presented in this chapter suggest that low frequency activity-generating neural networks are more active in response to sensory feedback in the dominant hemisphere compared to the non-dominant hemisphere. In contrast, high gamma frequency-generating neural networks appear to be active in both dominant and non-dominant hemispheres. This could suggest that the non-dominant hemisphere's BG may play a role in sensory signaling or

memory formation during attentional set shifting, whereas the dominant hemisphere BG plays a role primarily in motor error detection networks, regardless of the handedness of the subject. Our data may thus give a clue to how BG function differs between dominant and non-dominant hemispheres, but due to our limitations in recruiting subjects we have insufficient data to analyze these findings in further detail. Dedicated studies comparing right and left-handed subjects would be required to investigate this further.

2.4.6 Limitations

IED is a complex task that comes with potential confounders that make interpreting results difficult. Different types of rule changes, variation in objects, and changes in stimulus parameters within rules add a wealth of variables. An additional confounder we should keep in mind is that, as we cannot be truly aware of how confident or surprised a subject is, we must make assumptions regarding subjects' view of rules. Unexpected outcomes may be associated with distinct responses from a given subject trial-by-trial, and that could confound the result if unexpected and expected outcomes of the same valence are pooled. While we do have better control over our human subjects than we do animals, we must confront the fact that as much as we would like, we cannot truly get inside of a subject's head. We must be content that, because the valence of a given outcome is known trial-to-trial, we can pool correct and incorrect trials together. This might offer an insight into how valence of the outcome is represented or processed on an electrophysiological level. Recordings from PD and dystonic subjects are rare because DBS electrode leads are not often externalized. Our small number of patients resulted in a low number of trials which prevented us from testing the effects of a larger variety of rule-changes. IED features 9 different rule types, and we were unable to probe the effect these more complicated changes had upon our subjects. We sought to mitigate these factors by

concentrating our analyses on the time window centered within seconds of feedback. We assumed that this period of time was the most relevant to the study's aim. By averaging all data to the onset of auditory feedback, we could attempt to avoid the variations of object presentation, decision making, and variations in movement to screen. Through these efforts, we were able to reduce confounding variables such as visual stimulus presentation, decision making, and movement initiation.

The PD surgical group are non-typical of PD in general since neuropsychological impairment, especially memory impairment, common in PD, is a contraindication to surgery, therefore our group may have more cognitive reserve that improves their performance relative to the average PD population. This view is supported by the observation in the general PD population that IED performance is impaired in PD, whereas our study subjects were able to perform these parts of the IED task. Conversely, we propose that our dystonia group is more likely to be representative of normal BG function since all 5 in our study had non-genetic focal dystonia and comparable neuropsychological results to the general population. Furthermore, dystonia is not associated with neurodegeneration or dopamine-depletion (except in the rare familial dopamine-depleted form of dystonia) at least in the BG. However, these conjectures would require further study and corroboration with animal work to fully elucidate.

2.4.7 Concluding Remarks

These results demonstrate that GPi (as a representative of BG function) in subjects with PD and dystonia responds selectively to the valency of feedback in a motor task – whether feedback was correct or incorrect. In PD subjects, this is most dramatic in the theta frequency band. We also found that sensory feedback was associated with phasic high gamma oscillations in dystonic subjects but not in PD subjects either on or off medication. Furthermore, dystonic subjects had differences in the timing of the onset of high gamma oscillations depending on the valency of their choice, which echoes a similar finding from the ventral striatum (Lega et al. 2011). These findings suggest that there is more than one mechanism that contributes to BG-dependent learning function. The BG acts as a driver of thalamo-cortical circuits in the healthy condition, and this behavior is exaggerated after the degeneration of nigro-striatal dopaminergic pathways. Movement error processing appears to remain more intact in PD subjects and this may be possible through mediation of the hyperdirect pathway's ability to bypass the striatum. The GPi of dystonic subjects, in contrast, may be a better driver than the PD GPi as action-outcome association information processed through or in conjunction with dopamine in the striatum is still represented in the GPi. This data suggests that both positive and negative outcome signals are present in the GPi, although the specific origin of these signals cannot be confidently determined without simultaneous recordings in multiple areas. In summary, our data offer a valuable electrophysiological comparison in GP responses, available in awake behaving humans by no other method, to sensory feedback during a cognitive task requiring a selective motor response. By using dystonic subjects, we could compare a dopamine-depleted neurodegenerative condition (PD) with a non-dopamine depleted non-neurodegenerative condition (dystonia), and thus gain insight into the cellular network activity consequences of PD neurodegeneration on cognition.

3. Executive Function in the Prefrontal Cortex of Humans

The dorsal anterior cingulate cortex (dACC) is proposed to facilitate learning by signaling valence resulting from decisions yielding unexpected outcomes. However, direct electrophysiological recordings from human dACC to validate this have not been previously performed. We used the unique opportunity offered by DBS surgery in the dACC of 3 human subjects to test the electrophysiological response of the dACC to a cognitive task that involved presentation of object pairs, a motor response, and audiovisual feedback to guide future object selection choices. dACC displayed distinctly lateralized 3 – 8 Hz ERP responses – left dACC signaled outcome valence while right dACC was involved in prediction formation. Multivariate analysis provided direct evidence that human dACC acts as a discriminator differentiating correct from incorrect action outcomes. Further findings suggested that dACC does not respond to other phases of action-outcome-feedback tasks which supports the idea of lateralized, functional specialization of areas within the ACC.

3.1 Introduction and Rationale

The ACC, located in the medial PFC, has been associated with a broad range of 'cognitive control' functions including salience (Seeley et al. 2007), conflict monitoring (Botvinick 2007), error detection (Hyman et al. 2013; K. Ito et al. 2013), and reward-based decision making (T. E. Behrens et al. 2007; Kolling et al. 2016; Walton et al. 2003). This has led to attempts to propose generic, computational models that unify ACC functions focused on the vital role ACC plays in learning. Models based on single-unit recording and LFP recordings in NHPs support the claim that neurons in the ACC signal predictive information about the outcomes of one's behavior that drive learning to optimize future behavior (Alexander and Brown 2011; T. E. Behrens et al. 2007; Shenhav et al. 2013; Silvetti et al. 2014). Neurons in the ACC encode the outcomes of decisions or actions (Cai and Padoa-Schioppa 2012; Procyk et al. 2016), particularly when such outcomes are unexpected (Hayden et al. 2011; Kennerley et al. 2011). Questions remain regarding ACC function. Are these functions performed by anatomically discrete subregions? Is ACC function lateralized across hemispheres? How does the ACC, especially in the human PFC, encode such processes? This last question requires electrophysiological data, which is extremely rare in humans.

We recorded LFPs from the dorsal ACC (dACC) bilaterally, in 3 habitually right-handed subjects undergoing DBS for chronic pain, allowing for the precise examination of whether prediction (before feedback) and prediction error signals (reactions post-feedback to differences between predicted and eventual outcome) are localized to the dACC. By recording bipolar mode LFP, we were able to precisely localize LFP to dACC, take recordings from within a few mm of the electrode, minimize volume conduction effects from without, and record simultaneously from both hemispheres of the dACC (Lempka and McIntyre 2013).

Participants performed the modified Wisconsin card-sorting cognitive test, IED, introduced in Chapter 2. Using this design, we searched for electrophysiological correlates of predictive activity at the time that pairs of stimuli were presented and outcome valence or other error-related activity at the time of outcome feedback in left and right hemisphere dACC.

3.2 Methods

3.2.1 Patient Group

The patient group is described in detail in Table 3.2. Three patients with chronic pain (ages at time of testing 36, 42, and 48 years) were studied. All 3 patients were habitually right-handed.

Patients gave informed written consent; the study was approved by the Oxfordshire Research Committee A using references 08/H0604/58 and 11/SC/0229. The study conformed to the Declaration of Helsinki.

Table 3.2 Participants' characteristics

Patient	Sex	Diagnosis	Age at surgery	Handedness
1	m	Chronic pain	48	Right
2	f	Chronic pain	36	Right
3	m	Chronic pain	52	Right

3.2.2 Electrode Implantation and Electrode Placement Confirmation

ACC targets were selected on preoperative MRI scans. Selected targets for ACC electrodes were 20 mm posterior to the frontal horns and 8‐10 mm lateral to the midline to target the dACC. The tip of the electrode was targeted to contact the corpus callosum such that as many contacts lay within the cingulate bundle as possible (Boccard et al. 2015b). Surgery, electrode placement, and electrode placement confirmation are as described in Chapter 2.

3.2.3 Magnetic Resonance Imaging Acquisition

Before DBS surgery, subjects underwent a T1- and T2-weighted MRI scan on a 1.5 Tesla magnet (Philips Achieva, Amsterdam, Netherlands). Diffusion-weighted data were acquired using a single-shot echo planar sequence. The scanning parameters used were 65 ms echo time, 9390 ms repetition time, a 176 x 176 reconstructed matrix, a voxel size of 1.8 $\times$ 1.8 $\times$ 2 mm, and slice thickness of 2 mm.

3.2.4 Intra- Extradimensional Set Shifting Task

Subjects performed an on-screen variation of the Wisconsin card sorting test the IED set shifting task as in Chapter 2. One chronic pain subject performed 1 IED task while the other 2 subjects each performed 4 tasks. The subject that performed 1 task passed on the first attempt. One subject passed the 1st and 2nd tasks and then failed on the 3rd and 4th attempts. The 3rd subject failed the 1st and 2nd task, passed the 3rd task, and failed the 4th.

3.2.5 Electrophysiology and Analysis

Differential recordings were made from adjacent circumferential 1.5 mm contacts on each deep brain macroelectrode. A bipolar configuration was utilized to limit the effects of volume conduction and limit the spatial resolution of recordings to a few mm of adjacent tissue (Lempka and McIntyre 2013). ACC DBS electrode locations were identified by postoperative image-fused MRI and CT scans. Signals were high pass filtered at 0.5 Hz, amplified 10,000X using isolated 1902 CED amplifiers and digitized using 1401 CED Mark II at a rate of 2.5 kHz, or recorded via a Porti system (Twente Medical Systems International, B.V., Netherlands) and recorded onto disc using Spike2 software (CED, Cambridge, UK). Raw data was notch filtered

at 50, 100, and 150 Hz as required to remove mains noise using Spike2 infinite impulse response Bessel filters, Q-value adjusted to avoid unwanted filtering of adjacent frequencies as much as possible.

Preprocessing and analysis of LFPs was performed offline using MATLAB software and EEGLab (Brunner et al. 2013; Delorme and Makeig 2004; Delorme et al. 2011). Spike2 data were imported into EEGLab in MATLAB. Raw data were resampled at 512 Hz. 5 s epochs beginning 2000 ms prior to the start of auditory feedback and continuing to +3000 ms post-feedback were extracted from both left and right electrode contacts and divided into correct and incorrect trials. Trials were divided into correct trials and incorrect trials, as well as trials that had "novel" stimuli and trials that had "familiar" stimuli, as explained in 2.2.4. Baseline prior to feedback (-2000 ms) was subtracted and then data were normalized by individual mean and sample standard deviation using MATLAB z-score commands to allow for comparison between different subjects. EEGLAB commands were used to generate ERP, power spectra, and ERSP.

3.2.6 Multivariate Local Field Potential Discriminant Analysis

A linear multivariate classifier was applied to LFP data locked to the time of decision outcome, using a sliding window approach. Only results from subject 1 and subject 2 were used, as subject 3 did not produce enough incorrect trials to reliably train the multivariate discriminant. Specifically, a projection of the multidimensional LFP signals was estimated, $\boldsymbol{x_i}$(t), where $i = [1 \cdots T]$ and T was the total number of trials, within a short time window that maximally discriminated between positive and negative outcome trials. Each time window had a width of N = 50 ms and the window center was shifted from -200 to 600 ms relative to outcome onset, in 10 ms increments. Logistic regression was used to learn the spatial

weighting, $\boldsymbol{w}(\tau)$, that achieved maximal discrimination between positive and negative outcomes, arriving at the one-dimensional projection $y_i(\tau)$, for each trial *i* and a given window τ:

$$y_i(\tau) = \frac{1}{N}\sum_{t=\tau-N/2}^{t=\tau+N/2} \boldsymbol{w}(\tau)^{\perp}\boldsymbol{x_i}(t) \qquad \text{(Equation 3.1)}$$

where $\perp$ is used to indicate a transpose operator (Parra et al. 2005). Note that the classifier was designed to map positive and negative discriminant component amplitudes (i.e. $y_i(\tau)$) to positive and negative outcomes, respectively. The performance of the discriminator for each time window was quantified using the area under a receiver operating characteristic curve, referred to as an A_z value, using a leave-one-out trial cross-validation procedure (Duda et al. 2001). To assess the significance of the discriminator, we used a bootstrapping technique where we performed the leave-one-out test after randomizing the trial labels. We repeated this randomization procedure 1,000 times to produce a probability distribution for A_z, and estimated the A_z leading to a significance level of $P < 0.01$.

To visualize the temporal profile of the resultant discriminating components, we applied the spatial weighting vectors, $\boldsymbol{w}(\tau)$ from the short time windows that led to significant discrimination performance between positive versus negative outcomes, to an extended time window (200 ms before until 600 ms after the outcome).

3.2.7 Statistical Analyses

EELAB non-parametric permutation statistics with FDR correction were used to compare data between trials and between study groups. The statistical process is as follows: the difference in mean values between the 2 groups or conditions is calculated to serve as the observed test statistic. Next, the data from the 2 compared groups was pooled and divided into 2 groups in every possible combination. The mean differences were calculated between the resampled groups. The set of the mean differences calculated when the data were resampled in this manner was the distribution of possible mean differences, supposing the null hypothesis was correct. If the observed test statistic lies out with the middle 95 % distribution of resampled mean differences, then the null hypothesis can be rejected at the 5 % level ($p < 0.05$). In this case, FDR correction was necessary due to the large number of comparisons inherent in comparing time-frequency plots.

3.3 Results

3.3.1 Electrode Localization and Diffusor Tensor Imaging

Three electrode contact pairs at different coordinates were available for use in recording (Figure 3.3.1). The central pair, C2-1, was chosen to orient recordings anatomically directly within the dACC. MRI diffusion tensor imaging (DTI) was performed to assess the orientation and integrity of white matter tracts between the electrode position and multiple regions of interest. This analysis was available for 2 of the 3 subjects (Figure 3.3.1C and 3.3.3D). For both subjects and both electrodes, the strongest connectivity was found to be the left hemisphere's supplementary motor area. A notable connectivity was also found to the right hemisphere's superior frontal gyrus and the superior middle frontal gyrus. These DTI observations were consistent with known human and NHP ACC anatomical connectivity with regions of the frontal cortex and motor areas and confirmed that electrode placement was bilaterally in the dorsal part of the ACC (Asemi et al. 2015; Koski and Paus 2000; Neubert et al. 2015).

3.3.2 Trial-By-Trial Anterior Cingulate Cortex Event-Related Potentials

We hypothesized that, supposing the dACC is involved in executive function both before and after feedback, we would detect patterns of frequency changes related to novel versus familiar objects (pre-feedback) and expected versus unexpected outcomes (post-feedback), so time-frequency analysis was performed. A total of 797 trials were available for analysis, and subject data were pooled for respective hemispheres, stimulus type, and feedback variance‐whether the subject made a correct or incorrect choice. To identify temporally

A

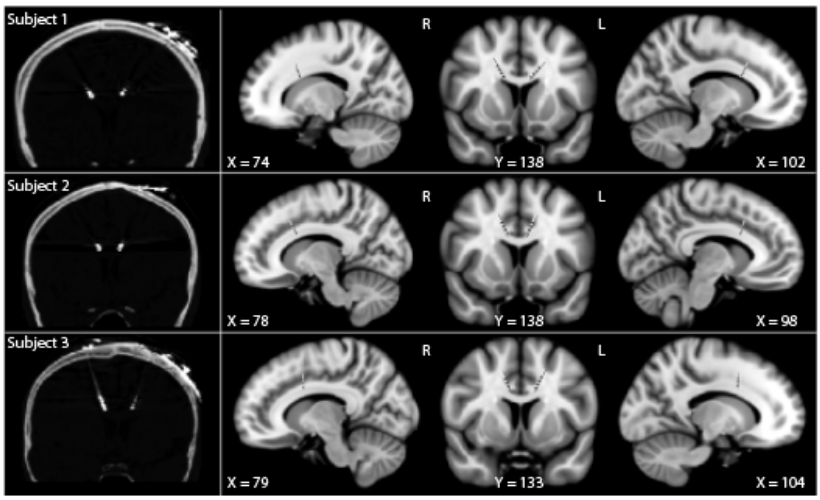

B

AC-PC Coordinates

		Left			Right		
		X	Y	Z	X	Y	Z
Subject 1	C3	105	140	102	72	140	104
	C2	103	139	100	73	138	101
	C1	101	138	97	75	137	98
	C0	99	137	95	77	136	95
Subject 2	C3	100	140	107	76	141	107
	C2	99	139	104	77	140	104
	C1	97	138	101	79	138	101
	C0	96	137	98	80	137	98
Subject 3	C3	106	133	113	77	133	111
	C2	105	133	110	78	133	108
	C1	104	133	107	79	133	105
	C0	103	134	104	80	133	102

MNI Space 1mm

		Left			Right		
		X	Y	Z	X	Y	Z
Subject 1	C3	-15	14	30	18	14	32
	C2	-13	13	28	17	12	29
	C1	-11	12	25	15	11	26
	C0	-9	11	23	13	10	23
Subject 2	C3	-10	14	35	14	15	35
	C2	-9	13	32	13	14	32
	C1	-7	12	29	11	12	29
	C0	-6	11	26	10	11	26
Subject 3	C3	-16	7	41	13	7	39
	C2	-15	7	38	12	7	36
	C1	-14	7	35	11	7	33
	C0	-13	8	32	10	7	30

C

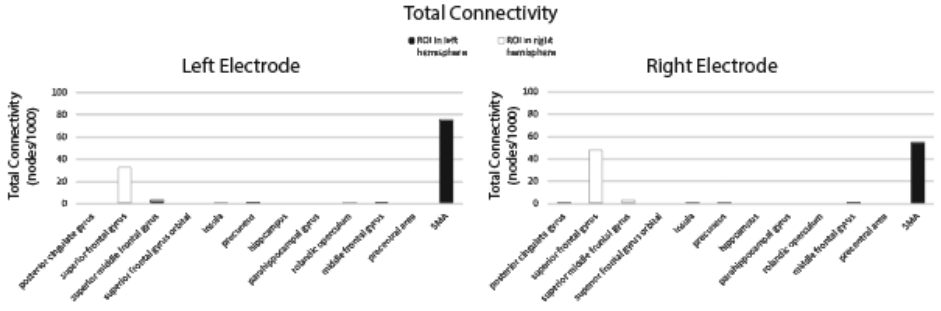

D

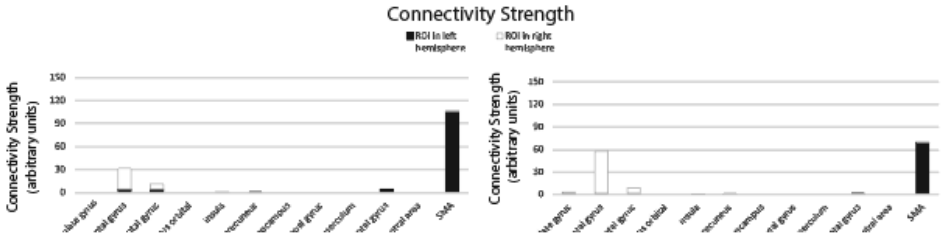

Figure 3.3.1 Subject electrode placement (3.3.1A-3.3.1B) and diffusor tensor imaging data (3.3.1C - 3.3.1D)
A. Post-operative CT-scans showing subjects' electrode placements. Electrodes registered and displayed in the common MNI space.
B. Electrode contacts in AC-PC coordinates and MNI space. Electrode order from most dorsal, C3, to most ventral, C0.
C. Diffusor Tensor Imaging (DTI)-computed total connectivity derived from the number of voxels with non-zero connectivity with several regions of interest (ROI) available from 2 of 3 subjects. DTI connectivity is from the middle electrode contact pair C2-C1. Both left and right electrodes displayed connectivity to right superior frontal gyrus and left supplementary motor areas.
D. DTI connectivity strength as mean intensity per non-zero voxels. Supporting total connectivity results, highest connectivity strength was with right superior frontal gyrus and left supplementary motor areas.

distinct neuronal population components associated with the value of outcome, we used single-trial multivariate discriminant analysis on LFP signals locked to the delivery of feedback to extract information on the valence and magnitude of the prediction error generated by the dACC (Lempka and McIntyre 2013).

LFPs from left and right dACC were averaged at time of stimulus presentation across all trials incorporating visual object presentation, motor action, and feedback phases (Figure 3.3.2). The most prominent feature of the averaged response, consistent across trials and subjects, was that feedback was associated with an ERP beginning 50 ms after the start of feedback in the left hemisphere with a mean peak magnitude of 0.8 μV, more prominently in the left hemisphere than the right hemisphere with a peak of 0.3 μV ($p < 0.05$; Figure 3.3.2.A).

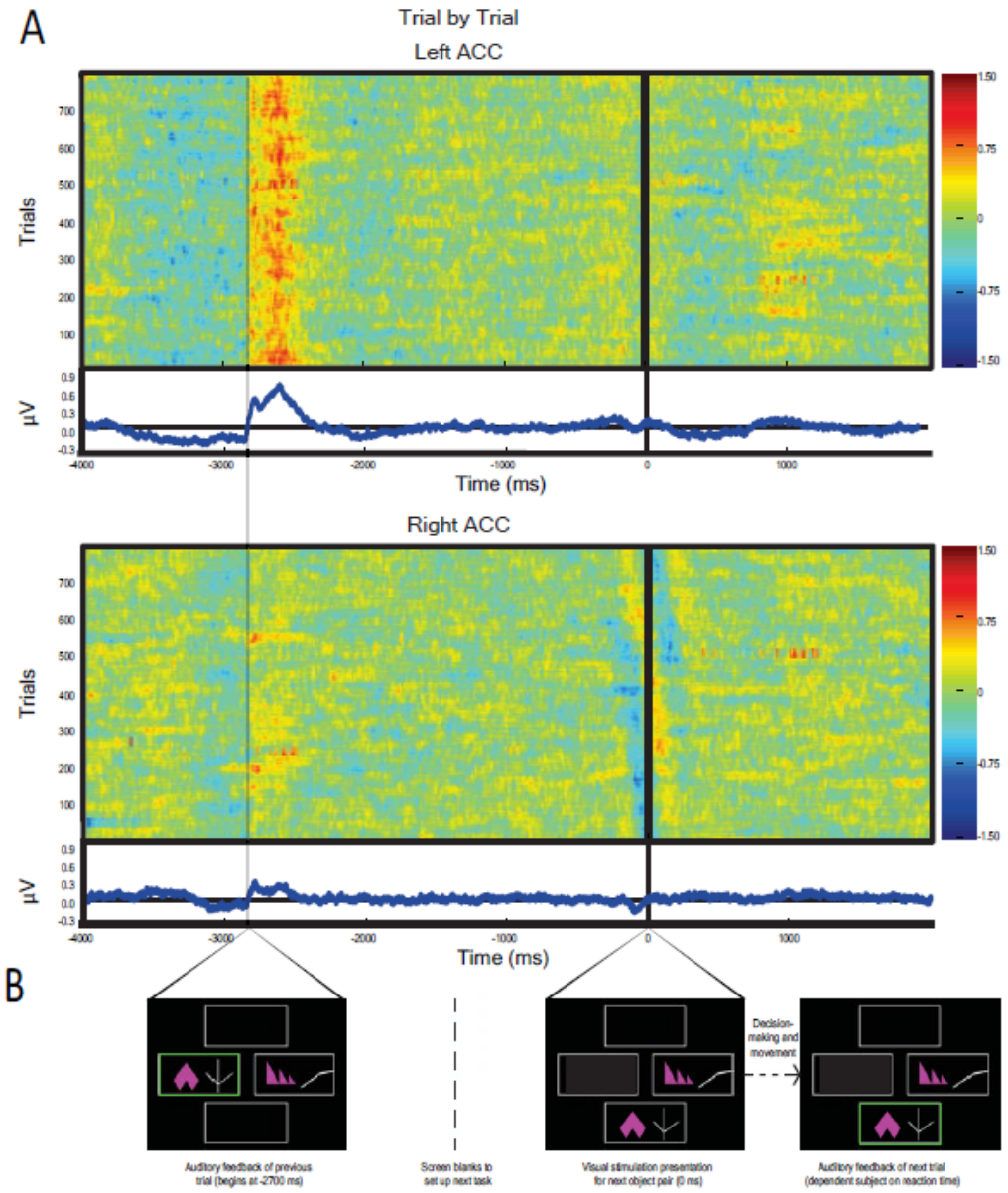

Figure 3.3.2 Average dACC bipolar mode local field potential (LFP) response in 3 subjects performing IED task, trial-by-trial responses

A. Trial-by-trial LFP responses (y axis, n = 798 trials, 3 subjects) from left and right hemisphere dACC (regardless of correct or incorrect result) versus time representing the decision making period composed of: selection of object (-4000 to -2700 ms); receipt of feedback (-2700 to -2100 ms); clearing of the screen (-1500 to -200 ms); and object pair presentation of the subsequent trial (0 ms onwards). Color represents magnitude of the LFP (red = higher voltage) such that individual pixels represent the magnitude of the LFP at a point in time in a trial. The trials were locked to stimulus presentation (0 ms). The time delay between start of feedback of the preceding trial and presentation of visual object pair in the next trial was constant (2700 ms). Responses were normalized (mean/standard deviation) but not filtered. Blue line graphs represent average of individual trial responses with Y-axis representing normalized voltage and X-axis representing time. The most notable result is the evidence of a left dACC ERP response to feedback at approximately -2700 ms with a magnitude of 0.8 μV. A lesser, but still significant ($p < 0.05$), response also appeared in right dACC at this time with a magnitude of 0.3 μV. There was no apparent response to visual object presentation (0 ms) nor to movement (prior to -2700 ms).

B. Sample IED images aligned with events from Figure 3.3.2A.

3.3.3 Multivariate Analysis Findings

We analyzed this post-feedback ERP in more detail by running a multivariate discriminant analysis on the broadband signal to integrate information across DBS electrodes and generate an aggregate discriminator channel that best dichotomized outcomes into positive (correct) and negative (incorrect) outcomes (Fouragnan et al. 2015). Discrimination performance increased in the range 200 - 400 ms following the outcome, with two distinct temporal components peaking roughly at 200 ms (early) and 350 ms (late) – corresponding to 6.6 Hz or one theta frequency oscillation (3 – 8 Hz) period apart (Figure 3.3.3.A and 3.3.3.B). Using a univariate discrimination instead – by considering individual LFP channels in isolation – was consistently less reliable, reinforcing the notion that the relevant neural representations are highly distributed within the dACC. Similarly, by comparing dACC subregions through examining spatially separated electrode contacts, the spatial weights discriminating outcome valence ($\boldsymbol{w}$ in Eq. 3.1) were only moderately correlated between the 2 components (Figure 3.3.3A and 3.3.3B), suggesting that different sub-groups of neurons within the dACC might be responsible for the early and late discriminating activity. Next, we computed the temporal profiles of the early (Figure 3.3.3C and 3.3.3D) and late (Figure 3.3.3E and 3.3.3F) components ($\boldsymbol{y}$ in Eq. 3.1) for each participant by processing the outcome-locked data through the spatial generators (weights) estimated at the peak times of the 2 components. These temporal profiles were highly consistent across the participants and revealed that both the early and late outcome valence components appear to be modulated primarily by negative outcomes and the early component appears to represent a more transient event compared to the late component, which exhibited a broader response profile.

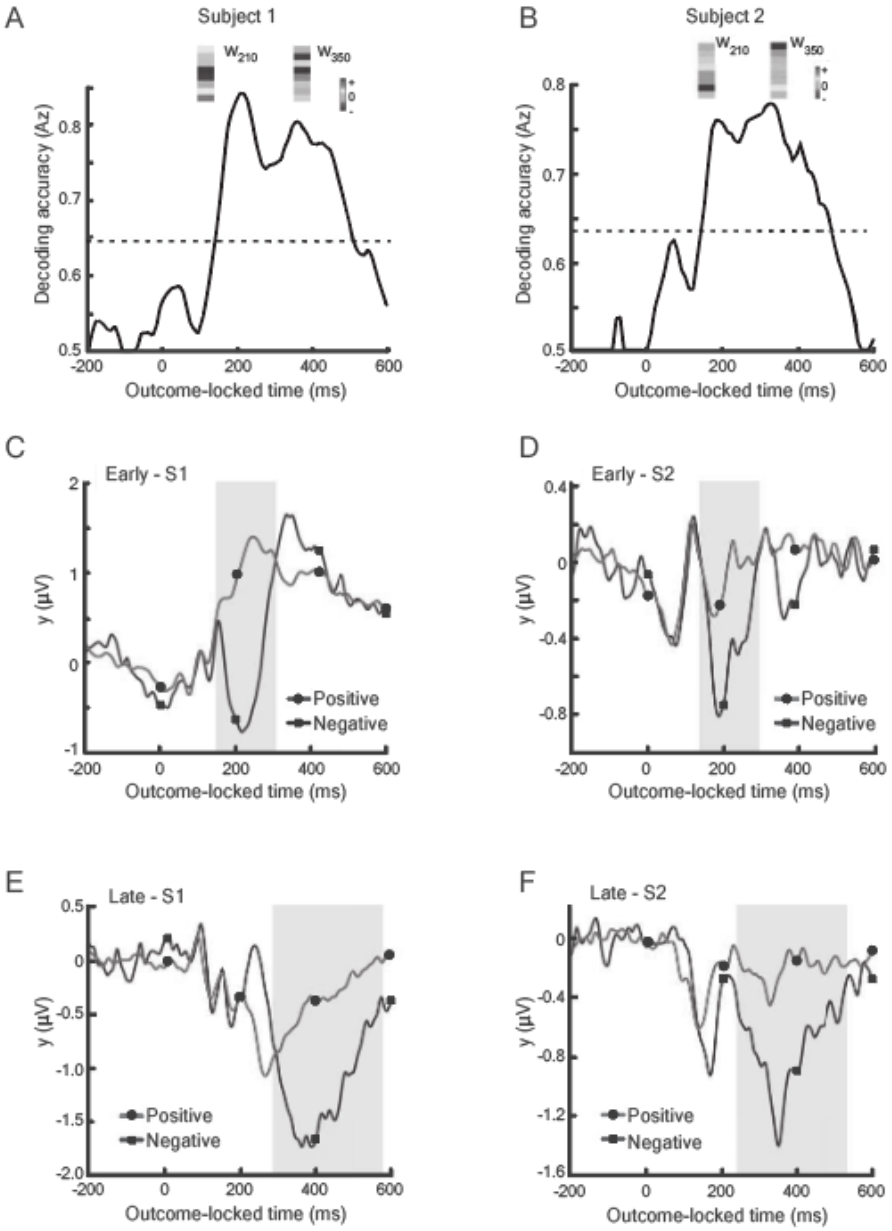

Figure 3.3.3 dACC discriminants positive versus negative feedback

A. and B. Decoding performance (Az) during outcome valence (positive-vs-negative outcome) discrimination of feedback-locked monopolar LFP data for subject 1 (A) and subject 2 (B). Subject 3 did not produce enough incorrect trials to reliably train the multivariate discriminant. The dashed line represents the subject-specific Az value leading to a significance level of P = 0.01, estimated using a bootstrap test. Spatial weights (w) of subject-specific discriminating (early and late) components are shown over the relevant peak component times. These weights represent the relative contribution of each LFP electrode to the overall discrimination performance (the sign of the weights is arbitrary and depends on the polarity of the corresponding electrode signals).

C. and D. Temporal profile of the early discriminating component activity (y(early)) averaged over trials (for the participants shown in A and B, respectively) for each of the positive (dark line with squares) and negative (light lines with circles) outcomes, obtained by applying the subject-specific spatial weights estimated at the time of maximum discrimination (see timing of w's shown in A and B) over an extended time window spanning the delivery of feedback (-200 - 600 ms post-feedback). The grayshaded area is used to highlight the range over which the difference between the two outcome types is more prominent. E. and F. The temporal profile of the late discriminating component activity (y(late)) for each of the positive and negative outcomes. Same convention as in C and D.

3.3.4 Event-Related Spectral Perturbation Findings

Given the prominence of the outcome-related activity in the dACC, we analyzed the LFP response to feedback in more detail using ERSP analysis. We compared trials with correct predictions and incorrect predictions without regard to the underlying trial rule (Figure 3.3.4A and 3.3.4B). The most prominent feature of the ERSP was that incorrect prediction was associated with a significantly greater response in the theta frequency band (3 - 8 Hz) than correct prediction in the left hemisphere (bootstrapping with FDR, $p < 0.05$). We found no difference in outcome-related theta frequency activity between correct and incorrect trials in the right dACC ($p > 0.05$) (Figure 3.3.4C). In contrast, during stimulus presentation, there were no significant differences between ERSP during presentation of novel stimuli and familiar stimuli in the left dACC, but the right dACC displayed significantly greater ERSP to novel stimuli than to familiar stimuli in the theta frequency band (Figure 3.3.4D – 3.3.4F).

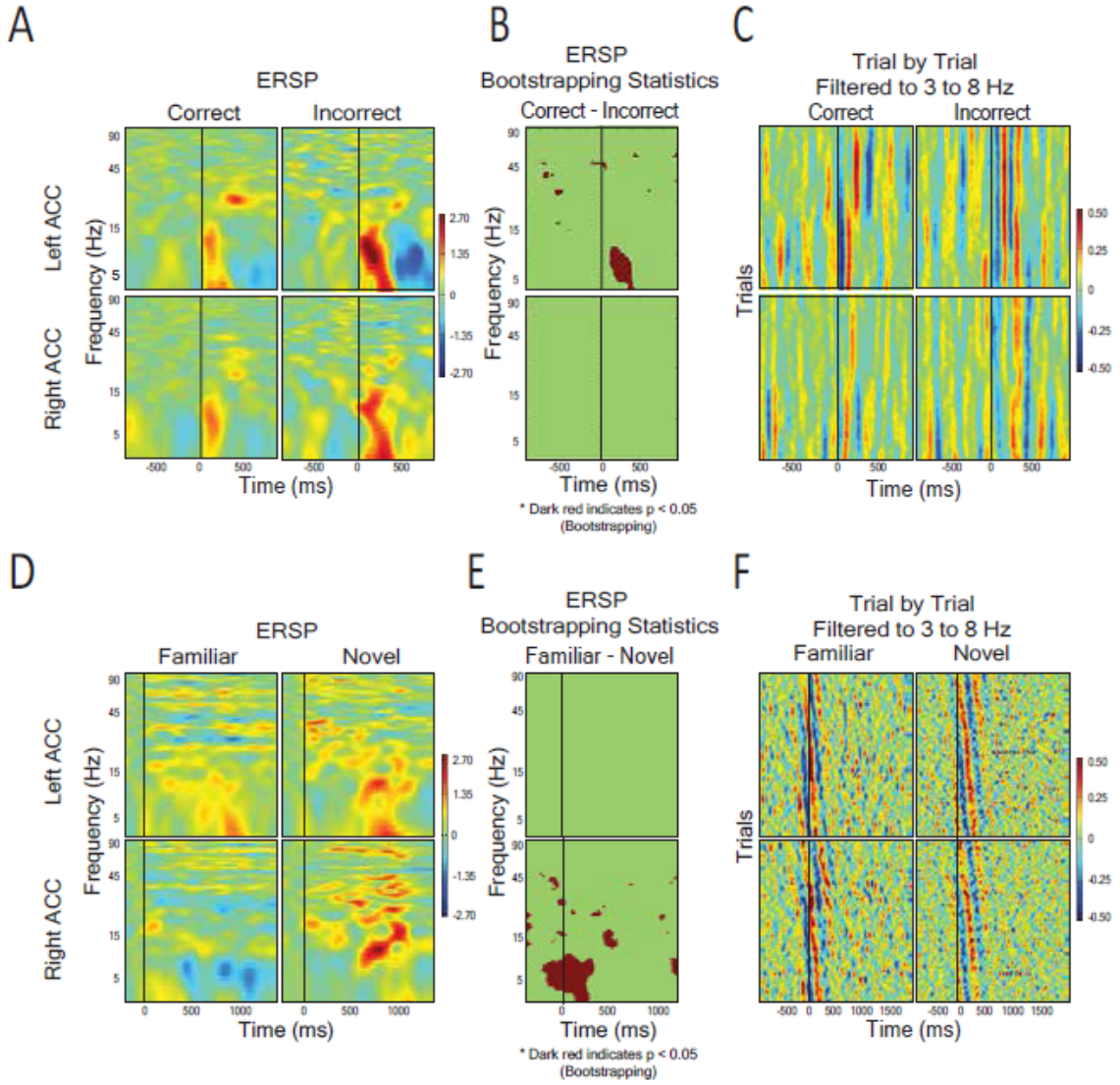

Figure 3.3.4 Local field potential (LFP) response to feedback (3.3.4A-3.3.4C) and visual object presentation (3.3.4D-3.3.4F).

A. 571 correct trials vs 227 incorrect trials. Graph shows event related spectral perturbance (ERSP) using EEGlab morlet wavelet-based analysis. Start of feedback = 0 ms and Y axis = log-based frequency (3 - 100 Hz).

B. Bootstrapping ($p < 0.05$) statistical comparison of difference in ERSP between correct and incorrect, showing frequency and time points of statistical significance.

C. Trial by trial LFP responses from left and right dACC during correct trials (n = 571) and incorrect trials (n = 227) filtered to theta frequency (3 - 8 Hz). The trials were averaged to receipt of feedback (0 ms). Color represents magnitude of the LFP (red = higher voltage) such that individual pixels represent the magnitude of the LFP at a point in time in a trial.

D. ERSP from left and right dACC in response to familiar stimulus pairs (i.e. stimulus of a sequence of 6 correct responses, n = 66) and novel stimulus pairs (i.e. first trials of 2 new object pairs, n = 33). Stimulus onset = 0 ms and Y-Axis as in 4A and 4B. We found a significantly greater theta frequency response of right dACC to novel stimuli but no significant differences in left dACC.

E. Bootstrapping ($p < 0.05$) statistical comparison of difference in ERSP between familiar and novel stimuli presentation.

F. Trial by trial data for visual object presentation filtered to theta frequency.

3.4 Discussion

3.4.1 Attentional Set Shifting

Neurodegeneration in the nigro-striatal dopamine system is a primary neuropathological feature of PD. While a consensus regarding the relationship between nigro-striatal pathologies and PD motor symptomology has been reached, PD cognitive symptomology is not as well understood (Kehagia et al. 2010). A possible hypothesis is that the cognitive deficits observed in PD arise from a disruption of PFC-striatal circuits arising from dysfunction of the dopamine system (Cools 2006; Emre 2003; Kehagia et al. 2010). This hypothesis is supported by several lines of evidence. Executive function deficits have been shown to dominate the cognitive symptomology of both PD subjects and subjects with PFC damage (Kehagia et al. 2010; Sawada et al. 2012). These deficits, including attentional set shifting ability, have been shown to be rescued by administration of L-DOPA medication (Au et al. 2012; Fera et al. 2007). In the previous chapter, we explored the effect of variations of the integrity of the dopamine system on the neurophysiology of the BG. Dystonic subjects represented normal dopamine levels while PD subjects represented dopamine dysfunction. Here, we explored executive function electrophysiology in the PFC of subjects with “normal” dopamine system function. While dopamine has been shown to play a role in chronic pain, these subjects should still have “normal” physiological dopamine levels in their BG and PFC, and can act as representative of “normal” executive function (Kim et al. 2015).

3.4.2 Outcome Valence Findings

Considerable evidence from neurophysiological recordings in NHPs support the claim that the dACC signals outcome valence post decision (Amiez et al. 2005; Kennerley et al. 2011; Sallet et al. 2007). Neuroimaging studies in humans support this but have failed to localize these signals to either the ACC or to the adjacent superior frontal gyrus (Yeung et al. 2004). Our results agree with recent accounts that the dACC plays a crucial role in cognition. Our data provide strong support that the human dACC signals both prediction confidence and prediction errors, and that these functions suggest a degree of lateralization across hemispheres in the dACC response to outcomes – right dACC is involved in the initial formation of predictions while left dACC does not signal coding or prediction error per se, but a fundamental dynamic signature of the rule-updating process as suggested by the late components in Figure 3.3.3, agreeing with functional MRI (fMRI) work by O'Reilly *et al.* showing that dACC signals update future behavior (O'Reilly et al. 2013). The timing and overall response profile of these components were generally consistent with those reported recently in human electroencephalography studies using a similar reward-learning task (Fouragnan et al. 2015). In those studies, the early component was shown to represent a quick evaluation of the outcome along a good/bad axis, whereas the later component was more directly involved in updating/learning stimulus-reward associations. That the early and late components are temporally separated by a single theta oscillation and are in reaction to negative outcome valency is reflected in Figure 3.3.4.C, where two theta band peaks were observed following incorrect feedback in the left dACC.

3.4.3 Laterality Findings

Functional subdivisions of ACC have been proposed before, with the evidence of inter-subject variability allowing for additional discrepancies (Lutcke and Frahm 2008; Polli et al. 2005; Taylor et al. 2006). While lateralization is not often reported in the majority of PFC studies, some groups have observed cingulate executive function processing specialization in either left or right hemisphere (Garavan et al. 1999; Garavan et al. 2003; Konishi et al. 1998; Menon et al. 2001; Rubia et al. 2001; Taylor et al. 2006). Our results are in agreement with these previous studies that investigated hemispheric lateralization of executive function in the ACC. We were able to show that individual, separate components could be observed following correct feedback in the left hemisphere dACC. This may indicate that both early and late components would be expected to be different between the 2 hemispheres only if one compared a correct guess at a familiar set of objects versus an incorrect guess at a novel set of objects. The presence of theta and high delta frequency activity in the left and right hemisphere dACC during the different phases of the task and theta's perceived involvement in a multitude of cognitive processes including decision making, outcome valence, reaction to novelty, and recalculation of predictions in medial frontal regions lend further credence to this theory (Cavanagh and Frank 2014; Jensen and Tesche 2002; Klimesch 1999; Lindsen et al. 2010; Womelsdorf et al. 2010).

Unfortunately, we can only make limited statements regarding hemisphere dominance in this study as we had no left hand dominant subjects.

3.4.4 Concluding Remarks

Our findings are relevant to evaluating competing schools of thought regarding dACC function. Experimental results put us squarely in the camp of Kolling et al. (Kolling et al. 2016), wherein the dACC is thought to play a leading role in the regulation of behavioral adaptation and persistence. Furthermore, we do not observe variation of dACC signal strength as suggested by the work of Shenhav et al. (Shenhav et al. 2016). The evidence of laterality in dACC function also indicates that executive function may be more understandable through functional specialization of cortical areas. Our laterality findings are further established through the inclusion of post-operative CT and diffusion tensor imaging analyses that confirm our electrode placement in the dACC and connectivity uniformity across hemispheres. Essentially, we offer clarifying evidence of lateralized decision-making in line with foraging theories in a fascinating cortical region supporting cognitive functions as varied as executive control, reward, learning and memory, and attention.

To our knowledge, this study represents the first bilateral dACC electrode recording study from awake humans performing a cognitive task with sensory cue, motor action, and sensory feedback components. Additionally, while there is precedence of discrete ACC lateralization of function with respect to verbal and figural fluency, the present study presents the first evidence of ACC lateralization during executive function (Geisseler et al. 2016).

4. The Electrophysiological Relationship between the Anterior Cingulate Cortex and the Basal Ganglia Thalamocortical Circuit in the Normal and Parkinsonian Brain during Movement in Rats

Dopamine loss in PD is thought to result in the increased transmission of oscillatory activity throughout the BG thalamocortical circuit. The ACC is connected with the output of the BG by way of the VM thalamus and provides input to the BG through the striatum and through the hyperdirect pathway to the STN. However, little is known about ACC activity under parkinsonian conditions. This chapter investigates the impact of dopamine cell lesion-induced changes in BG output on activity in the ACC through an examination of ACC LFP and spike timing with reference to VM and STN LFP and spiking activity in the 6-OHDA dopamine-lesioned, hemiparkinsonian rat.

4.1 Introduction and Rationale

The work of Ungerstedt *et al.* in 1968 on rats with unilateral lesions of the SNpc through the infusion of the neurotoxin 6-hydroxydopamine (6-OHDA) cemented what is known as the hemiparkinsonian rat as a valuable animal model for investigating the effects of dopamine loss on the transmission of oscillatory activity through the BG thalamocortical circuit (Ungerstedt 1968). Rats injected with 6-OHDA into the medial forebrain bundle (MFB) develop many of the hallmark motor symptoms of PD patients, including impaired function of the limb contralateral to the lesion accompanied by difficulties with gait resulting in rotation, which can be attenuated through standard dopaminergic drugs (Blandini et al. 2007; Da Cunha et al. 2008; Gerlach and Riederer 1996; Schwarting and Huston 1996; Yuan et al. 2005). Electrophysiologically, dopamine-lesioned rats also have some resemblance to PD humans (Figure 4.1B). By 1 week post-6-OHDA injection, rats develop increased oscillatory LFP activity in the high beta (25 – 40 Hz) range throughout the BG of the lesioned hemisphere during treadmill walking and this activity is coherent between areas (Avila et al. 2010; Brazhnik et al. 2012; Brazhnik et al. 2014; Brazhnik et al. 2016; Delaville et al. 2014; Delaville et al. 2015). This abnormal oscillatory behavior, like motor symptoms, are improved with dopaminergic drugs and modulate according to motor activity. This model provides the unique opportunity to explore the mechanisms through which brain circuits become recruited into a sustained, excessively synchronized and oscillatory state.

The oscillatory activity that is observed throughout the BG thalamocortical circuit following dopamine cell loss has not been previously demonstrated to also be transmitted to the ACC. However, evidence of connections from the output of the BG to the ACC through the VM thalamus in rats suggests that this indirect transmission of oscillatory activity is

theoretically possible. Excitatory glutamatergic efferents from the VM thalamus project widely to the outer layer of the cortex (Herkenham 1979; Kuramoto et al. 2015). The VM thalamus, through these projections, has also previously been shown to transmit Parkinsonian beta oscillatory activity to the MCx in the hemiparkinsonian rat, setting precedence for VM thalamus to cortical transmission (Brazhnik et al. 2016). It was hypothesized that this excitatory oscillatory input from the VM thalamus may thus shape oscillatory activity in the ACC in PD and potentially impact ACC function. While previous work by Delaville *et al*. has shown that other regions of the rat PFC (the PLC and ILC) do not exhibit excessively synchronized high beta activity in the hemiparkinsonian rat (Figure 4.1B), these regions are not believed to be strongly innervated by the VM thalamus, and thus may behave in a different manner than the ACC (Delaville et al. 2015).

The aim of the study presented in this chapter was to investigate whether the loss of dopamine in the parkinsonian state affects the relationship between neuronal activity in the STN, VM, and ACC in rats after 6-OHDA dopamine cell lesions. Effects of dopamine cell lesion on spectral coherence and spike timing relationships between the ACC and VM, and between the ACC and STN were assessed by simultaneously recording LFP spectral activity and spike trains in the ACC, VM, and STN in non-lesioned, intact rats and in the lesioned hemisphere of hemiparkinsonian rats 7, 14, and 21 days after a unilateral injection of 6-OHDA into the MFB.

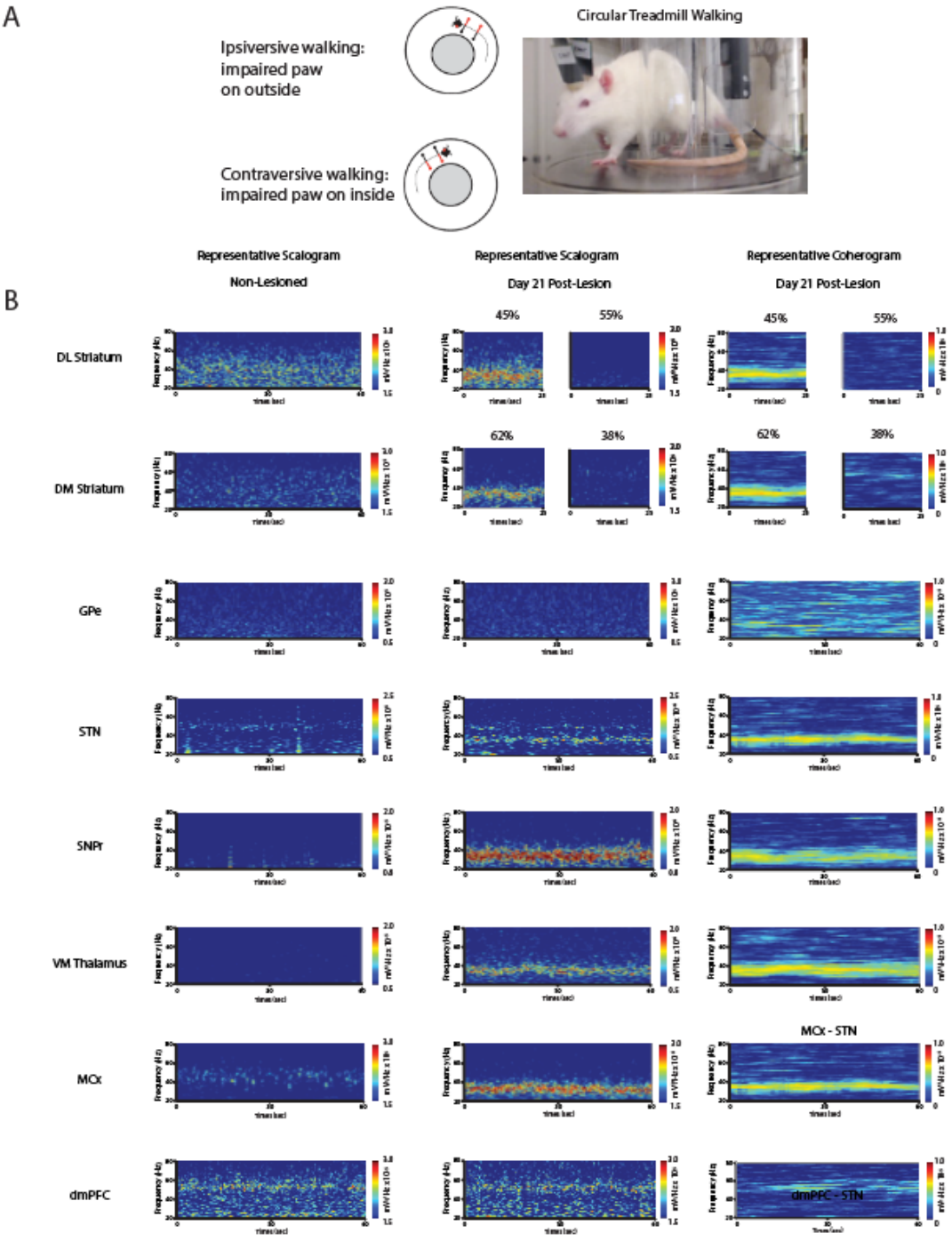

Figure 4.1 Previous findings in the hemiparkinsonian rat.

A. Image of a chronically implanted, hemiparkinsonian rat performing continuous treadmill walking in the ipsiversive direction.

B. Previous electrophysiological recordings from the hemiparkinsonian rat reveal the development of excessively synchronized oscillatory activity in the high beta band by 21 days post-lesion (4.1B, Middle), as compared to non-lesioned rats (4.1B, left) in approximately half of the DL and DM striatum, in the STN, SNpr, VM thalamus, and MCx. These regions also display high coherence in this frequency range (4.1B, Left) after 6-OHDA lesion. The GPe, dmPFC (ILC and PLC), and half of recorded sites in the DL and DM striatum do not develop this oscillatory band. Adapted from Avila et al., Brazhnik et al., and Delaville et al., (Avila et al., 2010; Brazhnik et al., 2012; Brazhnik et al., 2016; Delaville et al., 2015).

4.2 Methods

All experiments were conducted in accordance with the *NIH Guide for Care and Use of Laboratory Animals* and were approved by the NINDS Animal Care and Use Committee. Every effort was made to minimize the number of animals used and their discomfort.

4.2.1 Subjects and Behavioral Training

Male Long Evans rats (Taconic Farms, Rockville, MD, USA) weighing 275 - 325 g were housed with *ad libitum* access to rat chow and water in environmentally controlled vivarium conditions. The vivarium had a reversed 12 h light/ 12 h dark cycle, with lights turning on at 18:00 h. Starting a week before surgery, rats were handled daily and trained to walk on a 19 cm diameter circular rotating treadmill custom-built by the NIMH Section on Instrumentation (NIH) equipped with a paddle which could be lowered across the treadmill track to encourage continuous walking (Avila et al. 2010). Rats were trained in 5 - 7 daily sessions during which rats were encouraged to walk in the counter-clockwise direction (ipsiversive to their future dopamine-lesioned hemisphere) for 6 - 8 epochs of 3 - 5 min alternating with 2 min periods of treadmill-off “rest” (Figure 4.1A). This treadmill walking task involves both motor (locomotion) and cognitive (attention) processes. The treadmill walking task also had an audio component as explained in Chapter 5.2.1. At the end of a week of training, rats were capable of walking steadily on the treadmill at a speed of 9 RPM (approximately 0.325 km/hr) with minimum rearing or turning. After unilateral dopamine cell lesion, hemiparkinsonian rats could walk reasonably well on the circular treadmill when oriented in the direction ipsiversive to the 6-OHDA-lesioned hemisphere with their affected paws on the outside of the circular treadmill (counterclockwise). Rats had difficulty walking

consistently in the direction contraversive to the lesioned hemisphere with their affected paws on the inside of the circular treadmill (clockwise). This difficulty was averted by training rats to walk in the ipsiversive direction and only performing recordings in this direction.

4.2.2 Surgical Procedures

Male Long Evans rats (Taconic Farms, Rockville, MD, USA) weighing 300-325 g at the time of surgery were anesthetized with ketamine (70 mg/kg, intraperitoneally (i.p.)) and medetomidine (50 mg/kg, i.p.) and placed in a stereotaxic apparatus (David Kopf Instruments) with their heads restrained with atraumatic ear bars and the incisor bar at -3.5 mm. The incision area was shaved and cleaned with betadine and ethanol swabs. Ocular lubricant was applied to the eyes to prevent corneal drying during surgery. Small supplementary doses of ketamine and medetomidine were administered during surgery as needed to maintain anesthesia.

The post-operative diet of lesioned rats was supplemented with fruit and enriched gelatin to maintain weight.

4.2.3 Unilateral Nigrostriatal Pathway Lesions

Before the intracerebral injection of 6-OHDA (Sigma-Aldrich) neurotoxin into the left MFB, desmethylimipramine HCl (30 mg/kg, i.p.) was administered in order to protect noradrenergic neurons. A hole was drilled into the skull at 4.4 mm anterior to the lambdoid suture and 1.2 mm lateral to the sagittal suture. Six micrograms of 6-OHDA HBr in 3 µL of 0.9 % saline with 0.01 % ascorbic acid were infused at a rate of 1 µL/min over 3 min via a 27-gauge stainless steel cannula powered by a syringe pump (Harvard Apparatus) into the MFB, 8.3 mm ventral to the skull surface. The cannula was left at the target site for a period of 3 min

after the completion of infusion, raised 0.1 mm, and then left for a further 1 min to prevent excessive diffusion of the neurotoxin. Seven days after surgery, rats were screened for lesion efficacy by step testing (Olsson et al. 1995). In brief, rats were held about the waist with their hindlimbs and one forelimb elevated above a table. Rats were moved at a steady state 1 m laterally along the table, with one paw able to take steps. During this movement, the number of steps taken by the paw contralateral or ipsilateral relative to the injected hemisphere were counted over the distance. A ratio of steps taken by the contralateral limb to the number of steps taken by the ipsilateral limb below 5 % has previously been shown to correlate with 99 % loss of dopamine in the striatum ipsilateral to the lesioned hemisphere (Parr-Brownlie et al. 2007). Rats that demonstrated a strong lesion effect in behavior further confirmed histological monitoring of lesion strength and were used for electrophysiology. The extent of dopamine cell degeneration was verified postmortem through immunohistochemical staining for TH (see section 4.2.9).

4.2.4 Electrode Placement

A total of 21 rats (12 rats with ACC and VM electrodes, and 9 rats with ACC and STN electrodes) received 6-OHDA lesions in the same hemisphere. A second group of 9 rats (4 rats with ACC and VM electrodes, and 5 rats with ACC and STN electrodes) acted as controls and was unilaterally implanted with electrodes in the ACC, STN, and VM and received a saline injection into the MFB.

During surgery, holes were drilled into the skull for electrode placement in the ACC (anterior +3 mm from the bregma, lateral +0.8 mm from the sagittal suture, and ventral 2 mm from the skull surface), VM (posterior 2.6 mm from bregma, lateral +1.4 mm from the sagittal suture, and ventral -7.1 mm from the skull surface), and STN (anterior 5.4 mm from the

lambdoid suture, lateral +2.5 mm from the sagittal suture, and -7.8 - 8.0 mm from the skull surface). Electrode bundles were implanted in the above target regions and secured to the skull surface with screws and dental cement. Each bundle consisted of 8 stainless steel, 50 µm Teflon-insulated microwires plus a local reference wire with no insulation for 1 mm on the recording tip. Electrode bundles had diameters of approximately 350 µm. Ground wires for each set of electrodes were wrapped around an earth screw drilled into the skull above the cerebellum. One group of rats (n = 5) was not lesioned during surgery and was implanted with a guide cannula (26-gauge; Plastics One) above the MFB in the left hemisphere for later infusion of 6-OHDA. For rats with cannulas, stylets were inserted to keep debris from entering. After the completion of surgical procedures, atipamezole (0.5 mg/kg, s.c.) was administered to reverse anesthesia. Triple antibiotic ointment (bacitracin zinc, neomycin sulfate, and polymyxin B sulfate; Perrigo®, Allegan, MI) and lidocaine hydrochloride 2 % local anesthetic jelly (Actavis Pharma, Inc., Parsippany, NJ) were applied to the surgical site. Ketofluids were given subcutaneously to aid in recovery in the post-operative period. Recordings began after recovery of the animals, 1 week post-surgery.

4.2.5 Electrophysiological Recordings

LFP and extracellular unit recordings were performed before the 6-OHDA injection (for rats equipped with a cannula) and on days 7, 14, and 21 after lesion. Data were collected during epochs of walking on the rotating circular treadmill and during attentive/inattentive rest. LFPs and extracellular spike trains were amplified and filtered using Plexon (Plexon Inc., Dallas, Texas, USA) preamplifiers and sampled with a Micro1401 data acquisition interface (CED, Cambridge, UK). LFPs and spikes from the recording wires were referenced to the 9th wire in the same bundle. LFPs and spike trains were sampled at 1 or 2 kHz and 40 kHz,

respectively. LFPs were amplified 1,000x and bandpass filtered 0.07 – 500 Hz. Action potentials were amplified 10,000x and bandpass filtered from 0.15 – 9 kHz. LFPs and spike signals, once discriminated, were digitized, stored, and analyzed offline using Spike2 (CED) software.

4.2.6. Data Analysis

Periods of LFP and spike recordings, free of major artifacts such as those caused by rearing or turning, were taken for analysis. Direct observation and videotaped motor behavior were used for the selection of epochs representing different behavioral states. For LFP power and coherence, and for spike-triggered waveform averaging (STWA), epochs of approximately 100 s were taken during walking on the circular treadmill in the direction ipsiversive to the lesioned hemisphere, unless otherwise indicated. Variable length epochs of inattentive rest were also analyzed.

4.2.7 Spectral Analysis of Local Field Potential Recordings

Before power and coherence analysis, LFP signals were smoothed to 500 Hz. LFP power was measured by FFT with a frequency resolution of 1 Hz. Using a MATLAB script, total power was calculated for each structure in multiple frequency ranges: theta (4 – 11 Hz), alpha (12 – 19 Hz), low beta (20 – 29 Hz), and high beta (30 – 36 Hz). LFP power from 3 – 4 channels per bundle during epochs of each behavioral condition were averaged. Data are reported as mean ± standard error of the mean (SEM). FFT-based spectral coherence was calculated for each pair of electrodes (ACC-STN and ACC-VM) using a MATLAB script.

The following criteria were applied to identify significant peaks in power or coherence spectra. A relative maximum in the spectrum was identified that was greater than the surrounding 1 Hz bins (within the frequency band of a given spectral band). The slope of the curve changed from positive to negative (through taking the 1st derivative of the spectrum) around the identified maximum. Finally, the 2nd derivative at the relative maximum had to be negative, indicating a downward concavity (Brazhnik et al. 2012).

To identify a minimum significance value for coherence, each data segment was binned at 50 ms, using a block size of 256 which yielded 23 non-overlapping 12.8 s windows. Using these parameters, peak coherence > 0.127 was considered to be significant ($p < 0.05$) as determined using the equation

$$1 - (1 - \alpha)^{1/(L-1)}$$

where α is the 0.95 confidence interval and L is the number of windows used; in this case 23 (Rosenberg et al. 1989).

4.2.8 Cell Sorting and Spike-Triggered Waveform Averaging Analysis

Spike waveforms were sorted using principal components analysis (PCA) in Spike2. To assess sorting for single cells, inter-spike interval histograms were generated and inspected to ensure that spikes were not occurring within an assumed refractory period of 1 ms. To evaluate the temporal relationships between spiking activity of individual neurons and LFPs, STWAs were calculated during inattentive rest and treadmill walking epochs. LFPs were bandpass filtered to a desired frequency range. STWAs were generated from epochs of single-unit spike trains and LFP recordings and peak-to-trough amplitude, the period of the averaged waveform oscillation around a given spike, and the phase of a given spike with respect to maximum positive deflection of the surrounding averaged waveform oscillation were

measured. For each spike train, 20 additional STWAs were generated from 20 randomly shuffled versions of the original. The randomly generated 20 STWA peak-to-trough amplitudes were averaged and compared with the unshuffled STWA. If the unshuffled mean amplitude was greater than the shuffled mean's plus 3 standard deviations it was considered significantly correlated. Phase calculations were then only considered for significantly correlated spike trains. Epochs of spike trike trains with firing rates of < 2.0 Hz were not considered for analysis. Coherence between spiking and LFP activity were generated using a MATLAB script. Spiking occurring at the peaks or the troughs of LFP oscillations was at 0° and 180° phase, respectively. STWAs were determined to be significant if the peak-to-trough amplitude of the STWA around the time of spiking was greater than 4 significant deviations above the amplitude of a STWA generated from the same data using randomly distributed spiking.

4.2.9 Histology and Immunochemistry

Upon completion of recordings, rats were anesthetized with urethane (1.5-2.0 g/kg, i.p.) and recording sites were marked by passing a 10 µA positive current for 18 s through 2-3 microwires. Anesthetized rats were perfused intracardially with 200 ml of chilled saline followed by 200 ml of 4 % paraformaldehyde in phosphate-buffered saline (PBS). Brains were retrieved and post-fixed in paraformaldehyde solution overnight and then immersed in 10 % sucrose in PBS (0.1 M, pH 7.4). Coronal sections of 40 µm for electrode placement verification were mounted on glass slides and stained with cresyl violet and 5 % potassium ferricyanide / 9 % HCl to show deposited iron from the marking of electrode sites.

To assess the loss of dopaminergic neurons in the SNpc, a TH staining protocol was performed in freely floating sections (Avila et al. 2010; Brazhnik et al. 2012; Brazhnik et al. 2014). Brain sections were washed 3 times in PBS (0.01 M, pH 7.4) before incubation with

rabbit polyclonal anti-TH antibody (1:200 dilution; Pel-Freez Biologicals) with mild agitation for 12 – 18 h at room temperature. Brain sections were rinsed again 3 times in PBS and incubated with a secondary antibody of biotinylated anti-rabbit IgG (1:200 dilution; Vector Laboratories) for a period of 60 min, rinsed in 50 mM Tris (pH 7.4), and reacted with 0.05 % 3,3' -diaminobenzidine tetrahydrochloride and 0.01 % H_2O_2 (DAB kit; Vector Laboratories) for 2 – 10 min until intense staining occurred. Sections were washed in 50 mM Tris and then mounted on slides, dehydrated, and prepared for light microscopy.

To assess the extent of dopamine cell degeneration, stained slices were imaged under a light microscope using wide-field optics to properly capture both lesioned and non-lesioned hemispheres. These images were digitized and examined using ImageJ (NIH) software. The optical density of TH fibers and neurons of the SNpc in the lesioned hemisphere were compared with that of the un-lesioned hemisphere, and rats with a density < 90 % of that in the non-lesioned hemisphere were considered fully lesioned.

4.2.10 Statistical Analyses

A Student-Newman-Keuls *post hoc* test was applied to acquire significant differences between groups of total LFP power, pairwise coherence, and STWA ratios in both lesioned and non-lesioned hemispheres. This difference between variable groups was assessed using *t* test or by a Mann-Whitney test. A Rayleigh test was applied to polar data to show whether spiking was significantly phase-oriented to LFPs. Statistical analysis was performed using Sigma Plot (SyStat Software, San Jose, CA, USA) and Microsoft Excel (Microsoft Corporation, Redmond, WA, USA). The minimum criteria for significance was $\alpha = 0.05$.

4.3 Results

4.3.1 Lesion and Electrode Placement Confirmation

Overall, 9 non-lesioned rats, 7 poorly-lesioned rats (< 90 % dopamine cell death), and 21 well-lesioned rats (< 90 % dopamine cell death) were available for analysis. 5 non-lesioned rats and 9 lesioned rats were available with STN electrodes. 9 non-lesioned rats and 21 lesioned rats were available with ACC electrodes. 4 non-lesioned rats and 12 lesioned rats were available with VM electrodes.

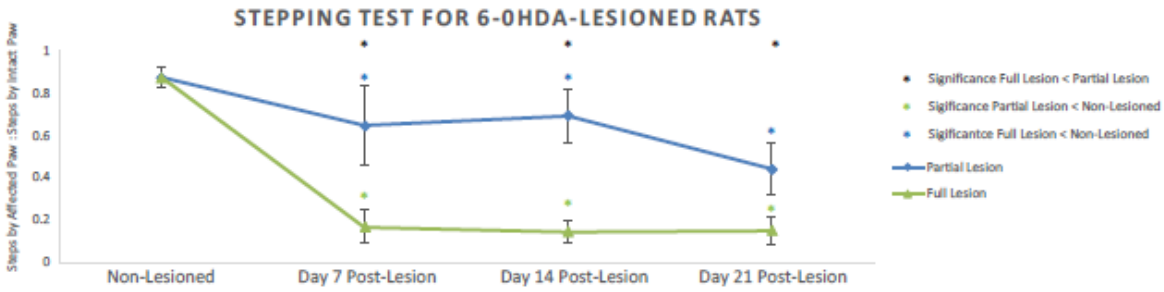

Figure 4.3.1.1 Results of step testing in non-lesioned (n = 9), partial (< 95% DA depletion, n = 7), and full 6-OHDA lesioned (> 95% DA depletion, n = 21) rats as ratio of steps taken by the affected paw to steps taken by the intact paw. Rats are held by the waist with their hindlimbs and one forelimb suspended above the table and moved at a steady rate so they moved 1 m over about 4 to 5 s. During this movement, the number of steps made by the contraleral or ipsilateral paw relative to the injected hemipshere were counted over the total distance. Three trials were performed per day and averaged for each rat and across all rats. Values are given as mean ± SEM. Rats with both partial lesion and full lesion show significant ($p < 0.05$) deficits in steps taken by the affected paw as compared to non-lesioned rats. Rats with full lesions take significantly less steps than partially lesioned rats.

Rats performed a stepping test to confirm lesion quality in the weeks post-lesion, with the number of steps taken by lesioned paw divided by steps taken by the intact paw providing a ratio (Figure 4.3.1.1). Rats were shown to generally bias to the left paw (intact paw after lesion) before lesion (mean ± SEM, 87.6 ± 4.6 %). After lesion, two distinct populations of rats could be categorized by the step test ratio. Rats regardless of lesion quality made significantly fewer steps with their affected paws as compared to non-lesioned rats ($p < 0.05$). Rats with a full dopamine cell lesion had significantly lower step test ratios than those rats with partial lesions by day 7 post-lesion (partial lesion 64.8 ± 19.2 % vs. full lesion 16.8 ± 7.7 %). Both partially lesioned and fully lesioned rats exhibited further decreases in step test ratios by the 21st day post-lesion. These ratios, while still significantly different, began to approach parity (partial lesion 44.3 ± 12.4 % vs. full lesion 15.1 ± 6.4 %). After perfusion, histology was performed and ACC, STN, and VM electrode locations were assessed. Rats with acceptable electrode placement are plotted in Figure 4.3.1.2. Lesioned rats are marked with green O's and non-lesioned rats are marked with red X's.

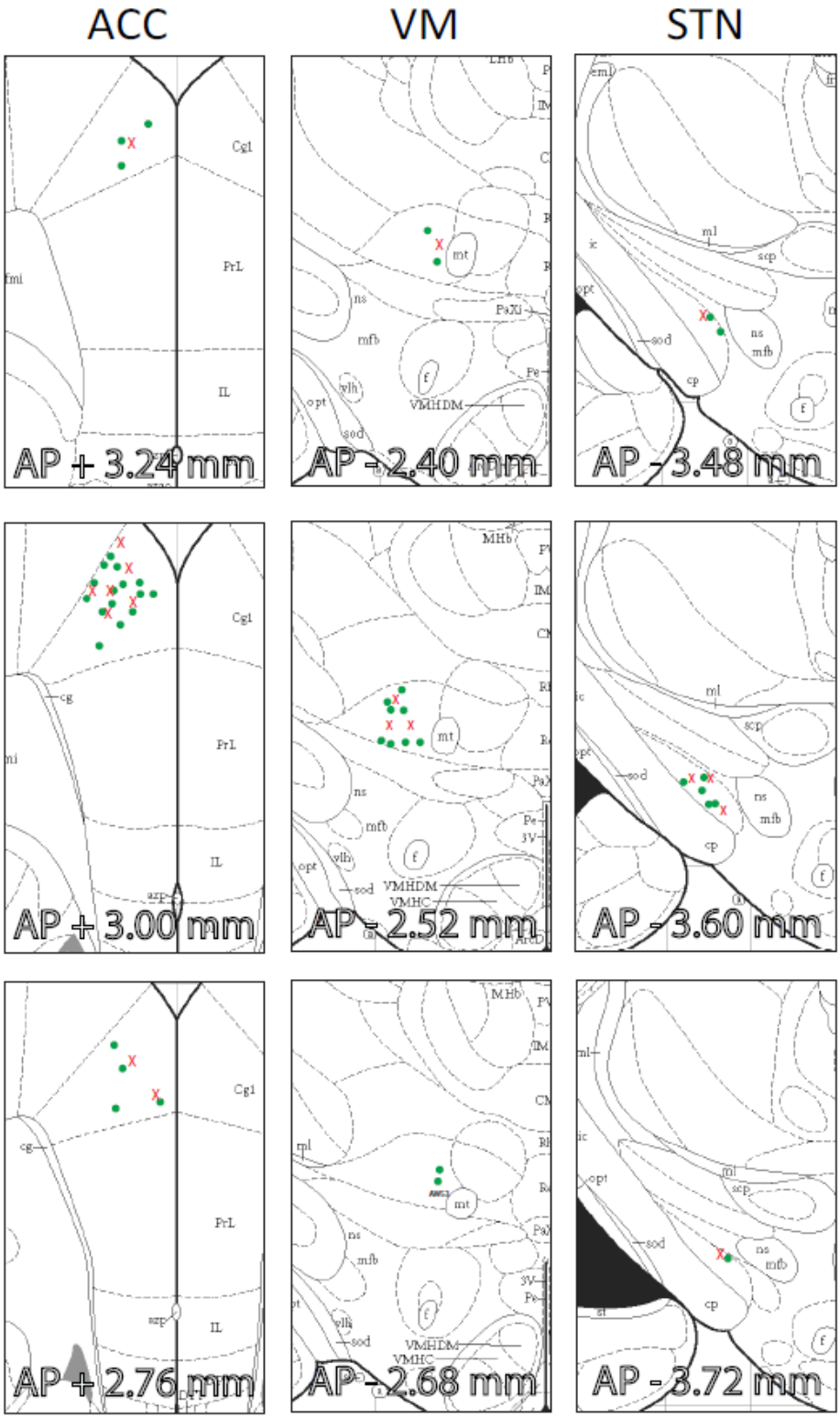

Figure 4.3.1.2 Location of ACC, STN, and VM recording sites in non-lesioned and 6-OHDA lesioned rats. 5 non-lesioned rats and 9 lesioned rats were available in STN. 9 non-lesioned rats and 21 lesioned rats were available in ACC. 4 non-lesioned rats and 12 lesioned rats were available in VM. Distance from bregma is indicated in each coronal slice in mm. Recordings in intact rats are shown as red X's and recordings in lesioned rats are shown as Green O's. Schematics of coronal slices are adapted from The Rat Brain in Stereotaxic Coordinates, 2nd Ed. (Paxinos and Watson, 1986).

4.3.2 Oscillatory Local Field Potential Activity in the Subthalamic Nucleus, Anterior Cingulate Cortex, and Ventral Medial Thalamus after Dopamine Cell Lesion

As has been shown previously (Brazhnik et al. 2016; Delaville et al. 2015), chronic recordings from electrodes implanted in the STN and VM demonstrate that excessively synchronized high beta (30 – 36 Hz) LFP power develops during treadmill walking in the 6-OHDA-lesioned rats as compared to the non-lesioned rat. Notably, the ACC also develops power in this frequency band as shown in power spectra and time-frequency analysis (Figure 4.3.2.1). This increase in the ACC is similar to that seen in the STN and VM, and also similar to increases shown previously in the SNpr and layer V and VI of the MCx after 6-OHDA dopamine cell lesion during treadmill walking (Avila et al. 2010; Brazhnik et al. 2012; Brazhnik et al. 2014; Brazhnik et al. 2016; Delaville et al. 2014; Delaville et al. 2015). In this chapter, LFP recordings were obtained from chronically implanted electrodes in the STN, ACC, and VM of the hemiparkinsonian rat during treadmill walking in a direction ipsiversive to the lesioned- hemisphere on days 7, 14, and 21 post-lesion. Representative wavelet-based scalograms (Figure 4.3.2.1, right) show the development of a distinct band of LFP oscillatory activity in the high beta range in the lesioned rat in all 3 brain regions at day 21 post-lesion. This high beta band is absent in the 3 regions while treadmill walking in the non-lesioned rat. This activity is reflected in the normalized mean power spectra from LFP recordings (Figure 4.3.2.1, left). The high beta band in the ACC can be seen in the power spectra to be much more “broad” as compared to the “sharp” bands in the STN and VM. A small gamma band can also be seen in the ACC in both lesioned and non-lesioned rats. Small, sharp peaks in the power spectra of STN and VM at 60 Hz reflect mains noise contamination of recordings.

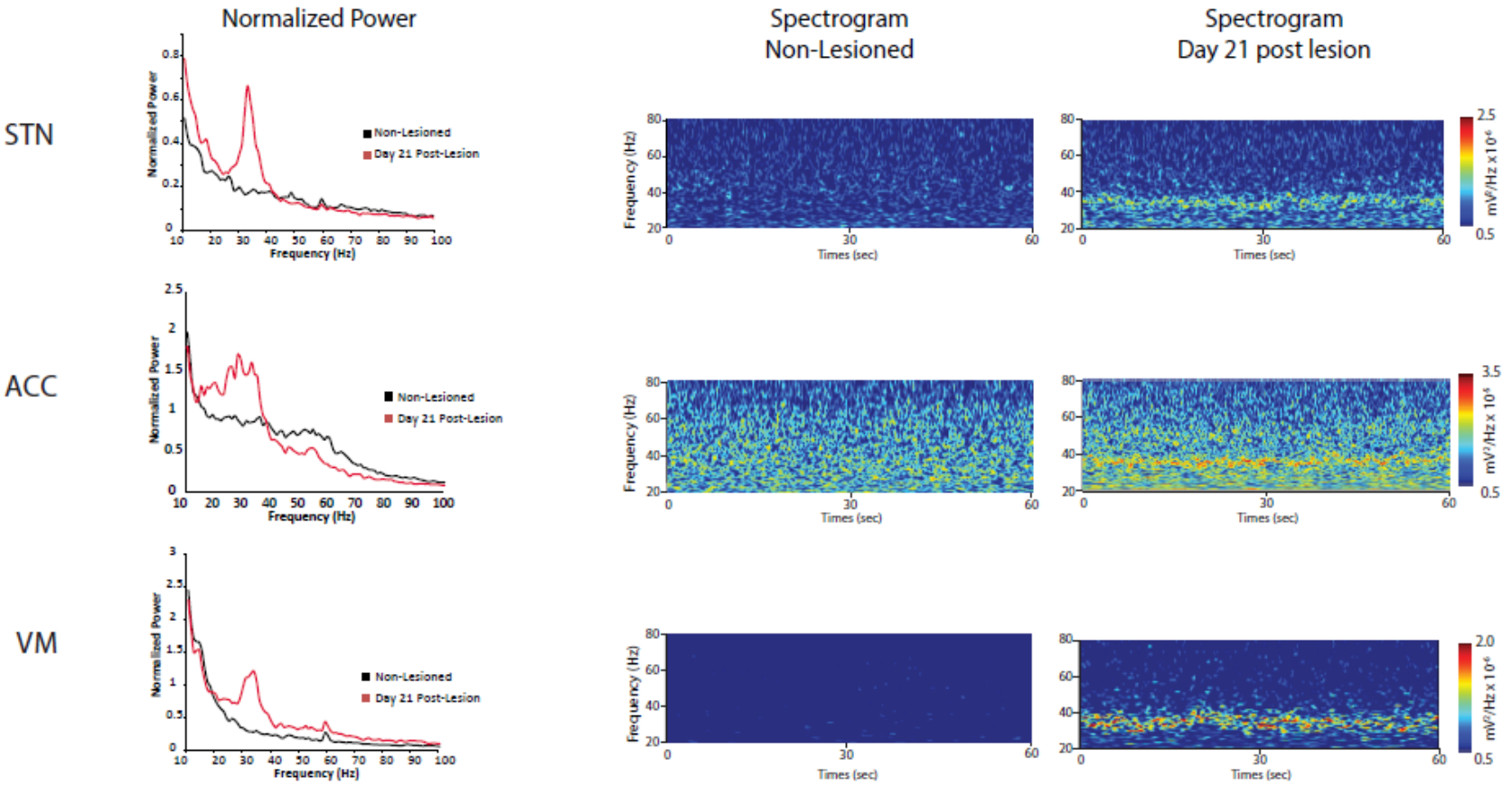

Figure 4.3.2.1 LFP oscillatory activity in the STN, ACC, and VM thalamus in 6-OHDA lesioned and non-lesioned rats during treadmill walking. Left, Averaged and normalized LFP power spectra. Right, Representative time-frequency wavelet-based spectrograms of LFP spectral power in the treadmill walking rat. Note the emergence of synchronized oscillations in the high beta-frequency range (30-36 Hz) in recordings from all 3 regions in the 6-OHDA dopamine-lesioned rat. High beta peaks are much "sharper" in the STN and VM, and "broad" in the ACC.

The mean peak frequency of high beta activity in the STN, ACC, and VM significantly increased ($p < 0.05$) in the 3 weeks after 6-OHDA lesion (Figure 4.3.2.2). Peak frequency in the STN increases by approximately 0.75 Hz/week, starting at 31.7 ± 0.1 Hz on day 7 post-lesion and rising to 33.0 ± 0.2 Hz on day 7 post-lesion. The ACC and VM both increase by less than 0.5 Hz/week. The ACC has a high beta peak frequency of 31.7 ± 0.1 Hz at day 7 post-lesion that rises to 32.5 ± 0.1 Hz on day 21. The VM, similarly, has a peak frequency of 31.9 ± 0.1 Hz on day 7 and a peak frequency of 32.4 ± 0.1 Hz on day 21. At day 7, there are no significant differences between the peak frequencies in the three regions, but by day 21 post-lesion, STN high beta peak frequencies are significantly higher than both ACC and VM peaks ($p < 0.01$).

Total high beta band (30 – 36 Hz) normalized power reflected what was observed in power spectra and time-frequency analyses in Figure 4.3.2.1, showing significant increases in all recordings post-lesion during treadmill walking relative to the non-lesioned rat (Figure 4.3.2.3). Normalized power in the STN modestly increased from 54.5 ± 3.5 in the non-lesioned

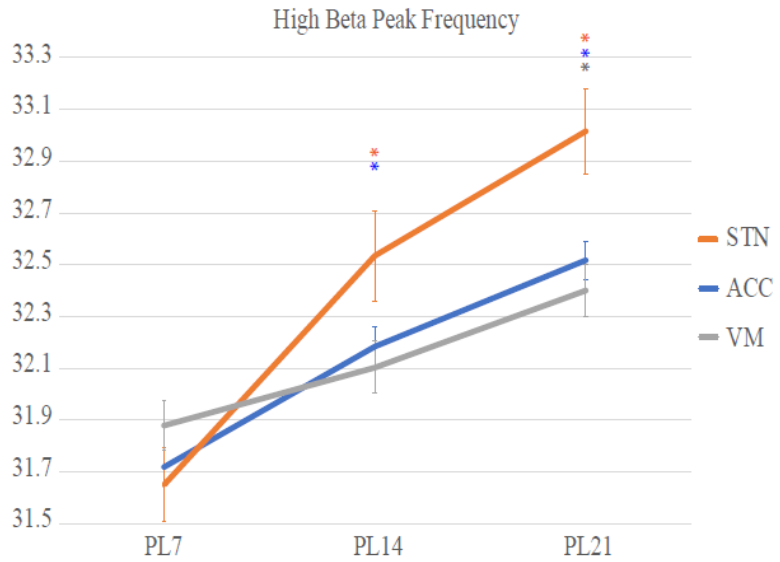

Figure 4.3.2.2 Peak Frequency of high beta (30-36 Hz) frequency band after 6-OHDA lesion in STN, ACC, and VM. All 3 regions exhibit significant increases in high beta peak-frequency over a period of 3 weeks after lesion ($p < 0.05$). Peak frequency increases approximately 1Hz/week in the STN and 0.5 Hz/week in the ACC and VM.

state to 68.1 ± 5.6 on day 7 post lesion ($p < 0.05$), further increasing to 82.7 ± 5.7 on day 14 ($p < 0.0001$) and 100.5 ± 8.9 on day 21 ($p < 0.00005$). ACC normalized power markedly increases from 190.5 ± 9.1 in the non-lesioned state to 365.2 ± 18.5 on day 7 ($p < 1 \times 10^{-15}$), 484.8 ± 28.3 on day 14 ($p < 1 \times 10^{-20}$), and 556.3 ± 37.15 on day 21 ($p < 1 \times 10^{-20}$). The VM increases from 30.8 ± 1.5 in the non-lesioned state to 42.6 ± 2.5 ($p < 1 \times 10^{-6}$) at day 7, 43.9 ± 2.0 on day 14 ($p < 1 \times 10^{-9}$), and 49.2 ± 2.0 on day 21 ($p < 1 \times 10^{-11}$).

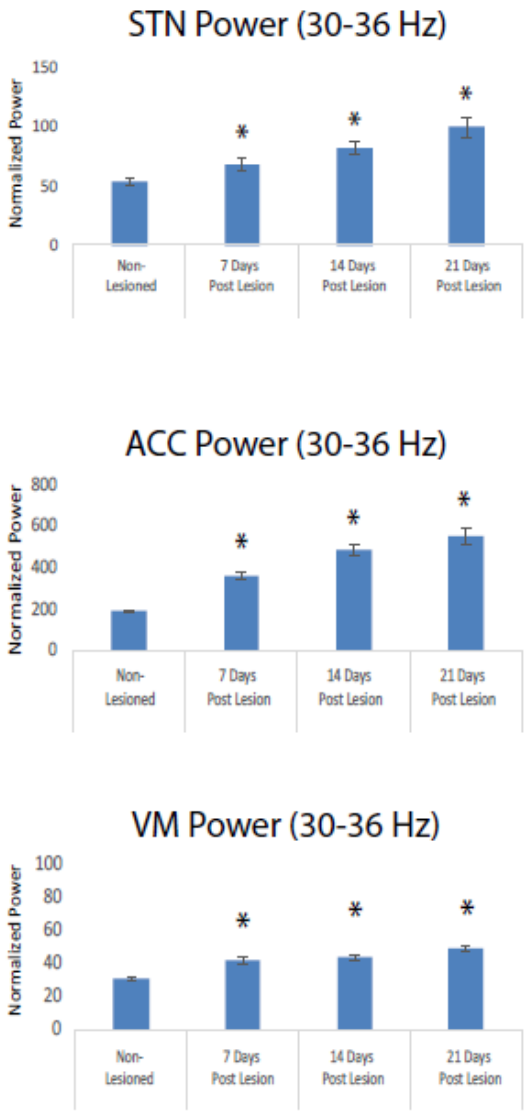

Figure 4.3.2.3 LFP oscillatory activity in the STN, ACC, and VM in non-lesioned and 6-OHDA-lesioned rats during periods of treadmill walking. Averaged, normalized LFP total power (mean ± SEM) in the high beta frequency range (30-36 Hz) during treadmill walking. After 6-OHDA lesion, all 3 regions exhibit the emergence of synchronized oscillations in the high beta frequency range, resulting in significant increases in STN, ACC, and VM power ($p < 0.05$).

4.3.3 High Beta Local Field Potential Coherence in the Subthalamic Nucleus, Anterior Cingulate Cortex, and Ventral Medial Thalamus after Dopamine Cell Lesion

To try to further probe the role of STN and VM thalamus in mechanisms that may underlie the emergence of high beta 30 – 36 Hz oscillatory LFP in the ACC after 6-OHDA dopamine cell lesion, coherence between STN and VM LFPs and between VM and ACC LFPs was examined during epochs of treadmill walking. Previously, increases in high beta LFP total power in the VM, STN, and MCx have been shown to emerge in parallel with an increase in coherence between these regions during treadmill walking (Brazhnik et al. 2014; Brazhnik et al. 2016; Delaville et al. 2014). Here, we similarly show that both STN-ACC and VM-ACC high beta coherence increased in the lesioned rat relative to non-lesioned rats (Figure 4.3.3). This robust increase can be clearly seen in time-frequency coherograms of spectral power at day 21 post-lesion (Figure 4.3.3, top), occurring broadly centered at the peak frequencies observed in Figure 4.3.2.2. Averaged, normalized coherence (Figure 4.3.3, bottom) show significant increases in high beta LFP coherence over the weeks after 6-OHDA lesion. Both STN-ACC and VM-ACC coherence are insignificant prior to lesion, but become significant (coherence value > 0.127) after 6-OHDA lesion. STN-ACC coherence increases from 0.12 ± 0.00 in the non-lesioned state to 0.21 ± 0.00 at day 7 post-lesion ($p < 1 \times 10^{-31}$), 0.23 ± 0.00 at day 14 ($p < 1 \times 10^{-51}$), and 0.29 at day 21 ($p < 1 \times 10^{-44}$). VM-ACC coherence increases even more significantly from 0.11 ± 0.00 in the non-lesioned state to 0.21 ± 0.00 at day 7 ($p < 1 \times 10^{-62}$), 0.28 ± 0.00 at day 14 ($p < 1 \times 10^{-100}$), and 0.31 ± 0.00 at day 21 ($p < 1 \times 10^{-81}$).

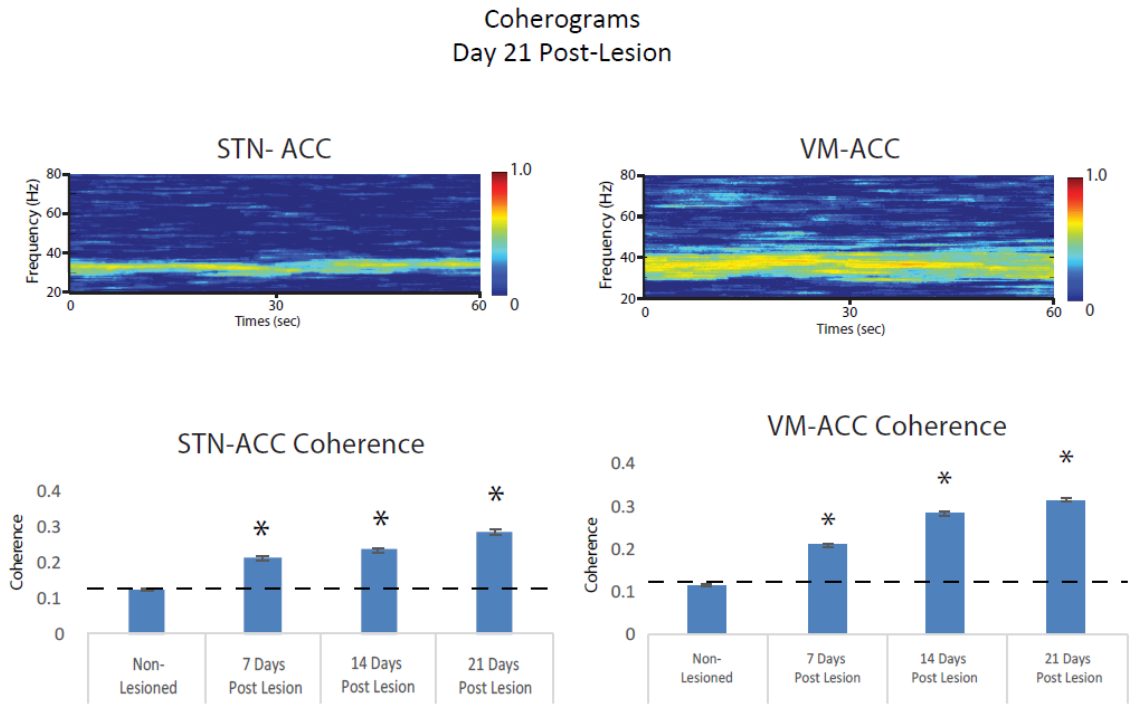

Figure 4.3.3 LFP oscillatory coherence between the STN, VM, and ACC in non-lesioned and 6-OHDA-lesioned rats during periods of treadmill walking. Top, Representative FFT-based time-frequency coherograms of LFP spectral power between the STN and ACC and between the VM and ACC in the lesioned rat plotted on a linear scale with greater values represented by red. Bottom, Averaged, normalized coherence (mean ± SEM) in the high beta frequency range (30-36 Hz) in non-lesioned rats and 7, 14, and 21 days post-lesion. Evident in both coherograms and bar plots are significant increases in STN-ACC and VM-ACC coherence ($p < 0.05$) within the high beta frequency range in the lesioned hemispheres. *Significant difference between lesioned and non-lesioned rats.

4.3.4 The Relationship between Anterior Cingulate Cortex Spiking Activity and Local Field Potentials

Spike-LFP relationships were examined in the STN, ACC, and VM to determine whether changes in spike timing correlate with the increases in LFP beta range activity observed after 6-OHDA dopamine cell lesion. First, the mean ratios of unshuffled to shuffled STWA peak-to-trough amplitudes of STN, ACC, and VM were compared between lesioned and non-lesioned rats (Figure 4.3.4, left).

As has been observed before, increases in STN and VM power in the 30 – 36 Hz high beta range in the lesioned rat during treadmill walking was associated with increased synchronization of STN and VM spikes to LFP oscillations in the same range (Brazhnik et al. 2016; Delaville et al. 2014). The mean of the unshuffled to shuffled peak-to-trough STWA amplitude ratios for all epochs of STN (non-lesioned 1.8 ± 0.2 vs. lesioned 4.2 ± 0.7) and VM (non-lesioned 1.2 ± 0.1 vs. lesioned 7.1 ± 0.7) spiking examined in lesioned rats was significantly greater than the mean of ratios from non-lesioned rats ($p < 0.05$). Significant increases in STWA ratios after lesion were coupled with a significant increase in the proportion of STN and VM spike trains correlated with their respective LFPs ($p < 0.05$). STN spikes to STN LFPs increased from 25 ± 5 % in the non-lesioned state to 53 ± 3 % in the lesioned rat. VM spikes to VM LFPs likewise increased from 0 % to 70 ± 3 %.

We hypothesize that the excessively synchronized high beta activity that arises in the ACC is influenced by spiking in the VM and STN. To investigate this, we looked at spike-LFP relationships between the three regions (Figure 4.3.4). The mean STWA amplitude ratios for epochs of both STN and VM spiking to ACC high beta LFPs was found to significantly increase after dopamine cell lesion ($p < 0.01$). STWA ratios of STN spiking to ACC LFPs increase after lesion from 1.2 ± 0.1 to 3.7 ± 0.4. STWA ratios of VM spiking to ACC LFPs increase from 0.9 ± 0.1 to 6.1 ± 0.6 after lesion. The proportion of spike trains in the STN or VM correlated to ACC LFPs also significantly increased after lesion ($p < 0.05$). STN spikes phase-locked to ACC LFPs rose from 0 % in the non-lesioned state to 66 ± 5 % after lesion. VM spikes phase-locked to ACC LFPs increased from 0 % in the non-lesioned state to 69 ± 5 % after lesion.

The above findings suggest that synchronous high beta input from the VM after 6-OHDA dopamine cell lesion would lead to entrainment of oscillatory spiking activity in the ACC in the same frequency range. However, when we investigated spike-LFP relationships in the ACC or originating in the ACC, we found the opposite (Figure 4.3.4). Mean unshuffled-to-

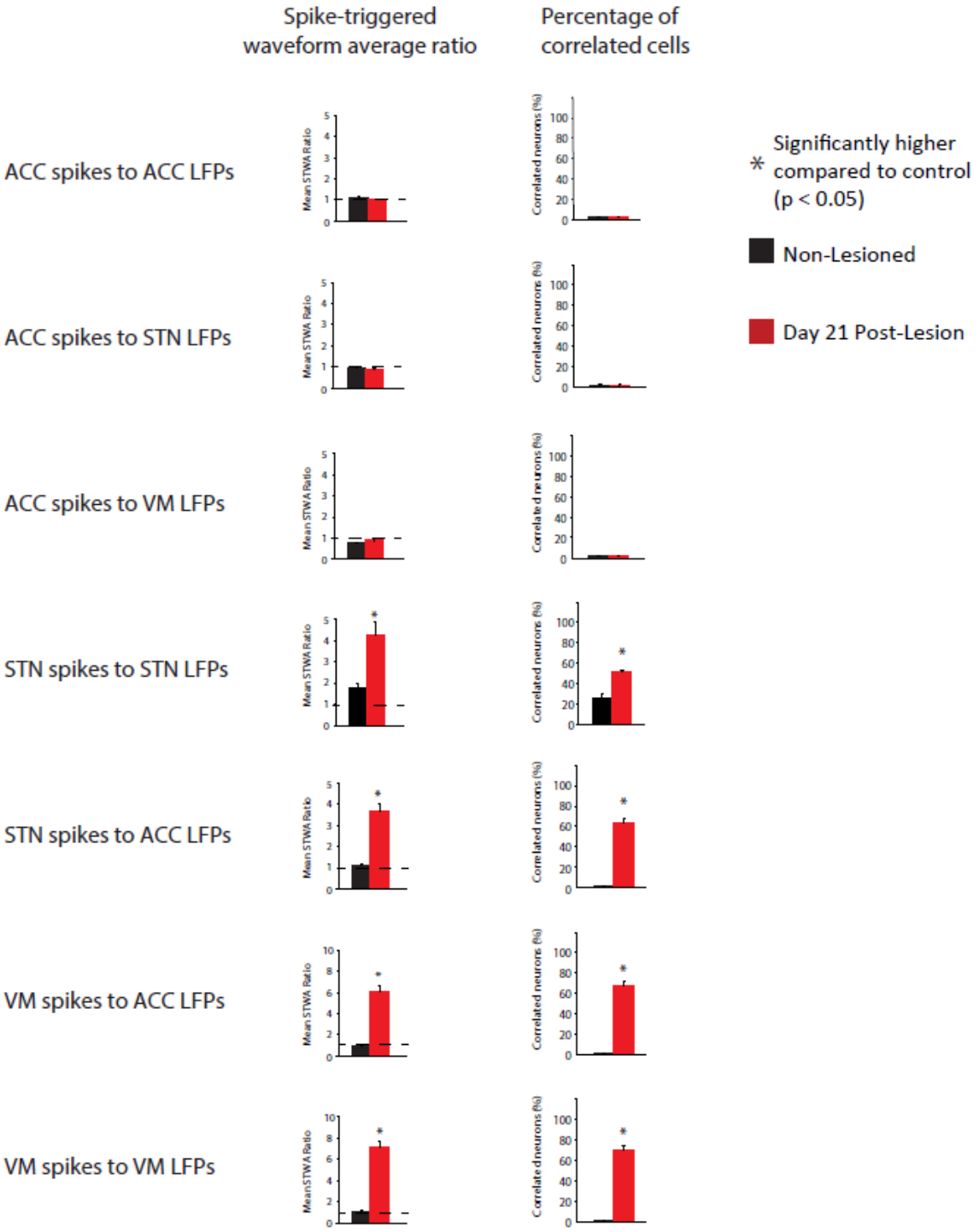

Figure 4.3.4 Spike-triggered waveform average (STWA) results from non-lesioned and 6-OHDA-lesioned rats during periods of treadmill walking. Recordings from lesioned rats are from 21 days post-lesion. Mean STWA-based amplitude ratios (Left) and the proportion of STN and VM STWAs showing significant phase locking of spike trains with local and ACC high beta LFP activity (right) are significantly higher in the lesioned rat (red bars) relative to the non-lesioned rat (black bars) ($p < 0.05$). ACC STWA ratios are below 1, and ACC does not exhibit significantly phase-locking of spike trains to high beta LFPs ($p > 0.05$). Dashed line in STWA Ratio plots indicate ratio of 1 representing significance. * Significant difference between lesioned and non-lesioned rats.

shuffled peak-to-trough STWA amplitude ratios reveal that there are no significant differences between non-lesioned and lesioned rats regarding ACC spike phase-locking to high beta LFPs in the ACC, VM, or STN ($p > 0.05$). STWA ratios are either within the margin of error of a ratio of 1, or well below that benchmark. Likewise, 0 % of ACC spike trains correlate with high beta LFPs in any of the 3 recording regions, and this lack of correlation occurs in both the lesioned and non-lesioned state.

4.3.5 Temporal Relationships between Spikes in the Subthalamic Nucleus, Anterior Cingulate Cortex, and Ventral Medial Thalamus in the 6-OHDA-Lesioned Rat

To explore the hypothesis that coherent LFP activity in the BG thalamocortical circuit reflect sequential spiking activity between circuit nodes, we examined temporal relationships between synchronized spiking activity in the STN, ACC, and VM of the non-lesioned and lesioned treadmill walking rat. To accomplish this, we first identified epochs of treadmill walking with spikes that significantly correlated to their regional LFP oscillations in the bandpass-filtered 30-36 Hz high beta range (Figure 4.3.4). These spikes and their corresponding LFPs were used to create STWAs for each epoch of treadmill walking for a given rat on a given recording day. With the exception of the ACC, the majority of spike trains showing significant spike-LFP relationships with their own regional LFPs were also significantly correlated to ACC high beta oscillations. The results showed that 0 % of ACC, 63 % of STN, and 68 % of VM spike trains had epochs with rates > 2 Hz that were significantly correlated with LFPs in the ACC of the lesioned rat. The high beta oscillation in the ACC was thus used as a common temporal reference to attempt to establish relative timing between spiking activity in each area.

Analysis revealed that spikes in the STN and VM in the lesioned hemisphere were, on average, occurring at different sequential time points with respect to components of ACC high

beta LFPs (Figure 4.3.5). Mean phase angles between spikes and cortical LFP oscillations (Figure 4.3.5, left) as assessed by STWAs, were significantly clustered around different phases of ACC high beta LFPs. ACC spikes did not significantly phase lock to ACC LFPs. STN spikes occurred at 58.4 ± 49.92 ° while VM spikes occurred at 244.7 ± 20.57 ° ($p < 0.05$). Because the mean dominant frequency from the spike-ACC LFP-derived STWA was approximately 33 Hz, the duration of a typical cortical STWA-based LFP oscillation (peak-to-peak) would be approximately 30 ms (reached from 1 s / 33 Hz). The temporal relationships between spiking in a given region could then be estimated using the relative differences in mean phase angles (Figure 4.3.5, top right). As the phase angle between STN and VM showed a difference of 186°, this corresponded to an 18.2 ms time difference, suggesting multisynaptic connectivity between the STN and VM. This difference would be compatible with the time that might be required for STN glutamatergic excitation of the SNpr to lead to GABAergic inhibition of VM thalamus neurons. These timings are similar to those shown previously by Brazhnik *et al*. and Delaville *et al.* between the STN, SNpr, VM, and MCx (Figure 4.3.5, bottom right).

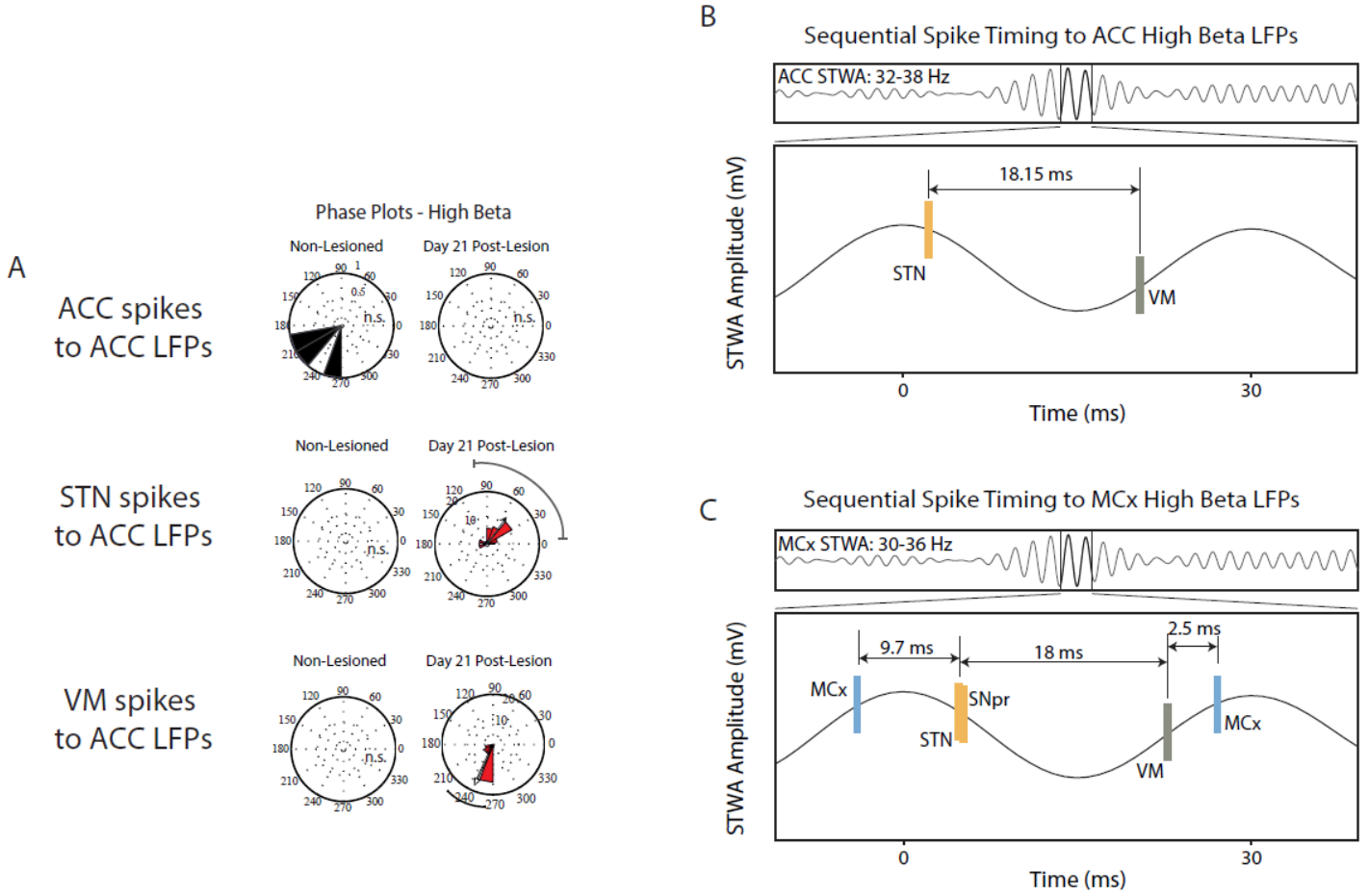

Figure 4.3.5 Relationships of spike trains in the ACC, VM, and STN relative to ACC LFPs band-pass filtered in the high beta (30-36 Hz) range in hemi-parkinsonian rats during treadmill walking.

A. Polar plots showing the distributions of phases of STWAs from correlated spike trains in the ACC, STN, and VM exhibiting significant correlations with the ACC high beta LFPs. Spikes are not significantly oriented in any region in the non-lesioned rat, or in the ACC after 6-OHDA lesion ($p > 0.05$). STN and VM spikes are significantly oriented to ACC LFPs and the mean phase is significantly different to the other ($p < 0.05$). The strengths of the mean phase values normalized to the radius of the circular plot are indicated by arrows.

B. Top, Representative ACC STWA. Bottom, Temporal relationships of representative spike trains in STN and VM with high beta ACC LFPs. LFP peak was used as the zero point.

C. Temporal relationships of spike trains in STN, SNPr, VM, and MCx to high beta MCx LFPs. Adapted from Delaville et al 2015 and Brazhnik et al. 2016.

4.4 Discussion

These results indicate that LFP activity in the ACC becomes significantly synchronized to the high beta band after dopamine cell lesion, exhibiting coherence with similar activity in both the VM thalamus and the STN during a walking task. This suggests the possibility that the constellation of cognitive symptoms observed in PD is due to either the development of this pathological activity or whatever physiological changes underlie high beta entrainment. This evidence was obtained from rats performing a sustained walking task that required a steady pace on a rotating circular treadmill.

4.4.1 Power Analysis Findings

The ACC showed increases in LFP power coherent with increases in both the STN and VM thalamus in the high beta range (30 – 36 Hz) during walking, only after lesion. This is consistent with previous findings from the MCx, STN, VM thalamus, and SNpr (Avila et al. 2010; Brazhnik et al. 2012; Brazhnik et al. 2014; Brazhnik et al. 2016; Delaville et al. 2014). Although the frequency range of high beta LFPs evident in our rats (30 – 36 Hz) is higher than that most commonly observed in PD subjects, the behavior- and dopamine-dependent nature of its activity suggests it is likely driven by similar processes to those observed in the BG of humans (P. Brown 2003; Levy et al. 2002). While beta frequency modulation has been observed in the ACC during normal function (Babapoor-Farrokhran et al. 2017) and in neurological disorders including treatment-resistant depression (Huebl et al. 2016; Merkl et al. 2016), this appears to be the first demonstration of such activity in the ACC of a hemiparkinsonian animal. These results may lead to further insight into the significance of excessive beta oscillatory activity in PD.

Normalized ACC total power was shown to be significantly higher than that seen in either the VM or the STN. Although these relative differences in total power in the high beta range remain to be further explored, the present results do show that synchronized activity is highly expressed in the high beta frequency band during treadmill walking and is coherent with similar increases in STN and VM LFPs.

We found the peak frequency of the high beta band in all three recorded regions to gradually increase over the 21 days post-lesion at a rate between 0.5 Hz and 0.75 Hz/week. This is similar to results observed Brazhnik *et al*. in the MCx and SNpr, and may suggest that these increases in frequency reflect ongoing plasticity within BG thalamocortical circuits after lesion (Brazhnik et al. 2012; Brazhnik et al. 2014; Brazhnik et al. 2016).

Pilot studies in a limited number of rats receiving chronic L-DOPA treatment displayed dyskinetic behaviors and initial findings of both the decrease in power of the parkinsonian high beta frequency band and the development of power in a new frequency range of high gamma (90 – 100 Hz) in the ACC. This activity was, in initial recordings, coherent with the STN and is similar to that seen by Delaville *et al.* (Delaville et al. 2015) and may represent the "finely-tuned gamma" observed during movement observed in the BG of PD subjects associated with L-DOPA treatment (Alonso-Frech et al. 2006; Jenkinson et al. 2013). Although L-DOPA medication has been shown to improve PD motor symptoms, it is known to have complex effects upon cognition with both positive and negative effects observed (Cools 2006). Future work on the electrophysiological effects of L-DOPA on ACC may have substantial implications for the understanding and treatment of the cognitive symptomology of PD.

Results from power spectra and time-frequency spectrograms (Figure 4.3.2.1) suggest that other frequency bands, such as gamma, may be affected by the integrity of the dopamine system in the ACC. The presence of both high beta and other frequency bands simultaneously

expressed in the ACC that fluctuate depending on dopamine (or other PD-related pathophysiology) may reveal potential electrophysiological roots for PD cognitive symptomology. This is explored in Chapter 5.

It is important to note the different patterns of power and coherence observed in the hemiparkinsonian rat that vary according to behavioral state. Brazhnik *et al*. showed that dramatically different patterns of power and coherence could be provoked by treadmill walking versus inattentive rest (Brazhnik et al. 2012).

4.4.2 Spike-Triggered Waveform Average Findings

High beta LFP power in the STN, VM, and ACC is thought to reflect net synchronized input to neurons in these areas. This data is consistent with the view that STN and VM spiking output is also synchronized by this output. STWA analysis thus agree with previous observations (Avila et al. 2010; Brazhnik et al. 2012; Brazhnik et al. 2014; Brazhnik et al. 2016; Delaville et al. 2015) of significant spike locking to increases in high beta LFP oscillations in the STN, VM, and SNpr of the dopamine-lesioned rat. Previous anatomical studies have shown the VM thalamus to act as one of the main targets of SNpr BG output in the rat (Herkenham 1979; Kuramoto et al. 2011), and to subsequently project widely to layers I and II of the cortex (Arbuthnott et al. 1990; Kuramoto et al. 2015). The temporal relationships between phase-locked spiking in our results are consistent with the above anatomical connections within the BG thalamocortical circuit and support the hypothesis that synchronous high beta input from the BG by way of the VM thalamus would lead to high beta LFPs in the ACC. In contrast, after dopamine-depletion, ACC spike trains were found to not significantly phase-lock to ACC LFPs or LFPs in either the STN (through hyperdirect or indirect innervation) or the VM (through potential cortical-thalamic innervation). This may suggest that

a common input may modulate the STN, VM, and ACC, but fails to induce significant spike-LFP synchronization in the ACC.

4.4.3 Effects of Dopamine Loss on Anterior Cingulate Cortex Output

An open question is how the loss of dopamine affects the outputs of the ACC. We have looked in this chapter at the possibility that the ACC contributes to the propagation of high beta activity elsewhere in the BG thalamocortical circuit as represented by the VM thalamus and the STN. Ultimately, ACC spike trains do not phase-lock to ACC, STN, or VM high beta LFPs. It is important to note that the ACC afferents project both directly to the STN through the hyperdirect pathway to the STN and indirectly through the striatum. Although ACC output was found to not be entrained to the parkinsonian high beta frequency range, the impact of synchronized input on the oscillations in net voltage in ACC neurons may still be disrupt information processing by ACC neurons.

4.4.4 Concluding Remarks

In conclusion, the research described in this chapter indicates that the ACC, which receives glutamatergic innervation from the VM thalamus, and thus the BG, develops the familiar parkinsonian excessively synchronized high beta oscillatory activity. ACC LFP activity becomes synchronized with, and potentially modulated by, activity in the STN and VM thalamus that varies by the integrity of the dopamine system. The relationship between ACC output and its connections to the BG and to the rest of the PFC remain to be clarified regarding the generation and propagation of high beta oscillations and their influence on cognitive dysfunction in PD. While we have not definitively shown that the ACC is the only part of the PFC that develops parkinsonian synchronized beta activity, we know that the ILC and PLC do not display activity similar to the ACC (Delaville et al. 2015). We hypothesize that synchronized beta activity may be more evident in areas receiving innervation from the area of the thalamus – such as the VM thalamus – that are the primary receivers of BG output. While the areas we have examined, now including the ACC, have not been revealed to be drivers of excessive synchronized beta activity, this does not rule out the possibility that other regions, such as the supplementary motor areas or the premotor cortex, are similarly affected in PD and are capable of propagating parkinsonian excessively synchronized activity further. In closing, these results support the utility of the rodent model in examination of LFP activity, coherence, and spiking behavior in the dopamine-depleted, parkinsonian ACC in the context of different behavioral states.

5. Modulation of Anterior Cingulate Cortex and Basal Ganglia Activity during a Simple Cognitive Task in Hemiparkinsonian Rats

The motor symptoms of PD have been linked to the emergence of exaggerated oscillatory activity in the 13 - 35 Hz beta range in LFP recorded throughout the BG thalamocortical circuit of PD patients and animal models. PD patients and parkinsonian animal models are also known to express dopamine-dependent cognitive impairments, implying effects of dopamine loss on PFC function. The electrophysiological correlates of these cognitive symptoms are not well understood. In light of the ACC's development of parkinsonian exaggerated beta activity (Chapter 4), this chapter investigates the involvement of BG thalamocortical circuits in dopamine-impaired and healthy rats in response to a salient cue that predicts the onset of either tone-to-treadmill-induced walking (an expected event) or tone-to-no-treadmill-induced walking (an unexpected event).

5.1 Introduction and Rationale

Excessive synchronization in the beta frequency range has been consistently observed in the BG and MCx in PD patients and animal models and are most commonly thought to be related to the motor symptoms associated with this disorder. PD patients and parkinsonian animal models are also known to express dopamine-dependent cognitive impairments, implying effects of dopamine loss on PFC function, but the electrophysiological correlates of these symptoms are not as well understood.

In chapter 2, we compared electrophysiological data from the BG of PD and non-PD patients during a cognitive task and showed that PD patients lacked phasic oscillations in frequency ranges associated with sensory feedback (Gillies et al. 2017). This result indicates the possible presence of electrophysiological abnormalities associated with cognitive function in the BG. In chapter 3, we examined the electrophysiological activity of the ACC during the same IED cognitive task, revealing ERP in the dACC in the theta (3-8 Hz) frequency range in response to stimuli varying by familiarity and the valence of feedback. We were restricted to specific subject conditions, however, due to our use of DBS patients in these studies. PD patients were only available with electrodes in the GPi, as the clinical validity of DBS stimulation during PD in this region is well accepted (Anderson et al. 2005; Tagliati 2012). ACC patients with chronic pain allowed for recordings in patients with “normal” executive function, but did not allow for any probing of the influences of dopamine-related disease state upon ACC function. Using the 6-OHDA dopamine cell-lesioned, hemiparkinsonian rat, we had the opportunity to probe questions that arise in chapter 2 and 3 that are currently difficult to answer in the human. By investigating the parkinsonian BG thalamocortical circuit and its connections with the ACC during a cognitive task using the rat model, we may be able to reveal

electrophysiological abnormalities that may be used as biomarkers to better understand the basis of PD cognitive impairment. At the same time, we may be able to gain insight into the significance of such biomarkers through understanding the electrophysiological factors underlying them, which may be further extrapolated to better understanding the human condition.

This study used awake, behaving 6-OHDA-lesioned hemiparkinsonian rats performing a circular treadmill walking task to compare synchronized activity in the ACC, STN, and VM. Electrode bundles were implanted in the ACC, STN, and VM of rats with either unilateral dopamine cell lesions or saline-controls. Rats were trained to expect epochs of treadmill walking after a tone, with subsequent epochs manipulating expectancy through tone-to-walk and tone-to-no-walk epochs. LFPs and spiking activity were recorded during epochs surrounding auditory stimuli and treadmill walking in control animals and 7, 14, and 21 days after dopamine cell lesion. We expanded our frequency bands of focus in Chapter 4 to now include theta (4 – 11 Hz), alpha (12 – 19 Hz), low beta (20 – 29 Hz), and high beta (30 – 36 Hz) frequency ranges. Theta is thought to be involved in a variety of executive function demands, including the adjustment of behavior following unexpected changes in task demands (Womelsdorf et al., 2010). Alpha band activity has been demonstrated to track with attention and stimulus predictability (Bauer et al. 2014; Friston et al. 2015). Beta has also been shown to have implications in cognitive function, including top-down stimulus-response mappings in trained behaviors (Bressler and Richter 2015).

5.2 Methods

All experiments were conducted in accordance with the *NIH Guide for Care and Use of Laboratory Animals* and were approved by the NINDS Animal Care and Use Committee. Every effort was made to minimize the number of animals used and their discomfort. All subjects, surgical procedures, lesions, electrode placement, histology and immunochemistry methods were performed identically to those appearing in the methods section of Chapter 4. Please refer to Chapter 4.2 for a more detailed description of the above techniques. Newly introduced methods for this chapter are detailed below.

5.2.1 Audio Stimuli Task

This cognitive task was designed to mimic some of the neural paradigms seen in the IED task used in Chapters 2 and 3 (Figure 5.2.1a). Starting a week before surgery, male Long Evans rats were trained 1 hr/day for 5 - 7 daily sessions during which rats were encouraged to walk on a circular treadmill in the counterclockwise direction for 6 - 8 epochs of 150 s. A 5 s long, 1 kHz tone was played 15 s prior to treadmill power onset. A tonal frequency of 1 kHz is known to be well within the normal hearing range of rats (J. G. Turner et al. 2005). Tones and walking epochs alternated with 100 s periods of treadmill-off "rest."

Seven days post-surgery, rats exhibited difficulty walking as explored in chapter 4. Rats performed the walking task again, with an introduced cognitive event (5.2.1b). After 4 consecutive tone-to-walk and rest epochs, a rule change occurred, wherein an epoch of tone-to-no-walk occurred. These events alternated across a recording session as shown in figure 5.2.1. The 4^{th} epoch in a consecutive series of 4 tone-to-treadmill-on epochs was considered an

"expected" walking epoch. The 1st instance of a rule change on a given recording day, wherein the treadmill fails to turn on after a tone is played, was treated as an "unexpected" epoch.

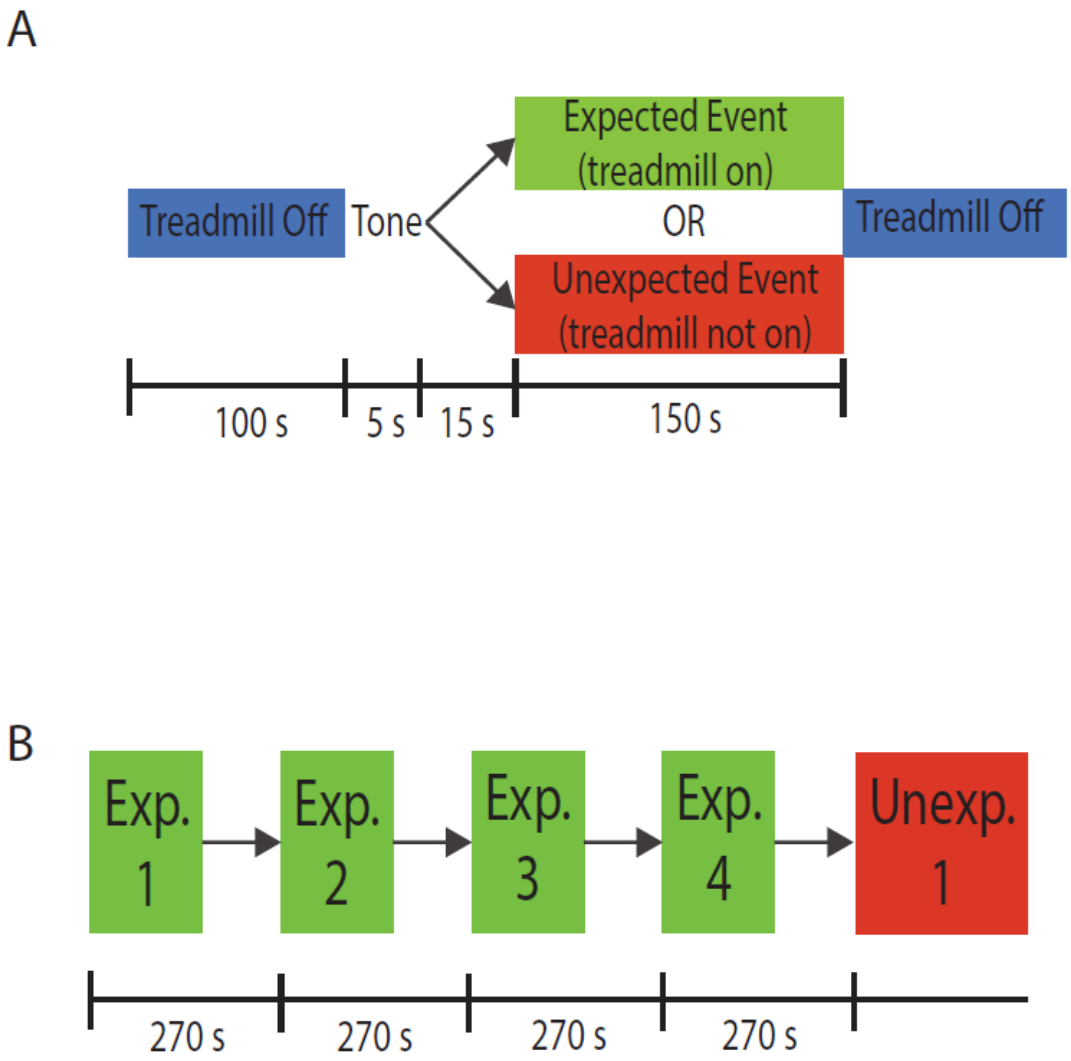

Figure 5.2.1. Schematic Representation of Event and Sequence of Events
A. Graphic representation of tone cognitive event. A 100 s epoch of treadmill off (periods where rat does not move during treadmill off provide the analyzed rest epochs) is followed by a 5 s tone. A 15 s interlude after tone is followed by either the expected event (the treadmill turns on) or the unexpected event (treadmill is not turned on). Either event lasts for 150 s and is followed by the next treadmill off rest epoch.
B. Sequence of events across a recording session. 4 consecutive epochs of expected events and their respective rests (each lasting a total of 270 s, the 4th expected event is the analyzed expected epoch) are followed by an unexpected treadmill off epoch (150 s, the analyzed unexpected epoch).

5.2.2. Signal Processing and Analyses

Periods of LFP and spike recordings, free of major artifacts such as those caused by rearing or turning, were taken for analysis. Direct observation and videotaped motor behavior were used for the selection of epochs representing different behavioral states. The three behavioral states analyzed on a given recording day were rest, epochs of "expected" walking following tone, and epochs of "unexpected" no walking following tone. For LFP power and coherence, and for STWA, epochs of approximately 100 s were taken during walking on the circular treadmill in the direction ipsiversive to the lesioned hemisphere, unless otherwise indicated. Variable length epochs of inattentive rest were also analyzed.

The techniques for spectral analysis of LFP recordings were the same as those described in Chapter 4.

Using a MATLAB script, total power was calculated for each structure in multiple frequency ranges: theta (4 – 11 Hz), alpha (12 – 19 Hz), low beta (20 – 29 Hz), and high beta (30 – 36 Hz). LFP power from 3 – 4 channels per bundle with one epoch/day/rat for each behavioral condition were averaged. Data are reported as mean ± SEM. FFT-based spectral coherence was calculated for each pair of electrodes (ACC-STN and ACC-VM) using a MATLAB script.

Wavelet-based time frequency representations of the signal were generated with Morlet wavelets using 128 frequency scales (Time-Frequency Toolbox). Time-frequency coherence was calculated using FFT-based coherence over a 10 s sliding window using EEGLAB (Brunner et al. 2013; Delorme and Makeig 2004; Delorme et al. 2011). Walk epochs were divided into expected treadmill on trials and unexpected treadmill off trials. Baseline prior to tone onset (-20 s to -15 s) was subtracted. EEGLAB commands were used to generate ERSP and coherence over 6 s surrounding the treadmill being turned on (expected) or not on

(unexpected). ERSP measure the average dynamic changes in amplitude of the power spectrum as a function of time relative to an event (Makeig et al., 1993).

5.2.3 Statistical Analyses

Data are presented as the mean ± SEM. Total LFP power, pairwise coherence, and STWA ratios in both lesioned and non-lesioned hemispheres were statistically compared using repeated-measures 1-way or 2-way ANOVA with time or frequency as the repeated measure. The difference between variable groups was statistically assessed using grouped *t* test. Statistical analysis was generated using Microsoft Excel or Sigma Plot. The minimum criteria for significance was $\alpha = 0.05$. Dashed horizontal lines on coherence and STWA percent correlated spike train plots indicate the $p = 0.05$ level of significance.

5.3 Results

5.3.1 Power Spectra, Spectrograms, Coherograms, and Peak Frequency Findings

To examine the oscillatory activity within and between the ACC and its connections, FFT-based power spectra were created from STN, ACC, and VM recordings in non-lesioned control animals (STN n = 5 rats, ACC n = 9 rats, VM n = 4 rats) and in animals 21 days after 6-OHDA lesion (STN n = 9 rats, ACC n = 21 rats, and VM n = 12 rats) (Figure 4.3.1.2). Power spectra were produced for epochs where the treadmill turned on after a tone ("expected") and epochs where the treadmill did not turn on after the tone ("unexpected"). The most distinctive finding was the development of a peak in the high beta (30 – 36 Hz) frequency band after 6-OHDA lesion in all three regions of interest in the expected walking epochs. These results are consistent with Chapter 4 results. A sharp peak in the theta (4 – 11 Hz) frequency band appears in the STN and in the VM thalamus, and appeared more broadly in the ACC. In the unexpected epoch where treadmills were not turned on, a similar (but weaker) high beta peak was also observed. Likewise, a small theta peak developed in lesioned and control animals in the STN and VM, and only in control animals in the ACC.

Wavelet-based spectrograms and coherograms were produced for both behavioral states for day 7 and day 21 post lesion (Figure 5.3.1). The development of a high beta frequency band, as seen in power spectra, is even more pronounced in the coherograms. This band develops in both conditions, in all 3 regions, with power in increasing order in the VM, STN, and ACC. The peak frequency of this phenomena appears to oscillate in the unexpected event from above 30 Hz

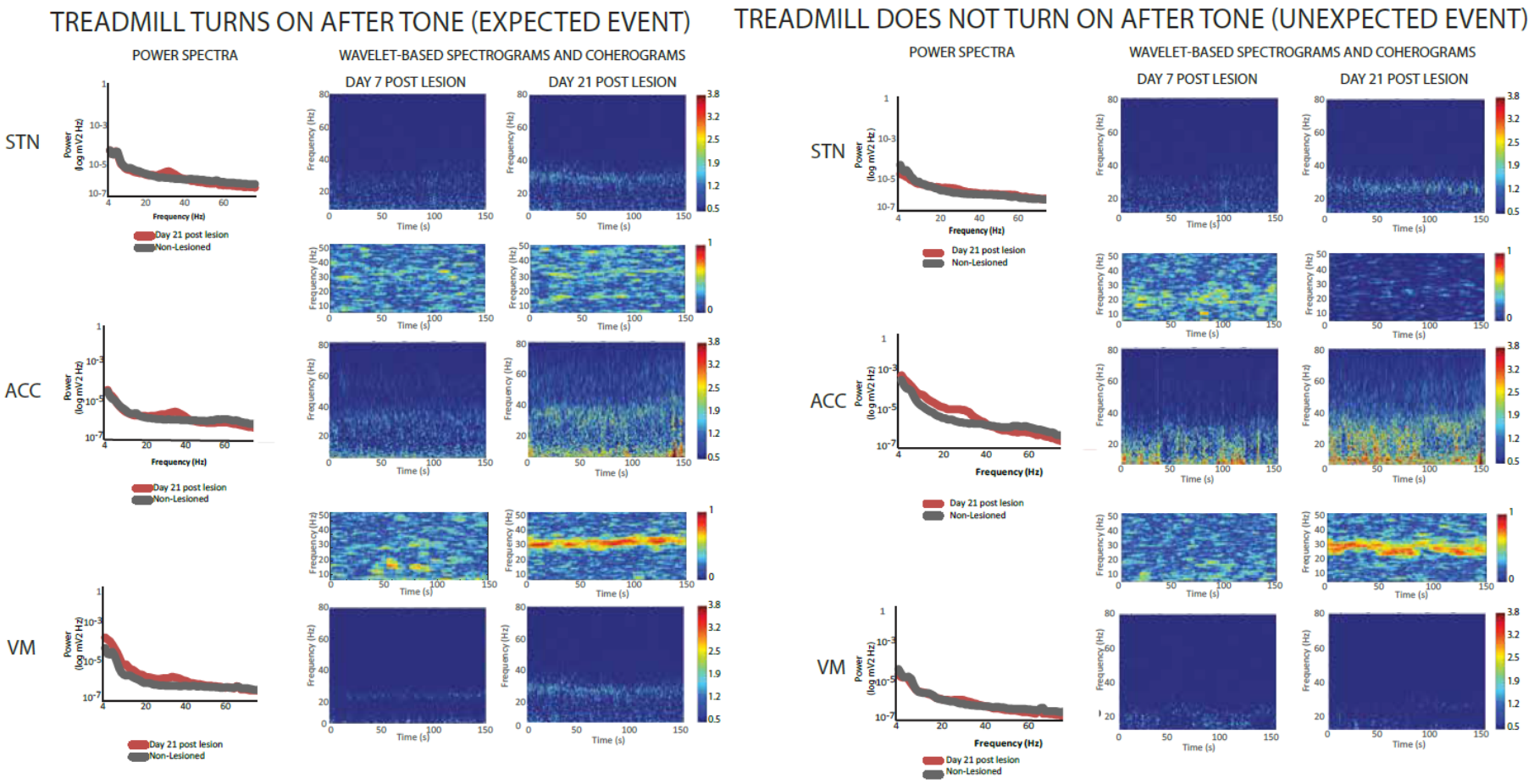

Figure 5.3.1. LFP power in paired recordings from the non-lesioned rats and from lesioned rats 7 and 21 days post lesion during expected and unexpected treadmill events

Log-scale averaged power spectra from STN, ACC, and VM from lesioned (red) and non-lesioned (gray) rats during expected and unexpected events. Representative time-frequency wavelet-based scalograms of LFP power (spectrograms) and coherence (coherograms) in recordings from VM, ACC, and VM during expected and unexpected epochs at day 7 and 21 post-lesion. Power is plotted on a logarithmic scale with greater values represented by red. Note the emergence of a high beta (30-36 Hz) band in the weeks after 6-OHDA lesion.

to below 30 Hz in coherence between the ACC and VM, perhaps justifying a cutoff between rat high and low beta at this point.

Table 5.3.1 shows the mean (± SEM) peak frequencies in each frequency band in the STN, ACC, and VM during expected walking epochs and unexpected non-walking epochs. For many frequency bands, there are no significant long-term variations in peak-frequency after 6-OHDA lesion ($p > 0.05$). Non-lesioned STN high beta (in-so-far that non-lesioned STN has high beta LFP) initially decreased in peak-frequency during the 1st week after lesion (non-lesioned 32.6 ± 0.5 Hz vs. lesioned 30.6 ± 0.1 Hz) but returned to non-lesioned levels by day 21 post lesion. During unexpected epochs, STN alpha (non-lesioned 15.8 ± 0.5 Hz vs. lesioned 14.1 ± 0.5 Hz) decreased while low beta (non-lesioned 21.2 ± 0.2 Hz vs. lesioned 23.1 ± 0.6 Hz) increased ($p < 0.05$). ACC theta peak-frequency in the expected event decreased after lesion (non-lesioned 5.7 ± 0.3 Hz vs. lesioned 4.8 ± 0.1 Hz) while both alpha (non-lesioned 13.7 ± 0.2 Hz vs. lesioned 14.7 ± 0.2 Hz) and low beta (non-lesioned 22.9 ± 0.3 Hz vs. lesioned 25.1 ± 0.3 Hz) increased post-lesion ($p < 0.05$). During unexpected epochs, the ACC also had a decrease in theta peak-frequency after lesion (non-lesioned 5.6 ± 0.2 Hz vs. lesioned 5.0 ± 0.2 Hz), while alpha band peak-frequencies initially increased over the 1st 2 weeks after lesion relative to the non-lesioned state, but returned to parity by day 21 post-lesion ($p < 0.05$). In the VM, low beta peak-frequencies significantly increased in the expected epochs post-lesion (non-lesioned 22.3 ± 0.2 Hz vs. lesioned 23.6 ± 0.4 Hz) while high beta has a slight decrease in peak-frequency at day 14 that returned to parity with non-lesioned frequencies by day 21 ($p < 0.05$). During the unexpected event, theta peak-frequencies in the VM initially decreased after lesion, but returned to pre-lesion levels by day 21 ($p < 0.05$).

EXPECTED EVENT

STN

		Non-Lesioned	Post Lesion 7	Post Lesion 14	Post Lesion 21
Theta	4 - 11 Hz	6.7 ± 0.4#	6.3 ± 0.5	6.0 ± 0.4	6.0 ± 0.3#
Alpha	12 - 19 Hz	14.0 ± 0.3#	14.2 ± 0.3#	14.2 ± 0.5	13.8 ± 0.3
Low Beta	20 - 29 Hz	21.7 ± 0.6	22.0 ± 0.5	22.3 ± 0.3	22.1 ± 0.6
High Beta	30 - 36 Hz	32.6 ± 0.5	30.6 ± 0.1*	32.7 ± 0.6#	33.2 ± 0.4

EXPECTED EVENT

ACC

		Non-Lesioned	Post Lesion 7	Post Lesion 14	Post Lesion 21
Theta	4 - 11 Hz	5.7 ± 0.3	5.3 ± 0.2	6.3 ± 0.3#	4.8 ± 0.1*
Alpha	12 - 19 Hz	13.7 ± 0.2	14.8 ± 15.1*	15.1 ± 0.3*	14.7 ± 0.2*
Low Beta	20 - 29 Hz	22.9 ± 0.3	23.5 ± 0.4	25.0 ± 0.4*	25.1 ± 0.3*#
High Beta	30 - 36 Hz	32.1 ± 0.2	31.7 ± 0.2	32.2 ± 0.2#	32.3 ± 0.2#

EXPECTED EVENT

VM

		Non-Lesioned	Post Lesion 7	Post Lesion 14	Post Lesion 21
Theta	4 - 11 Hz	6.3 ± 0.2	6.4 ± 0.2#	5.9 ± 0.2	5.8 ± 0.2
Alpha	12 - 19 Hz	14.2 ± 0.2	14.5 ± 0.2	14.1 ± 0.2	14.0 ± 0.2#
Low Beta	20 - 29 Hz	22.3 ± 0.2	22.6 ± 0.3	23.3 ± 0.5*	23.6 ± 0.4*
High Beta	30 - 36 Hz	32.2 ± 0.3	32.1 ± 0.2	31.5 ± 0.2*	32.1 ± 0.2

UNEXPECTED EVENT

STN

		Non-Lesioned	Post Lesion 7	Post Lesion 14	Post Lesion 21
Theta	4 - 11 Hz	5.1 ± 0.4#	6.1 ± 0.4	5.1 ± 0.3	4.4 ± 0.2#
Alpha	12 - 19 Hz	15.8 ± 0.5#	13.3 ± 0.2*#	14.4 ± 0.5	14.1 ± 0.5*
Low Beta	20 - 29 Hz	21.2 ± 0.2	21.3 ± 0.2	23.1 ± 0.7*	23.1 ± 0.6*
High Beta	30 - 36 Hz	31.6 ± 0.4	30.9 ± 0.3	31.3 ± 0.4#	32.0 ± 0.5

UNEXPECTED EVENT

ACC

		Non-Lesioned	Post Lesion 7	Post Lesion 14	Post Lesion 21
Theta	4 - 11 Hz	5.6 ± 0.2	5.7 ± 0.3	4.9 ± 0.2*#	5.0 ± 0.2*
Alpha	12 - 19 Hz	13.8 ± 0.2	15.1 ± 0.3*	14.7 ± 0.2*	14.3 ± 0.2
Low Beta	20 - 29 Hz	23.3 ± 0.4	22.5 ± 0.3	24.1 ± 0.3	23.8 ± 0.3#
High Beta	30 - 36 Hz	31.9 ± 0.2	31.6 ± 0.2	31.4 ± 0.2#	31.6 ± 0.2#

UNEXPECTED EVENT

VM

		Non-Lesioned	Post Lesion 7	Post Lesion 14	Post Lesion 21
Theta	4 - 11 Hz	6.5 ± 0.3	5.4 ± 0.2*	5.3 ± 0.2*#	6.2 ± 0.3
Alpha	12 - 19 Hz	14.2 ± 0.3	14.4 ± 0.3	13.9 ± 0.2	14.6 ± 0.2#
Low Beta	20 - 29 Hz	22.7 ± 0.3	22.2 ± 0.3	22.8 ± 0.4	22.6 ± 0.4
High Beta	30 - 36 Hz	31.8 ± 0.3	32.1 ± 0.3	31.5 ± 0.2	31.6 ± 0.2

Table 5.3.1 Mean Peak-Frequencies during Expected and Unexpected Epochs in STN, ACC, and VM in Each Frequency Band
All values show the mean peak-frequency (Hz) ± SEM, averaged across all animals. Peak-frequencies that are significantly different ($p < 0.05$) from the baseline peak-frequency in the non-lesioned condition are indicated with an asterisk (*). Values that are significantly different between behavioral paradigms are indicated with a number sign (#).

5.3.2 Theta Frequency Findings

To gain further insight into the roles of the STN, ACC, and VM in mechanisms underlying PD cognitive declines, mean LFP power analysis in the theta frequency band (4 – 11 Hz) was performed for STN, ACC, and VM (Figure 5.3.2). Coherence analysis between STN and ACC and between VM and ACC was also examined during epochs of expected treadmill walking and unexpected treadmill off (Figure 5.3.2). Normalized theta band power significantly increased after dopamine cell lesion (1485 ± 138), as compared to non-lesioned rats (1018 ± 208), in the ACC in expected events ($p < 0.05$). Theta band coherence was observed to significantly decrease between the STN and ACC after lesion during both expected (non-lesioned 0.22 ± 0.02 vs. lesioned 0.16 ± 0.01) and unexpected (non-lesioned 0.22 ± 0.01 vs. lesioned 0.15 ± 0.01) epochs ($p < 0.05$). Coherence between the VM and ACC increased (non-lesioned 0.21 ± 0.01 vs. lesioned 0.25 ± 0.01) after lesion during unexpected events ($p < 0.05$).

To gain further insight into the processes underlying the differences in LFP amplitude and coherence in the ACC, VM, and STN, analyses on the dynamics of spiking in the form of correlated spike trains locked to theta were performed and can be seen in Figure 5.3.2. Rats in the attentive rest behavioral state exhibited significant increases in spike to theta LFP correlation in every region and between regions, except in the STN ($p < 0.05$). The percent of correlated spike trains locked to theta became significantly larger after 6-OHDA lesion during unexpected events relative to attentive rest while during expected event, the percent of correlated spike trains decreased relative to rest ($p < 0.05$). Within the STN (n = 22 cells), and for STN spikes to ACC LFP correlation, these values did not change after lesion ($p > 0.05$). ACC (n = 50 cells) spiking to VM LFP correlations exhibited increases in percent in unexpected epochs relative to expected walking epochs ($p < 0.05$).

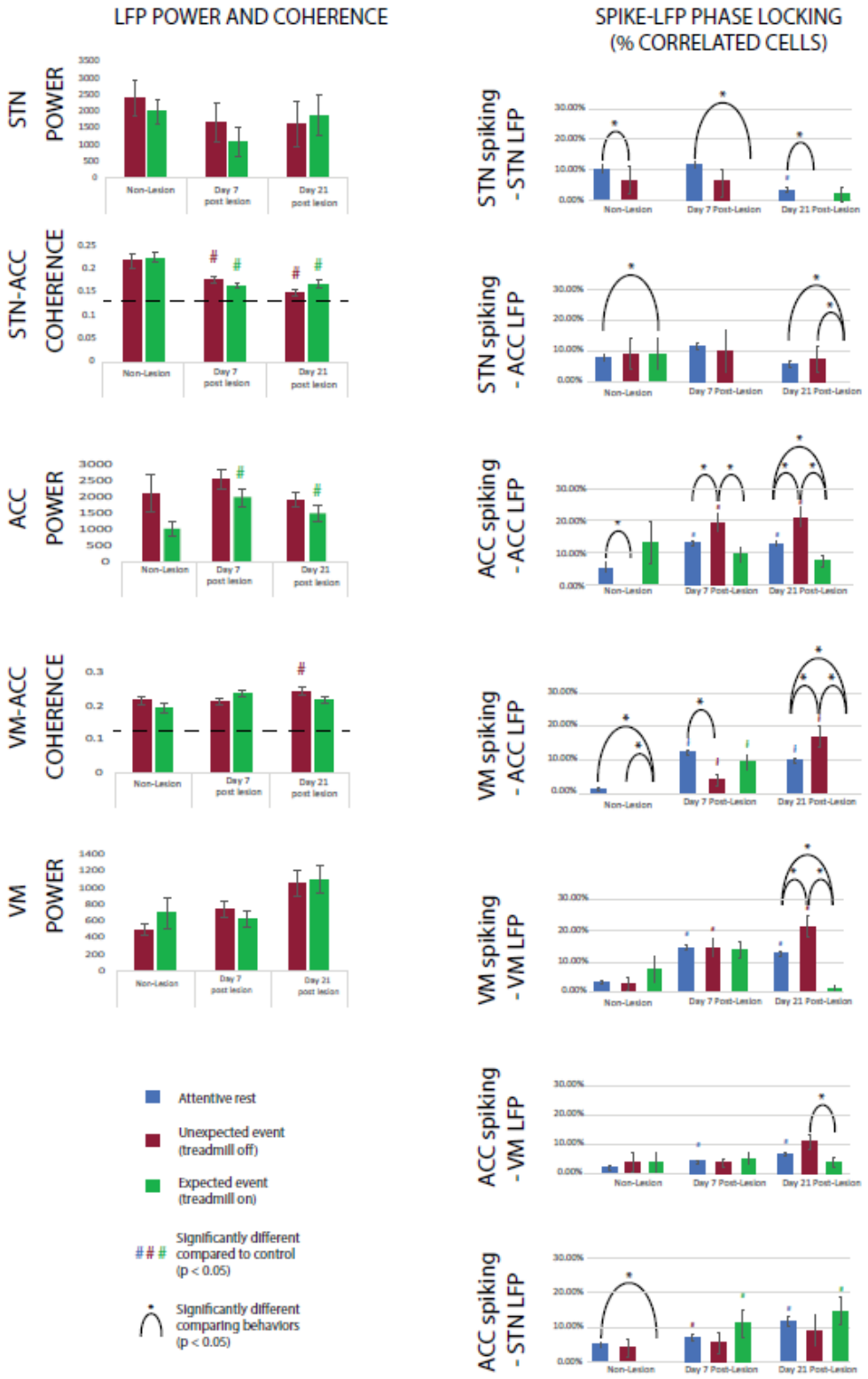

Figure 5.3.2. Theta (4-11 Hz) LFP power, coherence, and spike-LFP synchronization
Averaged total LFP power (mean ± SEM) within the discrete theta frequency band during expected (green) and unexpected (red) events show increases after lesion in ACC power during expected epochs, VM power during unexpected epochs, and decreases in STN-ACC coherence after both behaviors relative to non-lesioned rats ($p < 0.05$). Black horizontal line in coherence plots indicates significant coherence ($p < 0.05$) between regions. Spike-LFP phase locking plots display the proportion of spike-triggered waveform averages (STWA) showing significant phase-locking of spike trains with LFP activity in the theta range. These values become significantly higher during the unexpected event and during rest epochs after lesion relative to expected walking epochs in VM, ACC, and in STN- and VM-spiking phase locking to ACC ($p < 0.05$).

ACC spiking to STN LFP correlations increased during epochs of expected walking after lesion ($p < 0.05$).

5.3.3 Alpha Frequency Findings

For both behavioral paradigms, power analysis in the alpha frequency band (12 – 19 Hz) was performed for STN, ACC, and VM and coherence analysis between STN and ACC and between VM and ACC (Figure 5.3.3). In STN and VM, no significant changes in LFP power were seen between non-lesioned and lesioned animals. The ACC develops significant increases in normalized alpha power during unexpected treadmill off epochs (non-lesioned 745.47 ± 214.94 vs. lesioned 1151.18 ± 189.49) and a temporary increase on day 7 post-lesion during expected walking epochs (non-lesioned 385.37 ± 132.46 vs. lesioned 615.80 ± 86.21) that ceased by day 21. STN-ACC alpha-band coherence during both behaviors (unexpected 0.14 ± 0.01 and expected 0.14 ± 0.01) decreases to within the margin of error for coherence significance after lesion. ACC normalized power during unexpected epochs becomes significantly larger after lesion compared to expected epochs. VM power maintains the status quo after lesion wherein unexpected events have a significantly larger normalized power than expected events. Alpha coherence between the VM and ACC has significant differences between expected and unexpected epochs in the non-lesioned state that ceases after lesion. When examining spiking locked to alpha, the percent of spike trains locked to alpha band LFPs during expected walking epochs becomes significantly lower than that seen during rest after lesion. Unexpected treadmill epochs also develop significantly higher percents of spike-LFP correlations than expected walking epochs within the ACC and VM, and between the VM (n = 48 cells) and ACC.

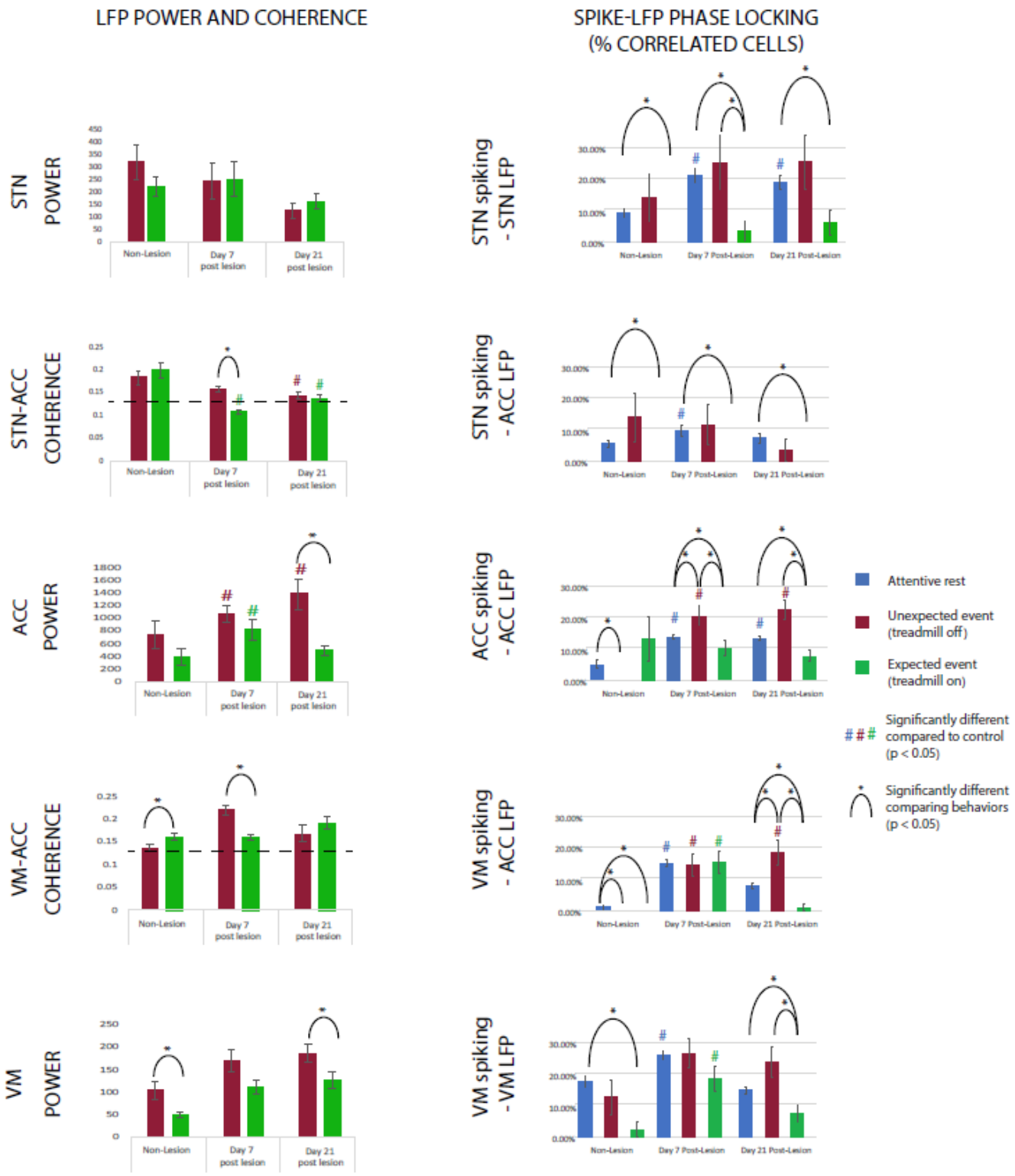

Figure 5.3.3. Alpha (12-19 Hz) LFP power, coherence, and spike-LFP synchronization
Averaged total LFP power (mean ± SEM) within the discrete alpha frequency band during expected (green) and unexpected (red) events show increases after lesion in ACC power during expected events and decreases in STN-ACC coherence during both behaviors relative to non-lesioned rats ($p < 0.05$) ACC power during unexpected epochs becomes higher relative to expected walking epochs. Black horizontal line in coherence plots indicates significant coherence ($p < 0.05$) between regions. Spike-LFP phase locking plots display the proportion of spike-triggered waveform averages (STWA) showing significant phase-locking of spike trains with LFP activity in the alpha range. These values generally become higher in unexpected and rest epochs relative to expected epochs.

5.3.4 Low Beta Frequency Findings

For both behavioral paradigms, power analysis in the low beta frequency band (20 – 29 Hz) was performed for STN, ACC, and VM and coherence analysis was performed between STN and ACC and between VM and ACC (Figure 5.3.4). As seen in alpha band power analysis (Chapter 5.3.3), there were no significant differences between low beta band normalized power before and after lesion, or across behaviors in the STN or VM ($p > 0.05$). ACC LFP low beta power increases during both expected (non-lesioned 359.18 ± 125.30 vs. lesioned 579.81 ± 86.64) and unexpected epochs (non-lesioned 432.29 ± 92.58 vs. lesioned 1112.82 ± 168.37) after 6-OHDA lesion ($p < 0.05$). During unexpected epochs, both STN-ACC (non-lesioned 0.14 ± 0.1 vs. lesioned 0.18 ± 0.01) and VM-ACC (non-lesioned 0.13 ± 0.01 vs. lesioned 0.22 ± 0.01) low beta coherence become significant after lesion ($p < 0.05$). During expected epochs, STN-ACC coherence decreases (non-lesioned 0.19 ± 0.1 vs. lesioned 0.14 ± 0.01) after lesion while VM-ACC coherence increases (non-lesioned 0.10 ± 0.00 vs. lesioned 0.23 ± 0.01) ($p < 0.05$). After lesion, ACC power during unexpected events becomes significantly larger than during expected ($p < 0.05$). STN-ACC coherence is higher in expected treadmill on than unexpected treadmill off in non-lesioned rats, and this comparison inverts after lesion ($p < 0.05$).

When examining spiking locked to the low beta frequency band, all three behavioral states see an across-the-board significant increase in spike-LFP locking after lesion ($p < 0.05$). After lesion in STN, ACC, VM, and between VM spikes to ACC LFPs, unexpected treadmill off entrains significantly higher percent of spike trains to low beta frequency than either attentive rest or expected walking epochs ($p < 0.05$). ACC spike trains do not at any point become significantly locked to low beta LFP in either STN or VM ($p > 0.05$).

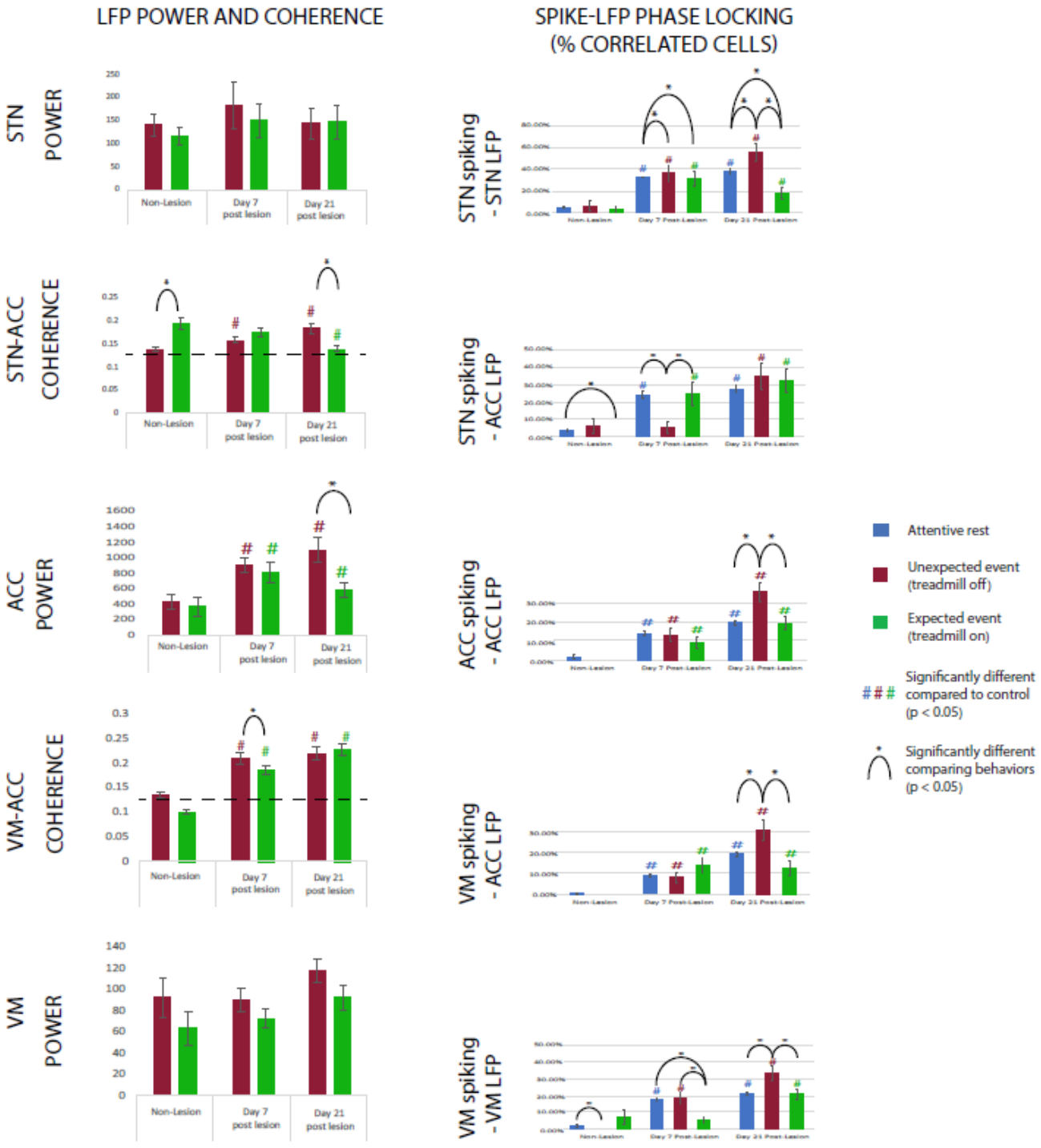

Figure 5.3.4. Low Beta (20-29 Hz) LFP power, coherence, and spike-LFP synchronization
Averaged total LFP power (mean ± SEM) within the discrete low beta frequency band during expected (green) and unexpected (red) events show increases after lesion in ACC power, STN-ACC coherence, and VM-ACC coherence during both behaviors relative to non-lesioned rats ($p < 0.05$). Black horizontal line in coherence plots indicates significant coherence ($p < 0.05$) between regions. Spike-LFP phase locking plots display the proportion of spike-triggered waveform averages (STWA) showing significant phase-locking of spike trains with LFP activity in the low beta range. These values become significantly higher in the weeks following lesion relative to the non-lesioned rat and show differences in phase-locking between behaviors.

5.3.5 High Beta Frequency Findings

For both behavioral paradigms, power analysis in the high beta frequency band (30 – 36 Hz) was performed for STN, ACC, and VM (Figure 5.3.5). Coherence analysis between STN and ACC and between VM and ACC was also performed. High beta spectral power increased during expected walking epochs in the STN (non-lesioned 44.93 ± 5.75 vs. lesioned 67 ± 7.16), ACC (non-lesioned 151.48 ± 22.15 vs. lesioned 247.12 ± 38.87), and VM thalamus (non-lesioned 26.61 ± 6.20 vs. lesioned 48.87 ± 4.30) by 21 days post-6-OHDA-lesion ($p < 0.05$). Likewise, coherence between the STN and ACC (non-lesioned 0.14 ± 0.01 vs. lesioned 0.31 ± 0.02) and between the VM and ACC (non-lesioned 0.12 ± 0.01 vs. lesioned 0.32 ± 0.02) increased after 6-OHDA lesion during expected walking epochs ($p < 0.05$). During the unexpected treadmill off epoch, ACC power (non-lesioned 200.77 ± 35.84 vs. lesioned 287.83 ± 27.50) and VM-ACC coherence (non-lesioned 0.10 ± 0.01 vs. lesioned 0.21 ± 0.01) also increased after lesion ($p < 0.05$). When comparing the 2 behavioral states, after lesion epochs of expected treadmill on invoked a significantly higher coherence between the STN and ACC and between the VM and ACC compared to epochs of unexpected treadmill off ($p < 0.05$).

Consistent with movement-related increases in oscillatory activity observed in LFP power analysis, the percent of spike trains with significant spike-LFP correlations within the STN and VM thalamus, as well as between STN and ACC and between VM and ACC spike-LFP correlations, increased after dopamine-lesion in rest, expected treadmill on, and unexpected treadmill off epochs ($p < 0.05$). ACC spiking to ACC theta LFP during attentive rest is the only exception to this trend ($p > 0.05$). As observed in data restricted to the alpha frequency band

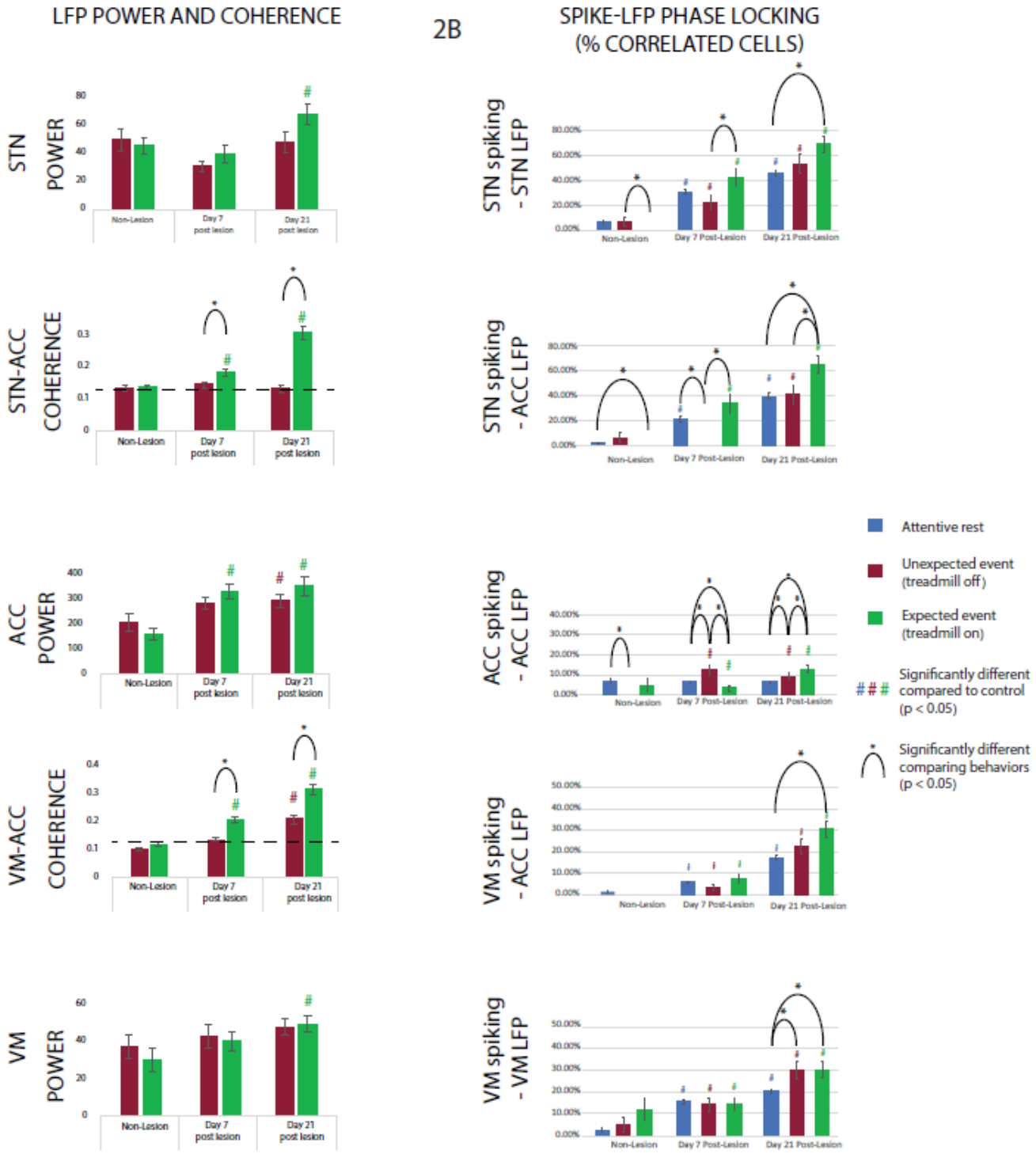

Figure 5.3.5. High Beta (30-36 Hz) LFP power, coherence, and spike-LFP synchronization
Averaged total LFP power (mean ± SEM) within the discrete high beta frequency band during expected (green) and unexpected (red) events show increases after lesion in power and coherence in all recorded regions during expected walking epochs relative to non-lesioned rats ($p < 0.05$). ACC power and VM-ACC coherence also increase following lesion. Expected events provoke significantly higher coherence between VM-ACC and STN-ACC compared to unexpected events. Black horizontal line in coherence plots indicates significant coherence ($p < 0.05$) between regions. Spike-LFP phase locking plots display the proportion of spike-triggered waveform averages (STWA) showing significant phase-locking of spike trains with LFP activity in the high beta range. These values become significantly higher in the weeks following lesion (modestly in ACC) relative to the non-lesioned rat and show phase-locking during expected walking to generally be higher than that seen during rest or unexpected events.

(Figure 5.3.3) and the low beta frequency band (Figure 5.3.4), there were no significant ACC spike trains locked to either STN or VM high beta LFPs, as STWA peak-to-trough ratios were below 1 ($p > 0.05$). Likewise, as seen in Chapter 3, spike trains locked to high beta LFP in the ACC had ratios bordering on 1, suggesting that ACC spiking may not significantly phase-lock to ongoing oscillatory activity. Both expected and unexpected epochs saw increases in the percent correlated spike trains, as compared to attentive rest, in VM spike trains locked to VM LFPs and ACC LFPs ($p < 0.05$). Expected treadmill on epochs saw increases in the percent correlated spike trains in STN and STN to ACC spike-LFP correlation ($p < 0.05$).

5.3.6 Event-Related Findings

As in Chapters 2 and 3, analyses were performed to attempt to identify event-related phenomena during cognition (Figure 5.3.6). ERSP and coherence was calculated for a 50 s window centered on either expected treadmill on or unexpected treadmill off. Coherence analysis between the ACC and STN reveals a baseline level of theta band coherence irrespective of behavior which is reduced after lesion. ERSP analysis reveals a decrease in theta and alpha frequency bands occurring approximately 1 s after the tone begins to play and continuing up to 5 s after the tone ends in the ACC and VM. The intensity of this phenomena decreases after lesion. In epochs of expected treadmill on both before and after lesion, an increase in theta band ERSP in STN and VM occurs after rats begin to walk. At the same time, as rats begin to walk, both alpha and low beta frequency band ERSP decrease. This decrease is paired with the development of the familiar parkinsonian high beta band, and the intensity of both increase in the weeks post-lesion. After lesion, high beta coherence between the VM and ACC and between the STN and ACC strengthens across both rest and walking epochs. The peak frequency of the high beta band coherence can be seen to increase after walk onset. An

increase in gamma band activity (> 30 Hz) occurs in the STN, ACC, and VM after treadmill walking begins in the non-lesioned animal. After lesion, the STN no longer develops gamma during walking, while the ACC and VM both exhibit large increases in gamma ERSP.

As seen during expected walking epochs, control rats exhibit theta band coherence between the ACC and STN that disappears after lesion. During unexpected treadmill off, a small increase in theta ERSP can be seen in ACC and VM. This may be a similar phenomenon to the unexpected theta signal seen in human subjects in Chapter 3. High beta coherence between the STN and ACC and between the VM and ACC increases after lesion during unexpected treadmill off similar to the increases seen during expected walking epochs.

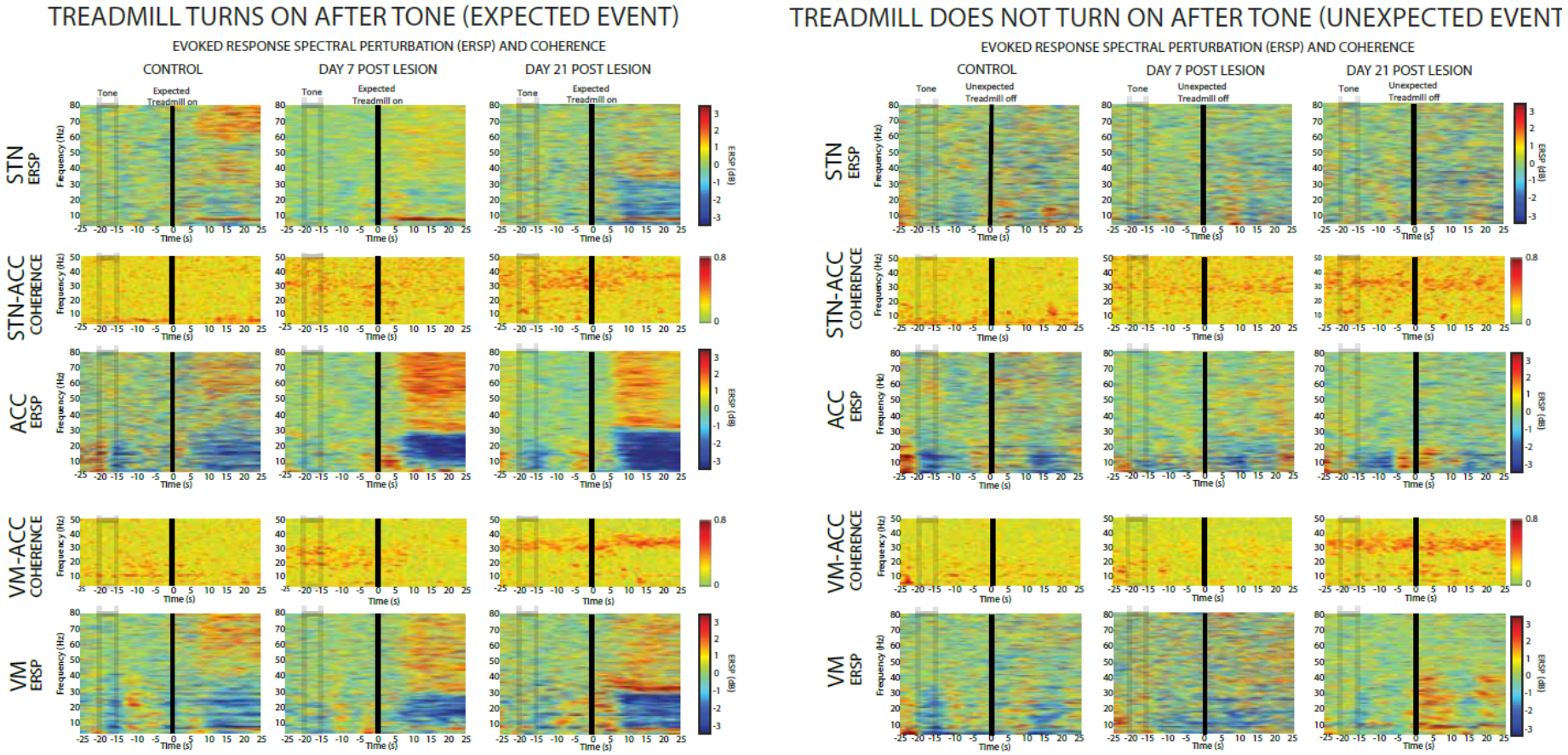

Figure 5.3.6. Event-Related Spectral Perturbation and Event-Related Coherence in STN, ACC, and VM Locked to Treadmill On/Off Event
The ERSP (Makeig, 1993) is a time-frequency analysis that shows mean event-locked deviations from resting baseline-mean power at each frequency. It reflects the extent to which the power at a given frequency of LFP is altered in relation to a specific time point, in this case the treadmill either turning on (expected) or not turning on (unexpected). The duration of the tone is marked on the plot, lasting from -20 s to -15 s prior to the treadmill event. LFP Coherence between STN-ACC and VM-ACC over the same time-period locked to the same treadmill event.

5.4 Discussion

Chapter 4 showed us that the connections between the ACC and the BG allow the ACC to be affected by changes in BG output after dopamine loss with the development of excessively synchronized high beta activity during a walking task (Herkenham 1979; Kuramoto et al. 2009). The aim of the research described in this chapter was to explore this connection further by determining if and how the loss of dopamine affects ACC (along with VM and STN) activity during a walking task with a cognitive component in the hemiparkinsonian rat model of PD. These results provided a series of observations supporting the view that the BG thalamocortical circuit develops both exaggerated oscillatory activity and spike-to-LFP phase locking during cognition in the hemiparkinsonian rat model of advanced-stage PD.

5.4.1 Theta Frequency Findings

After 6-OHDA lesion, theta (4 - 11 Hz) spike-LFP phase-locking in the ACC and VM increased during rest and unexpected treadmill off (Figure 5.3.2). The percent correlated phase locking in ACC and VM increased after dopamine lesion. This occurred, in increasing order, during epochs of expected treadmill on, rest, and unexpected treadmill off. Rats focused on walking exhibit the fewest cells phase-locked to theta. This may reflect increasing levels of attention or expectancy, and, as PFC theta is known to be involved in these functions, may disrupt normal function (Babapoor-Farrokhran et al. 2017; Basar et al. 1999, 2000; Hernandez-Gonzalez et al. 2017; Solomon et al. 2017). After 6-OHDA lesion, theta (4 - 11 Hz) STN-ACC coherence decreases while ACC theta LFP power increases (Figures 5.3.2 and 5.3.6). No differences were observed in theta power between event types. Coherence between the STN

and ACC in the theta band has been shown to reflect adjustments in conflict and error management (Zavala et al. 2016). This decrease in baseline theta coherence after lesion may suggest a cause for PD executive function deficits. Theta oscillatory bands have been shown to nest within and thus be directly affected by faster beta oscillations (Jensen and Lisman 2005; Kopell et al. 2000), so it is plausible that the increase in synchronized beta band activity observed in PD may disrupt normal physiological theta band activity.

5.4.2 Alpha Frequency Findings

Alpha band (12 - 19 Hz) power has been shown to express, not necessarily cortical inactivity, but an inverse relation to cortical arousal (Klimesch 1999; Laufs et al. 2003; Neuper and Pfurtscheller 2001). Conversely, a second view on alpha frequency response has described the involvement of alpha frequency increases during working memory tasks and cognitive performance (Klimesch et al. 1993; Klimesch 1996; Klimesch et al. 1997; Klimesch 1999). These 2 conflicting insights operate and reflect different cognitive requirements: alpha power decreases during cognitively demanding or arousing periods (such as reacting to stimuli) and increases during memory consolidation. In light of these views of the alpha frequency band, perhaps one should ask if event-related desynchronization can be considered a cognitive marker. In our recordings, alpha power was seen to increase in the lesioned ACC relative to the non-lesioned rat, during the unexpected treadmill off epoch. Additionally, after lesion, this difference in ACC alpha power becomes significant between expected and unexpected states. This brings the ACC in line with the behavior of alpha LFP power in the VM before and after lesion. Meanwhile, ERSP analyses show decreases in alpha power after the tone plays and after the start of treadmill walking or treadmill off. These findings agree to some extent with prior research. Alpha power can be observed to decrease as shown by ERSP analysis (Figure 5.3.6)

as these analyses are locked to the period of highest cognitive load: stimulus onset during both expected and unexpected epochs. Consequently, when observing alpha power and spike-locking over the entire 150 s (Figure 5.3.3), alpha power is seen to be highest in the non-lesioned rat only in the VM. This observation remains unchanged after lesion. The ACC and the STN paradoxically do not exhibit this phenomenon in the non-lesioned state. The ACC does come into line with the VM, but only after lesion in the dopamine-depleted state. This appears to reflect an excessive increase in alpha power relative to that seen in the non-lesioned state. The ACC's increase in alpha power in the unexpected non-walking behavior relative to the expected walking may reflect poor memory performance. Regardless, the findings here echo the complaints of Knyazev *et al*. (Knyazev et al. 2006). It is not clear how the same mechanisms might be linked with both perceptual activation, as seen in our phase-locked evoked alpha oscillations and described by Basar *et al.*, (Basar et al. 1999), and perceptual inhibition as proposed by event-related alpha synchronization seen in our power analyses (Basar et al. 2013). Meanwhile, relatively few studies have focused on task-related shifts in alpha frequency, although the work of Osaka does agree with our findings in the control state in the STN (Table 5.3.1), that as a task becomes more difficult, alpha peak-frequency increases in tandem (Osaka 1984). Alpha peak frequency significantly increases after lesion during both the expected event (days 7 through 21) and in the unexpected event (days 7 and 14). While power and spiking findings are not so easily explained, this change in peak-frequency may be a possible route through which alpha frequency-driven PD executive dysfunction occurs. Interestingly, alpha peak frequency in humans was found to be significantly higher in PD subjects experiencing L-DOPA-induced dyskinesias compared to PD subjects experiencing impulse control disorder symptoms, showing some additional precedence for behavior-related changes in alpha peak frequency in the parkinsonian state (Rodriguez-Oroz et al. 2011).

5.4.3 High Beta Frequency Findings

As previously shown in Chapter 4, 6-OHDA-induced dopamine cell lesion leads to significant increases in ACC LFP oscillatory activity in the high beta frequency range (30 – 36 Hz) as compared to non-lesioned rats. In the current results, during a walking task with an added cognitive component, we see similar increases in ACC high beta LFP power and ACC LFP coherence with both VM and STN. Mean LFP power in this 30 – 36 Hz range was significantly higher during expected treadmill walking epochs relative to rest and, for mean LFP coherence, relative to unexpected treadmill off epochs (Figures 5.3.1 and 5.3.5). These results are similar to reports in PD patients showing increases in synchronized oscillatory activity in the STN after the loss of dopamine (Alonso-Frech et al. 2006; P. Brown and Marsden 2001; Levy et al. 2002). They are also similar to findings from previous studies in hemiparkinsonian rats examining neuronal synchronization between and within the MCx and the BG-thalamus circuit in the dopamine-lesioned rat during treadmill walking (Brazhnik et al. 2012; Brazhnik et al. 2016; Delaville et al. 2015). Further, they agree with the results discussed in Chapter 3. STN and VM spike trains are strongly phase-locked to ACC high beta LFPs after dopamine-lesion during epochs of expected walking and to a lesser degree during rest and unexpected treadmill off epochs (Figure 5.3.5). High beta LFP power in ACC, VM, and STN LFP is thought to reflect net synchronized input to neurons in these areas. These results are consistent with the view that VM and STN spiking output are also synchronized by this input. In contrast, after dopamine cell lesion, ACC spike trains were less significantly phase-locked to ACC high beta LFP oscillations, suggesting that while common inputs may modulate the STN, VM, and ACC, they fail to induce significant spike-LFP synchronization in the ACC. The presence of high beta oscillatory activity in the ACC may influence cognitive processes, as the non-lesioned ACC does not have synchronized activity at this frequency. That the ACC only modestly expresses phase-locking to its own high beta LFP activity, and does not express

spike train phase-locking to LFPs in either the STN or VM may suggest that, while the ACC expresses high beta, it does not facilitate the propagation of high beta synchronization and possibly does not directly impede movement generation.

5.4.4 Event-Related Potential Findings

ERSP analysis of the epoch around the expected/unexpected treadmill paradigm reveals ERSP decreases in alpha (11 – 20 Hz) after the tone, and in alpha and low beta (11 - 30 Hz) after walking onset. High beta, and its peak frequency, increase after lesion during walking (Figure 4.3.6). Reductions in alpha ERSP relative to a rest baseline may reflect event-related desynchronization, wherein cortical arousal involves the replacement of relatively slow, spatiotemporally coherent cortical rhythms, with faster, more spatially differentiated activity (Makeig 1993; Pfurtscheller and Aranibar 1977). Similarly, event-related changes have been shown to indicate that both alpha desynchronization and theta synchronization are positively correlated with long-term memory performance and the ability to encode new information (Klimesch 1999). Thus, our ERSP findings of decreases in alpha (primarily in ACC and VM) and increases in theta in STN and VM agree with the suggestion that these regions aid in the encoding of new information through theta oscillations (during walking) and in search and retrieval processes reflected by alpha oscillations (after tone and after treadmill on/off). These findings deserve further exploration through ERSP analysis, and future work will explore how these frequency bands modulate over dopamine-state during a variety of behavioral and learning states.

Dopamine has been shown to play a central role in the executive function undertaken by the PFC (Bjorklund and Dunnett 2007; Puig et al. 2014b; Puig et al. 2014a; Schweimer and Hauber 2006; K. Zhang et al. 2007). When considering how the loss of dopamine might affect

information flow through the BG thalamocortical circuit, one must consider that the ACC projects both directly to the STN, as part of the hyperdirect pathway, and indirectly, through the striatum. (Jahanshahi et al. 2015). LFPs, as we record them, are thought to reflect net input to the neurons near a recording electrode. They may also be related to synchronized spiking and the ability of neuronal spiking to lock to a particular phase of ongoing oscillatory activity. Here, we have shown that ACC spiking becomes significantly phase-locked to all 4 examined frequency bands, varying with integrity of the dopamine system and behavior. That the ACC becomes significantly phase-locked with the VM (a source of BG output) and the STN (a BG input via the hyperdirect pathway), during what is both a motor and a cognitive task, is consistent with the idea that the ACC is a component of the greater BG thalamocortical circuit and that such activity is heavily dopamine-dependent.

5.4.5 Limitations

The 6-OHDA-lesioned, hemiparkinsonian rat has only recently been applied for the study of non-motor symptoms of PD (Solari et al. 2013). The animal model, itself, is a limiting factor for this study as in some ways it is not the most appropriate model for progressive, degenerative PD. PD non-motor symptoms are known to arise at an early stage of the disease, when motor faculties are still largely healthy and dopaminergic damage is still < 70 % (Gerlach and Riederer 1996). As our animal model is, instead, primarily designed with motor symptomology in mind, dopaminergic damage is > 90 %. To make a truly suitable non-motor symptom-focused 6-OHDA PD model, one should rather inject the neurotoxin bilaterally into the brain in order to avoid any possible compensatory effects of the non-lesioned hemisphere during behavioral performance (Solari et al. 2013). Bilaterally lesioned animals, however, are

rather high-maintenance (as they exhibit reduced foraging behavior due to their increased motor deficits), so are generally replaced with the more “user-friendly” hemiparkinsonian rat.

A lack of theta power differences between expected treadmill on and unexpected treadmill off may reflect limitations in the study design. Extrapolating electrophysiology over a full period of 150 s may reduce the visibility of the short-term cognitive effects of expected and unexpected occurrences (as seen in Figure 5.3.6). Next steps may be to focus LFP power, coherence, and STWA analyses on a shorter epoch time-locked to a regular event such as performed in Figure 5.3.6, which may better reveal theta band activity changes that are potentially averaged out over longer timespans.

Different frequency ranges have been shown to be associated with different behavioral states in PD animal models, and different frequencies could reflect activity in different neural networks, such as motor or cognitive networks (Brazhnik et al. 2014; Peter Brown et al. 2002; Delaville et al. 2014; Delaville et al. 2015; Fogelson et al. 2006; Oswal et al. 2013). While PD is most known for excessive beta range activity (12 – 30 Hz in humans), gamma (30 – 300 Hz in humans) oscillations have also been reported (Alegre et al. 2005; Alonso-Frech et al. 2006; P. Brown et al. 2001; Priori et al. 2004). We restricted the current rat research to theta, alpha, low beta, and high beta frequency bands, but in future work, we will expand to higher frequency bands. Previous work with hemiparkinsonian rats has shown low gamma coherence between STN and PFC that increases during walking and is affected in the initial days post-lesion (Delaville et al. 2015). The presence of both high beta and low gamma, and as we saw in this chapter, theta, being expressed simultaneously in the STN may suggest its participation in different neural networks. Going forward, looking at BG activity in conjunction with ACC and other PFC sites in gamma frequency ranges may help to probe these issues.

While ERSP reveals new and important information about event-related brain dynamics, it cannot reveal interactions between ERP and LFP modulation. These will be investigated in future works utilizing simultaneous analysis of LFP power and coherence, STWA, ERP, and ERSP.

5.4.6 Concluding Remarks

In the last few decades, the occurrence of nonmotor, cognitive symptoms in PD patients has become an increasingly recognized issue (Solari et al. 2013). As a result, preclinical animal models for the study of PD cognitive impairment have become increasingly necessary. Despite the limitations of the model, hemiparkinsonian rats display some of the most important cognitive symptoms seen in PD patients, including impairment of executive function. Regardless of some of the discrepancies in the data obtained, possibly due to the hemiparkinsonism of the animals, the present study has been able to reproduce some of the electrophysiological dysfunctions in the same anatomical sites found in human subjects. The ACC integrates activity from the STN and VM in a manner that varies with frequency and the integrity of the dopamine system, and this is evident across cognitive behavioral paradigms. These results may help future researchers gain further insight into PD electrophysiology and its influence on cognitive systems. As we go forward, clearer pathophysiological characterizations of the links between motor symptoms and cognitive deficits in PD will be necessary for future therapies designed to manage all aspects of PD.

6. Understanding the Role of the Basal Ganglia Thalamocortical Circuit in Cognition and Parkinson's Disease

This thesis has examined the electrophysiological function of the BG thalamocortical circuit in the dopamine-depleted state of PD and during cognitive and motor activity. Externalized DBS electrodes were used to study the influence of dopamine in the BG of PD and dystonic patients during a test of executive function in Chapter 2. Normal executive function and potential laterality of activity were explored in the dopamine-healthy ACC of chronic pain DBS patients in Chapter 3. Transmission of synchronized oscillatory activity from the BG, through the VM thalamus, to the ACC was examined using chronically implanted recording electrodes in awake, behaving hemiparkinsonian rats in Chapter 4. Modulation of STN, VM, and ACC activity during a simple cognitive/movement task was examined in hemiparkinsonian rats in Chapter 5. This final chapter summarizes the results from these experiments and explores the implications of the ACC's involvement in PD and its potential as a DBS target.

6.1 Summary of Results

6.1.1 Executive Function in the Human Basal Ganglia

Given their deleterious effects on quality of life in PD sufferers, the non-motor symptoms of PD are gaining recognition as an important facet of the disease. Cognitive deficits, including executive dysfunction, are common in PD subjects and are among the earliest symptoms observed in patients (Jankovic 2008; Kudlicka et al. 2011; Ravina et al. 2009). As these cognitive symptoms are believed to be at least partially dopamine- or striatum-dependent, we examined the electrophysiological output of the BG in PD and dystonic subjects (Sage et al. 2003; Schultz 1997).

In dystonic subjects, we found that auditory feedback was associated with the presence of high gamma oscillations nestled on a negative deflection morphologically similar to sharp wave ripple complexes described in the human rhinal complex (Figure 2.3.2) (Gillies et al. 2017; Ramadan et al. 2009). This high gamma burst was temporally modified by incorrect trial performance as compared to successful trial performance (Figure 2.3.5). Such high gamma activity has been associated with the formation of long-term memory in the neocortex and hippocampus and may reflect learning in the BG (C. J. Behrens et al. 2005). This high gamma band activity was not observed in PD subjects.

Both PD subjects and dystonic subjects exhibited robust theta frequency activity responses to incorrect trial performance in the GPi of their respective dominant hemispheres, but not in their non-dominant hemispheres, suggesting the mechanisms underlying valence-response might be lateralized in the BG (Figure 2.3.4). These processes remain impaired in PD subjects treated with dopaminergic medication, implying some of the cognitive deficits in PD are not strictly dopamine-dependent.

6.1.2 Executive Function in the Human Prefrontal Cortex

The ACC is proposed to facilitate learning by signaling outcome valence resulting from unexpected decision outcomes (T. E. Behrens et al. 2007; Botvinick et al. 2001; Cai and Padoa-Schioppa 2012; Hayden et al. 2011; S. Ito et al. 2003; Kennerley and Walton 2011; Kennerley et al. 2011; Procyk et al. 2016). This has not, however, been previously validated through direct electrophysiological recordings from human dACC. We had the rare opportunity to collect electrophysiological recordings from bilaterally implanted DBS patients shortly after they underwent electrode implantation in the ACC. We recorded LFP from the dACC, our hypothesis being that we would find electrophysiological correlates of predictive activity during stimuli presentation and outcome valence-related activity at the time of outcome feedback. The results provide strong support that the human dACC signals both prediction confidence and outcome valence, with these functions lateralized across hemispheres (the latter an unexpected finding). dACC laterality findings were similar to those obtained from GPi recordings in Chapter 2. We further established that lateralization of cognitive processing in the human cingulate is processed through activity in the theta frequency oscillatory band, with the right hemisphere active during memory formation and the left hemisphere modulating predictions (Figure 3.3.4).

Using a simple cognitive task, we compiled a large number of task trials and produced a robust body of unique data. Localized LFP recordings from the ACC in humans are rare, and this study contributes unique electrophysiological measurements not obtainable by fMRI nor EEG in humans. Our findings are relevant to evaluating competing schools of thought regarding dACC function. Experimental results put us squarely in the camp of Kolling *et al.*, wherein the dACC is thought to play a leading role in the regulation of behavioral adaptation and persistence (Kolling et al. 2016). Furthermore, we did not observe variation of dACC signal strength as suggested by the work of Shenhav *et al. (Shenhav et al. 2016)*. The evidence of

laterality in dACC function indicates that executive function may be more understandable through functional specialization of cortical areas (Figure 3.3.2). Our laterality findings were strengthened by the inclusion of post-operative CT and DTI analyses confirming our electrode placement in the dACC and connectivity uniformity across hemispheres (Figure 3.3.1). We therefore offer clarifying evidence of lateralized decision-making in line with foraging theories in a complex cortical region supporting cognitive functions as varied as executive control, reward, learning and memory, and attention.

6.1.3 Differences in the Electrophysiological Relationship between the Anterior Cingulate Cortex and the Basal Ganglia Thalamocortical Circuit in the Normal and Parkinsonian Rat Brain during Movement

Dopamine loss is thought to provoke the excessively synchronized oscillatory activity observed in the BG of PD patients. The hemiparkinsonian rat is a useful model for investigating the effects of dopamine loss on the transmission of excessive oscillatory activity throughout the BG thalamocortical circuit. Previous studies in the hemiparkinsonian rat have shown that they respond similarly to PD humans in that, after 6-OHDA-induced dopamine cell lesion, the hemiparkinsonian rat develops synchronous oscillatory activity that is propagated in some areas of the hemiparkinsonian striatum, the STN, SNpr, and VM thalamus (figure 4.1). This activity has also been observed in some areas of the hemiparkinsonian rat cortex, most notably the MCx, but not in other areas, such as the ILC and PLC (Delaville et al. 2014; Delaville et al. 2015). Historically, it was not known whether this activity was transmitted to the ACC, which neighbors and projects to the ILC and PLC, but anatomical connections promote the hypothesis of synchronized beta entrainment after dopamine cell lesion from the BG through the VM thalamus to the ACC.

After 6-OHDA dopamine cell lesion, the hemiparkinsonian rat ACC develops large increases in LFP power in the high beta (30 – 36 Hz) frequency range (Figure 4.3.2.1 and Figure 4.3.2.3). Similar to the increases observed in the STN and VM, the ACC exhibits significant increases in peak frequency in the high beta frequency band in the weeks following dopamine cell lesion. Coherence was drastically increased between LFP activity in this frequency range in the STN, VM thalamus, and ACC (Figure 4.3.3). Increases of spiking entrainment to ACC high beta LFP were observed in the STN and the VM thalamus while entrainment was modest at best in the ACC (Figure 4.2.4). The sequence of spike timing in the BG thalamocortical circuit was assessed by comparing the phase relationship of each spike train to a common ACC oscillation, and the temporal relationships between phase-locked spiking were consistent with the anatomical connections between the STN, VM thalamus, and ACC and support sequential entrainment of activity between these regions (Figure 4.3.5). Lesion-induced increases in oscillatory activity in the ACC in the high beta range were not correlated with synchronized spiking activity suggesting that the ACC may not participate in the further propagation of dopamine cell lesion-related synchronized oscillatory activity to downstream regions.

Potentially, cortical neurons are simply unable to synchronize through phase-locking to the beta frequency band. Results have failed to show substantial increases in spike synchronization to ongoing beta activity in the hemiparkinsonian rat model. Results from Walters *et al*. vary from non-significant spike phase-locking (Delaville et al. 2015) to modest but significant increases in spike phase-locking (Brazhnik et al. 2012). Similar modest results are seen if one looks at cortical spiking correlated with the finely tuned gamma associated with dyskinesia (Dupre et al. 2016). It is clear that there is thalamic drive inducing dramatic increases in beta (or gamma in the case of finely tuned gamma) local field in the cortex (Brazhnik et al. 2016; Lee and Jones 2013), but it does not appear to be the case that the

oscillations in voltage (due to thalamic innervation) around the neurons located near our recording electrodes result in dramatic changes in spike output in the lower layers.

6.1.4 Modulation of Anterior Cingulate Cortex and Basal Ganglia Activity during a Simple Cognitive Task in Hemiparkinsonian Rats

The electrophysiological correlates of dopamine-dependent cognitive dysfunction are not well understood in the ACC. After observing in Chapter 4 that the ACC was connected to the BG thalamocortical circuit and that it develops the excessively synchronized high beta activity that is the hallmark of the PD patient and hemiparkinsonian rat, the electrophysiological relationship between the VM, STN, and ACC were examined during a simple task with cognitive and movement components in Chapter 5.

As seen in Chapter 4, 6-OHDA-induced dopamine cell lesion led to significant increases in ACC beta frequency band LFP oscillatory activity and coherence with the STN and VM (Figure 5.3.1, Figure 5.3.4, and Figure 5.3.5). Likewise, STN and VM spike trains were strongly phase-locked to ACC high beta LFPs after dopamine cell lesion during expected walking epochs and less so during epochs of rest and unexpected treadmill off. After 6-OHDA lesioning, theta spike-LFP phase-locking in the ACC and VM increased during rest and unexpected treadmill off, but not during expected treadmill walking epochs (Figure 5.3.2). Theta band ACC LFP power was seen to increase after lesioning while STN-ACC coherence decreased in all behavioral states (Figure 5.3.2 and Figure 5.3.6). Chapters 2 and 3 explored the role of theta activity in dopamine-healthy states during conflict and error management. Results suggest that disruption of normal theta band oscillatory activity in the BG thalamocortical circuit may suggest possible avenues for executive dysfunction. Through examination of event-related phenomena, desynchronization of alpha frequency activity during

stimuli presentation observed before lesioning in the ACC and VM thalamus was found to decrease after dopamine cell lesioning (Figure 5.3.6), possibly reflecting a decrease in attention-related synchronization and a subsequent decrease in decision making ability.

6.2 Implications for the Involvement of the Anterior Cingulate Cortex in Parkinson's Disease

PD is a complex neurodegenerative condition stemming from dopamine depletion in the BG thalamocortical circuit. Cognitive and behavioral changes are common in early PD and throughout the progression of the disease (McKinlay et al. 2010; Muslimovic et al. 2005; Schrag et al. 2015). The causes of these symptoms are probably multifactorial, but they are at least partially related to decreasing levels of dopamine in the BG thalamocortical circuit. We chose to focus on the ACC, a region of the brain shown from imaging studies to be involved in a wide variety of executive functions that also exhibits the highest rates of [18F]-Fluoro-L-dopa uptake – a measure used to quantify dopamine metabolism – in the frontal cortex (Alvarez and Emory 2006; W. D. Brown et al. 1999; Firnau et al. 1988; Funahashi and Andreau 2013; C. L. Gallagher et al. 2015; Moore et al. 2003). Furthermore, dopamine levels in the PFC have been observed to influence executive function in the non-PD population, raising the likelihood of ACC dysfunction in PD (Meyer-Lindenberg et al. 2005). The purpose of the studies performed herein was to examine the influence of PD on the ACC and its connections with the BG thalamocortical circuit as well as to further our understanding of the electrophysiological basis for the executive dysfunction observed in PD.

We examined whether LFPs in the ACC of the dopamine cell-lesioned hemisphere of hemiparkinsonian rats show increases in oscillatory activity in the same high beta frequency range during treadmill walking as observed throughout the BG thalamocortical circuit. ACC LFP activity recorded in the 3 weeks following dopamine depletion showed clear increases in the 30 - 36 Hz range and was highly coherent with similar LFP activity in the STN and VM thalamus. Meanwhile, ACC spiking does not, in contrast with the VM and the STN, become

phase-locked to ongoing high beta LFPs after lesion, suggesting that the ACC is unlikely to contribute to the propagation of excessive PD high beta synchronization throughout the BG thalamocortical circuit. While these observations are consistent with our hypothesis that PFC (or at least the ACC) activity is entrained to oscillatory activity in the BG after dopamine cell lesion, it is unclear how, if at all, this activity affects normal ACC function. Prior to 6-OHDA lesion, there is very little activity in the 30 – 36 Hz range in the ACC, so the emergence of high beta synchronization in the ACC is not merely a potentiation of activity normally seen in the ACC during treadmill walking.

What does the emergence of parkinsonian high beta excessive oscillatory activity in the ACC mean for cognition? This remains a controversial and open question. Cognition has been shown to rely on the context-dependent selection of relevant inputs and the availability of flexible interareal brain communication, but the mechanisms that underlie this are poorly understood (Palmigiano et al. 2017). One possibility is that neuronal oscillations direct interareal communications through systems of oscillatory coherence in neuronal circuits (Fries 2005; Palmigiano et al. 2017). Cognitive, limbic, and motor circuits alike communicate through interareal bursts of coherence in various frequency bands as is experimentally confirmed through observations in human and animal models (Babapoor-Farrokhran et al. 2017; Buzsaki and Schomburg 2015; Fujimoto et al. 2016; Grion et al. 2016; Lipsman et al. 2014; Womelsdorf and Fries 2006, 2007). Coherent phase relationships between different frequency bands depend upon distinct dynamic functional hierarchies of oscillatory behaviors, and can be potentially disrupted by abnormal and excessive synchronization (Bastos et al. 2015). In this way, the high beta synchronization seen in humans and animal models may mediate interareal interactions within and between the ACC and its sphere of influence, disrupting normal function (Salazar et al. 2012). We observed in 6-OHDA lesioned, hemiparkinsonian rats modulation of normal LFP coherence between the STN, VM thalamus, and ACC during cognitive activity, lending

credence to this proposal. While the ACC does not exhibit spike phase-locking to parkinsonian beta synchronization, as much of the BG thalamocortical circuit does, it promotes a route for executive dysfunction through the over-synchronization of high beta LFP coherence which inhibits normal function.

It remains to be seen whether excessively synchronized parkinsonian beta will be seen in the ACC of humans. We certainly see exaggerated beta throughout the hemiparkinsonian rat BG and indeed in the hemiparkinsonian rat ACC. The importance of this finding once again hinges on the value of the hemiparkinsonian rat as a functional and "human-like" model of PD.

In light of our PD IED results, one might ask whether one might find similar deficiencies in other non-motor, "cognitive" conditions such as pain or depression. Given our strong laterality results in both the ACC and the GPi, it remains to be seen whether these other conditions do indeed have electrophysiology that is correlative with overlying behavioral changes. Pain and depression, like PD, have symptoms treatable through DBS. One might therefore theorize that these conditions have similar underlying electrophysiological phenomena that drive (or at least correlate with) the mechanisms behind symptomology (Boccard et al. 2014b; Boccard et al. 2015a; Bruchim-Samuel et al. 2016; Cleary et al. 2015; Gee et al. 2016; Pereira and Aziz 2014). Given that both pain (as seen by our ACC chronic pain subjects) and depression (Drevets et al. 2008; Mayberg et al. 2005; Pandya et al. 2012) have been tied to ACC circuit dysfunction and the observation that pain and depression have deficits responsive to DBS treatment raises the question of whether the underlying neurophysiological changes responsible for their symptoms might manifest similarly altered responses to IED and other executive function tasks as those seen in PD subjects. This remains to be seen and deserves future attention.

6.3 Implications for Parkinson's Disease Clinical Assessment Protocols and Diagnoses

We have shown functional correlates of decision making in the BG and ACC of the healthy brain that are disrupted after dopamine depletion. If the ACC is part of the BG thalamocortical circuit and is affected by the excessively synchronized beta band activity observed therein, how might this knowledge be leveraged clinically?

Executive dysfunction, as observed in PD, occurs at an earlier stage of the disease than do the motor symptoms (Dubois and Pillon 1997; Owen 2004; Zgaljardic et al. 2003; Zgaljardic et al. 2006). Can we therefore use the electrophysiological markers of executive dysfunction in the ACC, that we observed herein, for early disease diagnosis? If this is possible, then these electrophysiological biomarkers have the potential to be invaluable additions to clinical assessment protocols. The use of brain oscillations as biomarkers in pathology is based on several fundamentals. According to Basar, all structures of the brain work together to facilitate the many mechanisms that underlie cognition (Basar 2006; Yener and Basar 2010). These mechanisms are altered and modulated by neurological diseases. As such, efforts to identify disease biomarkers must recognize the myriad of mechanisms that operate in cognitive circuits. Biomarker identification strategies should be derived from a combination of observations from electrophysiological measures including frequency shifts, changes in oscillatory responses, and fluctuations of connectivity in the form of power or spike-LFP coherence. The electrophysiological changes that occur in pathology are often built upon biochemical or structural changes. Observing these neurophysiological markers in conjunction with changes in electrophysiology would enhance disease treatment development.

The signatures observed in electrophysiological brain dynamics can prove to be useful as functional biomarkers for both physiology and pathophysiology. Animal model research

allows us to examine the mechanisms that support oscillations and their synchronization across different frequency bands. Through these methods, the correlations between brain dynamics and disease states permit us to pursue more targeted searches for disturbances in mechanisms that can pave the way for new clinical therapeutic interventions.

DBS has been shown to be a highly effective treatment for PD. The flexibility of the technology permits its adaptation for other treatments. Using stereotactic techniques, neurosurgeons are applying DBS to mitigate the effects of a growing number of pathological conditions that cannot be adequately managed through medication alone. The clinical use of DBS has expanded to treat conditions such as dystonia and tremor, and more recently epilepsy, OCD, depression, and chronic pain. As the limitations of drug-based therapies have become apparent, neurologists are increasingly inclined to recommend surgical therapies and a majority of patients are managed by teams that include both neurosurgeons and neurologists (Ackerman 2006). Despite the growing popularity of surgical therapies, it remains essential to proceed with caution when using invasive, sometimes ethically problematic surgical tools like DBS in research contexts. The safe and responsible use of DBS necessitates the use of clinical assessment tools to identify treatable patients. The emergence of these assessment tools and outcome measures allow the efficacy of treatments to be verified by third parties and provide objective data to support and inform the recommendations of clinicians (Gardner 2013).

ACC DBS has shown promise as a treatment for the nociceptive and neuropathic symptoms of chronic pain (Boccard et al. 2013; Boccard et al. 2014b; Boccard et al. 2015a). Might DBS of the ACC also mitigate PD symptomology in any way? DBS, at least in the human STN and GPi, is thought to improve symptoms in PD through disrupting the excessive and pathological oscillations that emerge in the BG (Benazzouz and Hallett 2000). The ACC does exhibit direct and indirect reciprocal connections with the BG, and it has been shown to modulate both SMA and MCx activity during motor behavior (Asemi et al. 2015; Paus 2001).

The functional overlap of pain, motor, and cognitive circuits in the ACC may make the ACC a unique potential target for DBS. It is possible that DBS of the ACC might prove an effective PD treatment by disrupting the pathological ACC oscillatory activity we observed in the studies performed herein during both motor and cognition tasks.

In view of the appearance of motor symptoms prior to the development of beta oscillatory activity following 6-OHDA lesion, one might ask whether the presence of excessively synchronized beta oscillations could function as an early biomarker for incipient PD. Certainly, one might infer this from the hemiparkinsonian rat in the included results and from previous findings (Avila et al. 2010; Brazhnik et al. 2012; Brazhnik et al. 2014; Brazhnik et al. 2016; Delaville et al. 2015; Parr-Brownlie et al. 2007). This is dependent on several assumptions. Firstly, the 6-OHDA-lesioned rat functions as a good model of PD. Secondly, that acute 6-OHDA lesions resulting in greater than 90 % reduction in dopaminergic SNpc cells are a good representation of PD. While we and others have observed in the hemiparkinsonian rat motor symptoms that occur prior to the emergence of a synchronized beta oscillatory band, this effect requires a substantial dopaminergic lesion. It is unclear whether this would be the case in humans, or whether this activity requires either a sudden loss of dopaminergic cells or merely the passing of a threshold in the integrity of the dopaminergic system. This certainly deserves increased attention.

6.4 Future Directions

Herein, we displayed evidence of excessively synchronized parkinsonian beta band activity in the ACC of the hemiparkinsonian rat. This leads us to ask whether such activity might develop in the ACC of humans with PD. The method of externalized DBS electrode lead recording used here is a poor technique for probing this question. DBS electrode placement is restricted to its clinical practicality. As, at the present time, there is no clinical reason to localize a DBS lead in the ACC for the treatment of PD symptoms, one would not be able to use this depth recording technique to capture possible PD-induced synchronized beta in the ACC. We must look to other techniques to probe PD electrophysiology in the PFC. Such techniques as magnetoencephalography (MEG), fMRI, and EEG may prove to be useful research techniques, but these current state-of-the-art non-invasive tools have practical research limitations. MEG is capable of providing a direct measure of electrical activity in the brain with a high level of temporal resolution, albeit with a tradeoff in spatial resolution, and has already been shown as a useful measure of probing ACC activity (Mohseni et al. 2012). Broadband electrophysiological power has been demonstrated to directly couple with the global component of fMRI signals and may be probable with such a method, although fMRI has poor temporal resolution compared with MEG or EEG (Mohseni et al. 2012; Wen and Liu 2016). High density EEG has been shown to localize activity significantly more accurately than MEG, but may have limited functionality in probing deeper structures like the ACC (Klamer et al. 2015). Certainly, these tools used on their own offer their advantages. Their use in combination may act to counterbalance their respective disadvantages and are a promising direction for future work in non-invasive, practical attempts at studying the role of the ACC in human PD.

Pain is an additional PD clinical symptom relevant to the ACC's connection with the BG thalamocortical circuit that is worthy of comment. Pain affects 40 – 75 % of PD patients, leading to a decrease in quality of life (Ford 1998a; D. A. Gallagher et al. 2010; Martinez-Martin 2011; Snider et al. 1976). Though pain can be present throughout all the stages of PD, like cognitive dysfunction, it is a major feature of early-stage PD and it has been rated the most bothersome non-motor symptom of PD for many patients (Bjorklund and Cenci 2010). Pain is believed to be underreported in PD patients due to a lack of standard definitions of chronic pain, the distinction between pain related to PD and pain unrelated to PD, and public awareness (Negre-Pages et al. 2008). Despite the underreporting of pain, there is a high prevalence of pain reported by PD patients that could be the result of hypersensitivity. Decreased pain thresholds to heat and cold have been observed in PD patients when compared to healthy controls (Brefel-Courbon et al. 2005b; Djaldetti et al. 2004). PD patients also report lower pain thresholds to electrical stimulation to the leg (Mylius et al. 2009). This hypersensitivity to thermal and electrical stimulation may be the result of abnormalities in pain processing pathways and their interaction with the BG thalamocortical circuits we focused on in the studies performed herein.

Pain processing occurs through two separate pathway systems passing from the spinal cord to the brain: the lateral and medial systems. The lateral system relies upon the spinothalamic tract that projects through the lateral sensory thalamus to the sensory cortices and is responsible for processing the duration, intensity, localization, and sensory discrimination of pain (Scherder et al. 2005; Willis and Westlund 1997). The medial system projects through the medial thalamic nuclei to cognition-focused and emotion-focused areas of the brain and is involved in the cognitive-affective and motivational-affective dimensions of pain (Scherder et al. 2005; Willis and Westlund 1997). Within these pathways, there are many overlapping pain-processing circuits. Most relevant, the spino-reticulo-thalamic pathway routes nociceptive information through the most caudal aspect of the medulla, the medullary subnucleus reticularis

dorsalis (SRD) (Mehler et al. 1960; Villanueva et al. 1996). The SRD has large receptive fields that comprise the whole body and receives projections from noxious stimuli-activated laminae I, IV-VII and X of the dorsal horn (Dubner and Bennett 1983; Lima and Coimbra 1990; Villanueva et al. 1988; Villanueva et al. 1989). The SRD most notably sends nociceptive projections to the VM thalamus (Bernard et al. 1990; Villanueva et al. 1995).

We have explored the VM thalamus' projections to the ACC. The ACC is known to be involved in the processing of pain and DBS is utilized here to treat chronic pain (Boccard et al. 2014a; Herkenham 1979; Hutchison et al. 1999; Johansen et al. 2001; Lorenz et al. 2003; Welker 1971). As one of the prefrontal areas involved in affective pain processing, it stands to reason that abnormal oscillatory activity in the ACC of PD patients may alter pain perception. As part of the nociceptive spino-reticulo-thalamic pathway, the VM thalamus may also be expected to have increased activity during pain. It is unknown how loss of dopamine and the excessively synchronized high beta oscillatory activity that arises from it might affect pain-related processing in the BG thalamocortical circuit. This makes for an interesting area for future study that we have the ability to uniquely address in the chronically implanted, hemiparkinsonian rat model.

6.5 Concluding Remarks

Additional recordings from a larger pool of patients are required to confirm the findings presented here. Additional work is also warranted to define the specific contributions of various elements of the BG thalamocortical circuit in PD non-motor symptomology. Despite these shortcomings, we believe our findings help to outline an electrophysiological approach to understanding the physiological foundation for cognitive dysfunction in patients with PD. Our findings specifically suggest grounds for the ACC to be implicated in executive dysfunction in PD.

Much can be gained through further research into the nature of oscillatory brain activity. The electrophysiological oscillation-based approach has proven to be an effective alternative to drug-based interventions as a treatment for a growing number of pathologies. Studying and quantifying network oscillations and their cross-frequency interactions in awake, behaving humans and animal models can help us better understand basic brain mechanisms, pathology, and new avenues for treatment of disease. Clinical treatments such as pattern-guided, closed-loop DBS, sensory feedback, transcranial magnetic stimulation, and electrical stimulation are all potential treatments that can benefit from the electrophysiological biomarkers explored here.

Our results demonstrate that after disruption of the dopamine system, the ACC (unlike the ILC and PLC subunits of the PFC) can become highly entrained with, and potentially modulated by, oscillatory activity within the BG thalamocortical circuit. Under-stimulation of dopamine receptors appears to favor the development of an abnormal oscillatory state (either directly, epiphenomenally, or neuroplastically) with frequencies that are ostensibly dependent upon behavioral state and species, and this behavior extends to the ACC, a region of the brain

known for its involvement in a wide array of cognitive and affective processes. Our data suggests that through an examination of a combination of event-related activities, LFP, coherence, and spike-LFP relationships in both humans and animal models one can begin to identify the unique contributions of the BG thalamocortical circuit in generating, propagating, and interacting with excessive oscillatory activity. Further research into ACC function in the parkinsonian state may help us gain additional insights into the functional significance of pathological oscillatory phenomena in motor, cognitive, and pain systems and may lead to the potential for innovative methods for diagnoses and therapeutic intervention.

7. References

Ackerman, S (2006), *Hard science, hard choices : facts, ethics, and policies guiding brain science today* (Dana Foundation series on neuroethics; New York: Dana Press) xiii, 152 p.

Albin, R. L., Young, A. B., and Penney, J. B. (1989), 'The functional anatomy of basal ganglia disorders', *Trends Neurosci,* 12 (10), 366-75.

Alegre, M., et al. (2005), 'Movement-related changes in oscillatory activity in the human subthalamic nucleus: ipsilateral vs. contralateral movements', *Eur J Neurosci,* 22 (9), 2315-24.

Alexander, W. H. and Brown, J. W. (2011), 'Medial prefrontal cortex as an action-outcome predictor', *Nat Neurosci,* 14 (10), 1338-44.

Alkire, M. T., Hudetz, A. G., and Tononi, G. (2008), 'Consciousness and anesthesia', *Science,* 322 (5903), 876-80.

Allman, J. M., et al. (2001), 'The anterior cingulate cortex. The evolution of an interface between emotion and cognition', *Ann N Y Acad Sci,* 935, 107-17.

Alonso-Frech, F., et al. (2006), 'Slow oscillatory activity and levodopa-induced dyskinesias in Parkinson's disease', *Brain,* 129 (Pt 7), 1748-57.

Alvarez, J. A. and Emory, E. (2006), 'Executive function and the frontal lobes: a meta-analytic review', *Neuropsychol Rev,* 16 (1), 17-42.

Amiez, C., Joseph, J. P., and Procyk, E. (2005), 'Anterior cingulate error-related activity is modulated by predicted reward', *Eur J Neurosci,* 21 (12), 3447-52.

Anderson, V. C., et al. (2005), 'Pallidal vs subthalamic nucleus deep brain stimulation in Parkinson disease', *Arch Neurol,* 62 (4), 554-60.

Androulidakis, A. G., et al. (2007), 'Dopaminergic therapy promotes lateralized motor activity in the subthalamic area in Parkinson's disease', *Brain,* 130 (Pt 2), 457-68.

Antoniades, C. A., et al. (2014), 'Deep brain stimulation abolishes slowing of reactions to unlikely stimuli', *J Neurosci,* 34 (33), 10844-52.

Arbuthnott, G. W., et al. (1990), 'Distribution and synaptic contacts of the cortical terminals arising from neurons in the rat ventromedial thalamic nucleus', *Neuroscience,* 38 (1), 47-60.

Asemi, A., et al. (2015), 'Dorsal anterior cingulate cortex modulates supplementary motor area in coordinated unimanual motor behavior', *Front Hum Neurosci,* 9, 309.

Ashby, P., et al. (2001), 'Potentials recorded at the scalp by stimulation near the human subthalamic nucleus', *Clin Neurophysiol,* 112 (3), 431-7.

Au, W. L., et al. (2012), 'Levodopa and the feedback process on set-shifting in Parkinson's disease', *Hum Brain Mapp,* 33 (1), 27-39.

Avila, I., et al. (2010), 'Beta frequency synchronization in basal ganglia output during rest and walk in a hemiparkinsonian rat', *Exp Neurol,* 221 (2), 307-19.

Babapoor-Farrokhran, S., et al. (2017), 'Theta and beta synchrony coordinate frontal eye fields and anterior cingulate cortex during sensorimotor mapping', *Nat Commun,* 8, 13967.

Baker, S. N. (2007), 'Oscillatory interactions between sensorimotor cortex and the periphery', *Curr Opin Neurobiol,* 17 (6), 649-55.

Balleine, B. W., Liljeholm, M., and Ostlund, S. B. (2009), 'The integrative function of the basal ganglia in instrumental conditioning', *Behav Brain Res,* 199 (1), 43-52.

Barbas, H. and Pandya, D. N. (1989), 'Architecture and intrinsic connections of the prefrontal cortex in the rhesus monkey', *J Comp Neurol*, 286 (3), 353-75.
Barbeau, A. (1969), 'L-dopa therapy in Parkinson's disease: a critical review of nine years' experience', *Can Med Assoc J*, 101 (13), 59-68.
Barnett, J. H., et al. (2010), 'Assessing cognitive function in clinical trials of schizophrenia', *Neurosci Biobehav Rev*, 34 (8), 1161-77.
Basar-Eroglu, C., et al. (1992), 'P300-response: possible psychophysiological correlates in delta and theta frequency channels. A review', *Int J Psychophysiol*, 13 (2), 161-79.
Basar, E. (2006), 'The theory of the whole-brain-work', *Int J Psychophysiol*, 60 (2), 133-8.
Basar, E., et al. (1999), 'Are cognitive processes manifested in event-related gamma, alpha, theta and delta oscillations in the EEG?', *Neurosci Lett*, 259 (3), 165-8.
--- (2000), 'Brain oscillations in perception and memory', *Int J Psychophysiol*, 35 (2-3), 95-124.
Basar, E., et al. (2013), 'Brain's alpha, beta, gamma, delta, and theta oscillations in neuropsychiatric diseases: proposal for biomarker strategies', *Suppl Clin Neurophysiol*, 62, 19-54.
Bastos, A. M., Vezoli, J., and Fries, P. (2015), 'Communication through coherence with inter-areal delays', *Curr Opin Neurobiol*, 31, 173-80.
Bauer, M., et al. (2014), 'Attentional modulation of alpha/beta and gamma oscillations reflect functionally distinct processes', *J Neurosci*, 34 (48), 16117-25.
Beckstead, R. M. and Cruz, C. J. (1986), 'Striatal axons to the globus pallidus, entopeduncular nucleus and substantia nigra come mainly from separate cell populations in cat', *Neuroscience*, 19 (1), 147-58.
Bedard, C., Kroger, H., and Destexhe, A. (2006), 'Does the 1/f frequency scaling of brain signals reflect self-organized critical states?', *Phys Rev Lett*, 97 (11), 118102.
Behrens, C. J., et al. (2005), 'Induction of sharp wave-ripple complexes in vitro and reorganization of hippocampal networks', *Nat Neurosci*, 8 (11), 1560-7.
Behrens, T. E., et al. (2007), 'Learning the value of information in an uncertain world', *Nat Neurosci*, 10 (9), 1214-21.
Benazzouz, A. and Hallett, M. (2000), 'Mechanism of action of deep brain stimulation', *Neurology*, 55 (12 Suppl 6), S13-6.
Berens, P., et al. (2008), 'Comparing the feature selectivity of the gamma-band of the local field potential and the underlying spiking activity in primate visual cortex', *Front Syst Neurosci*, 2, 2.
Berg, D., et al. (2013), 'Changing the research criteria for the diagnosis of Parkinson's disease: obstacles and opportunities', *Lancet Neurol*, 12 (5), 514-24.
Bergman, H. and Deuschl, G. (2002), 'Pathophysiology of Parkinson's disease: from clinical neurology to basic neuroscience and back', *Mov Disord*, 17 Suppl 3, S28-40.
Bernard, J. F., et al. (1990), 'Efferent projections from the subnucleus reticularis dorsalis (SRD): a Phaseolus vulgaris leucoagglutinin study in the rat', *Neurosci Lett*, 116 (3), 257-62.
Bertran-Gonzalez, J., et al. (2010), 'What is the Degree of Segregation between Striatonigral and Striatopallidal Projections?', *Front Neuroanat*, 4.
Beurrier, C., et al. (2001), 'High-frequency stimulation produces a transient blockade of voltage-gated currents in subthalamic neurons', *J Neurophysiol*, 85 (4), 1351-6.
Bhattacharya, J. and Petsche, H. (2001), 'Universality in the brain while listening to music', *Proc Biol Sci*, 268 (1484), 2423-33.
Birkmayer, W. and Hornykiewicz, O. (1961), '[The L-3,4-dioxyphenylalanine (DOPA)-effect in Parkinson-akinesia]', *Wien Klin Wochenschr*, 73, 787-8.

Bjorklund, A. and Dunnett, S. B. (2007), 'Dopamine neuron systems in the brain: an update', *Trends Neurosci,* 30 (5), 194-202.
Bjorklund, A. and Cenci, M. A. (2010), 'The challenge of non-motor symptoms in Parkinson's disease', *Recent Advances in Parkinsons Disease: Translational and Clinical Research,* 184, 325-41.
Blanchard, T. C. and Hayden, B. Y. (2014), 'Neurons in dorsal anterior cingulate cortex signal postdecisional variables in a foraging task', *J Neurosci,* 34 (2), 646-55.
Blandini, F., et al. (2007), 'Time-course of nigrostriatal damage, basal ganglia metabolic changes and behavioural alterations following intrastriatal injection of 6-hydroxydopamine in the rat: new clues from an old model', *Eur J Neurosci,* 25 (2), 397-405.
Boccard, S. G., Pereira, E. A., and Aziz, T. Z. (2015a), 'Deep brain stimulation for chronic pain', *J Clin Neurosci,* 26, 26.
Boccard, S. G., et al. (2013), 'Long-term outcomes of deep brain stimulation for neuropathic pain', *Neurosurgery,* 72 (2), 221-30; discussion 31.
Boccard, S. G., et al. (2014a), 'Targeting the affective component of chronic pain: a case series of deep brain stimulation of the anterior cingulate cortex', *Neurosurgery,* 74 (6), 628-35; discussion 35-7.
Boccard, S. G., et al. (2014b), 'Deep brain stimulation of the anterior cingulate cortex: targeting the affective component of chronic pain', *Neuroreport,* 25 (2), 83-8.
Boccard, S. G., et al. (2015b), 'A tractography study of Deep Brain Stimulation of the Anterior Cingulate Cortex in chronic pain: a key to improve the targeting', *World Neurosurg,* 3, 3.
Bogacz, R. and Gurney, K. (2007), 'The basal ganglia and cortex implement optimal decision making between alternative actions', *Neural Comput,* 19 (2), 442-77.
Botvinick, M. M. (2007), 'Conflict monitoring and decision making: reconciling two perspectives on anterior cingulate function', *Cogn Affect Behav Neurosci,* 7 (4), 356-66.
Botvinick, M. M., et al. (2001), 'Conflict monitoring and cognitive control', *Psychol Rev,* 108 (3), 624-52.
Brazhnik, E., et al. (2014), 'Functional correlates of exaggerated oscillatory activity in basal ganglia output in hemiparkinsonian rats', *Exp Neurol,* 261, 563-77.
Brazhnik, E., et al. (2016), 'Ventral Medial Thalamic Nucleus Promotes Synchronization of Increased High Beta Oscillatory Activity in the Basal Ganglia-Thalamocortical Network of the Hemiparkinsonian Rat', *J Neurosci,* 36 (15), 4196-208.
Brazhnik, E., et al. (2012), 'State-dependent spike and local field synchronization between motor cortex and substantia nigra in hemiparkinsonian rats', *J Neurosci,* 32 (23), 7869-80.
Brefel-Courbon, C., et al. (2005a), 'Effect of levodopa on pain threshold in Parkinson's disease: a clinical and positron emission tomography study', *Mov Disord,* 20 (12), 1557-63.
--- (2005b), 'Effect of levodopa on pain threshold in Parkinson's disease: A clinical and positron emission tomography study', *Movement Disorders,* 20 (12), 1557-63.
Bressler, S. L. and Richter, C. G. (2015), 'Interareal oscillatory synchronization in top-down neocortical processing', *Curr Opin Neurobiol,* 31, 62-6.
Brissaud, Édouard and Meige, Henry (1895), *Leçons sur les maladies nerveuses (Salpêtrière, 1893-1894) Recueillies et publićes* (Paris,: G. Masson) 2 p.l., iii, 644 p.
Brogden, R. N., Speight, T. M., and Avery, G. S. (1971), 'Levodopa: a review of its pharmacological properties and therapeutic use with particular reference to Parkinsonism', *Drugs,* 2 (4), 262-400.

Brown, J. W. and Braver, T. S. (2005), 'Learned predictions of error likelihood in the anterior cingulate cortex', *Science,* 307 (5712), 1118-21.
Brown, P. (2003), 'Oscillatory nature of human basal ganglia activity: relationship to the pathophysiology of Parkinson's disease', *Mov Disord,* 18 (4), 357-63.
--- (2007), 'Abnormal oscillatory synchronisation in the motor system leads to impaired movement', *Curr Opin Neurobiol,* 17 (6), 656-64.
Brown, P. and Marsden, C. D. (1998), 'What do the basal ganglia do?', *The Lancet,* 351 (9118), 1801-04.
Brown, P. and Marsden, J. F. (2001), 'Book Review: Cortical Network Resonance and Motor Activity in Humans', *The Neuroscientist,* 7 (6), 518-26.
Brown, P. and Williams, D. (2005), 'Basal ganglia local field potential activity: character and functional significance in the human', *Clin Neurophysiol,* 116 (11), 2510-9.
Brown, P. and Eusebio, A. (2008), 'Paradoxes of functional neurosurgery: clues from basal ganglia recordings', *Mov Disord,* 23 (1), 12-20; quiz 158.
Brown, P., et al. (2001), 'Dopamine dependency of oscillations between subthalamic nucleus and pallidum in Parkinson's disease', *J Neurosci,* 21 (3), 1033-8.
Brown, Peter, et al. (2002), 'Oscillatory Local Field Potentials Recorded from the Subthalamic Nucleus of the Alert Rat', *Experimental Neurology,* 177 (2), 581-85.
Brown, W. D., et al. (1999), 'FluoroDOPA PET shows the nondopaminergic as well as dopaminergic destinations of levodopa', *Neurology,* 53 (6), 1212-8.
Bruchim-Samuel, M., et al. (2016), 'Electrical stimulation of the vmPFC serves as a remote control to affect VTA activity and improve depressive-like behavior', *Exp Neurol,* 283 (Pt A), 255-63.
Brunner, C., Delorme, A., and Makeig, S. (2013), 'Eeglab - an Open Source Matlab Toolbox for Electrophysiological Research', *Biomed Tech (Berl).*
Buschman, T. J. and Miller, E. K. (2007), 'Top-down versus bottom-up control of attention in the prefrontal and posterior parietal cortices', *Science,* 315 (5820), 1860-2.
--- (2009), 'Serial, covert shifts of attention during visual search are reflected by the frontal eye fields and correlated with population oscillations', *Neuron,* 63 (3), 386-96.
Buzsaki, G. and Draguhn, A. (2004), 'Neuronal oscillations in cortical networks', *Science,* 304 (5679), 1926-9.
Buzsaki, G. and Schomburg, E. W. (2015), 'What does gamma coherence tell us about inter-regional neural communication?', *Nat Neurosci,* 18 (4), 484-9.
Buzsaki, G., Logothetis, N., and Singer, W. (2013), 'Scaling brain size, keeping timing: evolutionary preservation of brain rhythms', *Neuron,* 80 (3), 751-64.
Buzsáki, G. (2006), *Rhythms of the brain* (Oxford: Oxford University Press) xiv, 448 p.
Cai, X. and Padoa-Schioppa, C. (2012), 'Neuronal encoding of subjective value in dorsal and ventral anterior cingulate cortex', *J Neurosci,* 32 (11), 3791-808.
Carlsson, A., et al. (1958), 'On the presence of 3-hydroxytyramine in brain', *Science,* 127 (3296), 471.
Carpenter, M. B. (1976), 'Anatomical organization of the corpus striatum and related nuclei', *Res Publ Assoc Res Nerv Ment Dis,* 55, 1-36.
Carter, C. S., et al. (1998), 'Anterior cingulate cortex, error detection, and the online monitoring of performance', *Science,* 280 (5364), 747-9.
Cassidy, M., et al. (2002), 'Movement-related changes in synchronization in the human basal ganglia', *Brain,* 125 (Pt 6), 1235-46.
Castle, M., et al. (2005), 'Thalamic innervation of the direct and indirect basal ganglia pathways in the rat: Ipsi- and contralateral projections', *J Comp Neurol,* 483 (2), 143-53.

Cavanagh, J. F. and Frank, M. J. (2014), 'Frontal theta as a mechanism for cognitive control', *Trends Cogn Sci,* 18 (8), 414-21.
Chamberlain, S. R., et al. (2011), 'Translational approaches to frontostriatal dysfunction in attention-deficit/hyperactivity disorder using a computerized neuropsychological battery', *Biol Psychiatry,* 69 (12), 1192-203.
Chang, H. T., Kita, H., and Kitai, S. T. (1983), 'The fine structure of the rat subthalamic nucleus: an electron microscopic study', *J Comp Neurol,* 221 (1), 113-23.
Chang, H. T., Tian, Q., and Herron, P. (1995), 'GABAergic axons in the ventral forebrain of the rat: an electron microscopic study', *Neuroscience,* 68 (1), 207-20.
Charcot, J. M. and Bourneville (1872), *Leçons sur les maladies du système nerveux faites à la salpêtrière,* 2 vols. (Paris: A. Delahaye).
Chen, C. C., et al. (2007), 'Excessive synchronization of basal ganglia neurons at 20 Hz slows movement in Parkinson's disease', *Exp Neurol,* 205 (1), 214-21.
Cleary, D. R., et al. (2015), 'Deep brain stimulation for psychiatric disorders: where we are now', *Neurosurg Focus,* 38 (6), E2.
Cohen, M. X. (2014), 'A neural microcircuit for cognitive conflict detection and signaling', *Trends Neurosci,* 37 (9), 480-90.
Cools, R. (2006), 'Dopaminergic modulation of cognitive function-implications for L-DOPA treatment in Parkinson's disease', *Neurosci Biobehav Rev,* 30 (1), 1-23.
Cooper, J. A., et al. (1994), 'Slowed central processing in simple and go/no-go reaction time tasks in Parkinson's disease', *Brain,* 117 (Pt 3), 517-29.
Cooper, J. A., et al. (1992), 'Different effects of dopaminergic and anticholinergic therapies on cognitive and motor function in Parkinson's disease. A follow-up study of untreated patients', *Brain,* 115 (Pt 6), 1701-25.
Cotzias, G. C., Papavasiliou, P. S., and Gellene, R. (1969), 'Modification of Parkinsonism--chronic treatment with L-dopa', *N Engl J Med,* 280 (7), 337-45.
Courtemanche, R., Robinson, J. C., and Aponte, D. I. (2013), 'Linking oscillations in cerebellar circuits', *Front Neural Circuits,* 7, 125.
Da Cunha, C., et al. (2008), 'Hemiparkinsonian rats rotate toward the side with the weaker dopaminergic neurotransmission', *Behav Brain Res,* 189 (2), 364-72.
Dahlstrom, A. and Fuxe, K. (1964), 'Localization of monoamines in the lower brain stem', *Experientia,* 20 (7), 398-9.
de Lau, L. M. and Breteler, M. M. (2006), 'Epidemiology of Parkinson's disease', *Lancet Neurol,* 5 (6), 525-35.
Degos, B., et al. (2008), 'Evidence for a direct subthalamo-cortical loop circuit in the rat', *Eur J Neurosci,* 27 (10), 2599-610.
Dehaene, S., Kerszberg, M., and Changeux, J. P. (1998), 'A neuronal model of a global workspace in effortful cognitive tasks', *Proc Natl Acad Sci U S A,* 95 (24), 14529-34.
Dehghani, N., et al. (2010), 'Comparative power spectral analysis of simultaneous elecroencephalographic and magnetoencephalographic recordings in humans suggests non-resistive extracellular media', *J Comput Neurosci,* 29 (3), 405-21.
Delaville, C., et al. (2015), 'Subthalamic nucleus activity in the awake hemiparkinsonian rat: relationships with motor and cognitive networks', *J Neurosci,* 35 (17), 6918-30.
Delaville, C., et al. (2014), 'Oscillatory Activity in Basal Ganglia and Motor Cortex in an Awake Behaving Rodent Model of Parkinson's Disease', *Basal Ganglia,* 3 (4), 221-27.
DeLong, M. R. (1990), 'Primate models of movement disorders of basal ganglia origin', *Trends Neurosci,* 13 (7), 281-5.

Delorme, A. and Makeig, S. (2004), 'EEGLAB: an open source toolbox for analysis of single-trial EEG dynamics including independent component analysis', *J Neurosci Methods,* 134 (1), 9-21.
Delorme, A., et al. (2011), 'EEGLAB, SIFT, NFT, BCILAB, and ERICA: new tools for advanced EEG processing', *Comput Intell Neurosci,* 2011, 130714.
Desmurget, M. and Turner, R. S. (2008), 'Testing basal ganglia motor functions through reversible inactivations in the posterior internal globus pallidus', *J Neurophysiol,* 99 (3), 1057-76.
--- (2010), 'Motor sequences and the basal ganglia: kinematics, not habits', *J Neurosci,* 30 (22), 7685-90.
Destexhe, A., Contreras, D., and Steriade, M. (1999), 'Spatiotemporal analysis of local field potentials and unit discharges in cat cerebral cortex during natural wake and sleep states', *J Neurosci,* 19 (11), 4595-608.
Deuschl, G., et al. (2001), 'The pathophysiology of tremor', *Muscle Nerve,* 24 (6), 716-35.
Deuschl, G., et al. (2000), 'The pathophysiology of parkinsonian tremor: a review', *J Neurol,* 247 Suppl 5, V33-48.
Di Nocera, F. and Ferlazzo, F. (2000), 'Resampling approach to statistical inference: bootstrapping from event-related potentials data', *Behav Res Methods Instrum Comput,* 32 (1), 111-9.
Dias, R., Robbins, T. W., and Roberts, A. C. (1996), 'Dissociation in prefrontal cortex of affective and attentional shifts', *Nature,* 380 (6569), 69-72.
Dimitrov, M., et al. (1999), 'Concept formation and concept shifting in frontal lesion and Parkinson's disease patients assessed with the California Card Sorting Test', *Neuropsychology,* 13 (1), 135-43.
Djaldetti, R., et al. (2004), 'Quantitative measurement of pain sensation in patients with Parkinson disease', *Neurology,* 62 (12), 2171-5.
Donner, T. H., et al. (2009), 'Buildup of choice-predictive activity in human motor cortex during perceptual decision making', *Curr Biol,* 19 (18), 1581-5.
Donoghue, J. P. and Herkenham, M. (1986), 'Neostriatal projections from individual cortical fields conform to histochemically distinct striatal compartments in the rat', *Brain Res,* 365 (2), 397-403.
Dostrovsky, J. and Bergman, H. (2004), 'Oscillatory activity in the basal ganglia--relationship to normal physiology and pathophysiology', *Brain,* 127 (Pt 4), 721-2.
Dostrovsky, J. O., Hutchison, W. D., and Lozano, A. M. (2002), 'The globus pallidus, deep brain stimulation, and Parkinson's disease', *Neuroscientist,* 8 (3), 284-90.
Doyle, L. M., Yarrow, K., and Brown, P. (2005), 'Lateralization of event-related beta desynchronization in the EEG during pre-cued reaction time tasks', *Clin Neurophysiol,* 116 (8), 1879-88.
Drevets, W. C., Savitz, J., and Trimble, M. (2008), 'The subgenual anterior cingulate cortex in mood disorders', *CNS Spectr,* 13 (8), 663-81.
Dubner, R. and Bennett, G. J. (1983), 'Spinal and trigeminal mechanisms of nociception', *Annu Rev Neurosci,* 6, 381-418.
Dubois, B. and Pillon, B. (1997), 'Cognitive deficits in Parkinson's disease', *J Neurol,* 244 (1), 2-8.
Duda, Richard O., Hart, Peter E., and Stork, David G. (2001), *Pattern classification* (2nd edn.; New York ; Chichester: Wiley) xx, 654 p.
Dupre, K. B., et al. (2016), 'Effects of L-dopa priming on cortical high beta and high gamma oscillatory activity in a rodent model of Parkinson's disease', *Neurobiol Dis,* 86, 1-15.

Durschmid, S., et al. (2013), 'Phase-amplitude cross-frequency coupling in the human nucleus accumbens tracks action monitoring during cognitive control', *Front Hum Neurosci,* 7, 635.
Eckert, T., Tang, C., and Eidelberg, D. (2007), 'Assessment of the progression of Parkinson's disease: a metabolic network approach', *Lancet Neurol,* 6 (10), 926-32.
Ehringer, H. and Hornykiewicz, O. (1960), '[Distribution of noradrenaline and dopamine (3-hydroxytyramine) in the human brain and their behavior in diseases of the extrapyramidal system]', *Klin Wochenschr,* 38, 1236-9.
Eidelberg, D. (2009), 'Metabolic brain networks in neurodegenerative disorders: a functional imaging approach', *Trends Neurosci,* 32 (10), 548-57.
Eling, P., Derckx, K., and Maes, R. (2008), 'On the historical and conceptual background of the Wisconsin Card Sorting Test', *Brain Cogn,* 67 (3), 247-53.
Emre, M. (2003), 'Dementia associated with Parkinson's disease', *Lancet Neurol,* 2 (4), 229-37.
Engel, A. K. and Fries, P. (2010), 'Beta-band oscillations--signalling the status quo?', *Curr Opin Neurobiol,* 20 (2), 156-65.
Engel, A. K., Fries, P., and Singer, W. (2001), 'Dynamic predictions: oscillations and synchrony in top-down processing', *Nat Rev Neurosci,* 2 (10), 704-16.
Engel, A. K., et al. (1992), 'Temporal coding in the visual cortex: new vistas on integration in the nervous system', *Trends Neurosci,* 15 (6), 218-26.
Erro, R., et al. (2013), 'Non-motor symptoms in early Parkinson's disease: a 2-year follow-up study on previously untreated patients', *J Neurol Neurosurg Psychiatry,* 84 (1), 14-7.
Falkenstein, M., et al. (2001), 'Action monitoring, error detection, and the basal ganglia: an ERP study', *Neuroreport,* 12 (1), 157-61.
Farina, E., et al. (2000), 'Researching a differential impairment of frontal functions and explicit memory in early Parkinson's disease', *Eur J Neurol,* 7 (3), 259-67.
Fera, F., et al. (2007), 'Dopaminergic modulation of cognitive interference after pharmacological washout in Parkinson's disease', *Brain Res Bull,* 74 (1-3), 75-83.
Firnau, G., et al. (1988), 'Metabolites of 6-[18F]fluoro-L-dopa in human blood', *J Nucl Med,* 29 (3), 363-9.
Fogelson, N., et al. (2006), 'Different functional loops between cerebral cortex and the subthalmic area in Parkinson's disease', *Cereb Cortex,* 16 (1), 64-75.
Foix, Charles and Nicolesco, J. (1925), *Anatomie cérébrale; les noyaux gris centraux et la région mésencéphalo-sous-optique* (Paris,: Masson et cie).
Ford, B. (1998a), 'Pain in Parkinson's disease', *Clinical Neuroscience,* 5 (2), 63-72.
--- (1998b), 'Pain in Parkinson's disease', *Clin Neurosci,* 5 (2), 63-72.
Fouragnan, E., et al. (2015), 'Two spatiotemporally distinct value systems shape reward-based learning in the human brain', *Nat Commun,* 6, 8107.
Fries, P. (2005), 'A mechanism for cognitive dynamics: neuronal communication through neuronal coherence', *Trends Cogn Sci,* 9 (10), 474-80.
--- (2009), 'Neuronal gamma-band synchronization as a fundamental process in cortical computation', *Annu Rev Neurosci,* 32, 209-24.
Friston, K. J., et al. (2015), 'LFP and oscillations-what do they tell us?', *Curr Opin Neurobiol,* 31, 1-6.
Fujimoto, T., et al. (2016), 'Sex Differences in Gamma Band Functional Connectivity Between the Frontal Lobe and Cortical Areas During an Auditory Oddball Task, as Revealed by Imaginary Coherence Assessment', *Open Neuroimag J,* 10, 85-101.
Funahashi, S. and Andreau, J. M. (2013), 'Prefrontal cortex and neural mechanisms of executive function', *J Physiol Paris,* 107 (6), 471-82.
Fuster, J. M. (2008), 'Anatomy of the Prefrontal Cortex', *Prefrontal Cortex, 4th Edition,* 7-58.

Gallagher, C. L., et al. (2015), 'Anterior cingulate dopamine turnover and behavior change in Parkinson's disease', *Brain Imaging Behav,* 9 (4), 821-7.
Gallagher, D. A., Lees, A. J., and Schrag, A. (2010), 'What Are the Most Important Nonmotor Symptoms in Patients with Parkinson's Disease and Are We Missing Them?', *Movement Disorders,* 25 (15), 2493-500.
Gan, J. O., Walton, M. E., and Phillips, P. E. (2010), 'Dissociable cost and benefit encoding of future rewards by mesolimbic dopamine', *Nat Neurosci,* 13 (1), 25-7.
Garavan, H., Ross, T. J., and Stein, E. A. (1999), 'Right hemispheric dominance of inhibitory control: an event-related functional MRI study', *Proc Natl Acad Sci U S A,* 96 (14), 8301-6.
Garavan, H., et al. (2003), 'A midline dissociation between error-processing and response-conflict monitoring', *Neuroimage,* 20 (2), 1132-9.
Gardner, J. (2013), 'A history of deep brain stimulation: Technological innovation and the role of clinical assessment tools', *Social Studies of Science,* 43 (5), 707-28.
Gee, L. E., et al. (2016), 'Subthalamic deep brain stimulation alters neuronal firing in canonical pain nuclei in a 6-hydroxydopamine lesioned rat model of Parkinson's disease', *Exp Neurol,* 283 (Pt A), 298-307.
Geisseler, O., et al. (2016), 'Cortical thinning in the anterior cingulate cortex predicts multiple sclerosis patients' fluency performance in a lateralised manner', *Neuroimage Clin,* 10, 89-95.
Gerdelat-Mas, A., et al. (2007), 'Levodopa raises objective pain threshold in Parkinson's disease: a RIII reflex study', *J Neurol Neurosurg Psychiatry,* 78 (10), 1140-2.
Gerfen, C. R. (1992), 'The neostriatal mosaic: multiple levels of compartmental organization', *Trends Neurosci,* 15 (4), 133-9.
Gerfen, C. R., et al. (1982), 'Crossed connections of the substantia nigra in the rat', *J Comp Neurol,* 207 (3), 283-303.
Gerlach, M. and Riederer, P. (1996), 'Animal models of Parkinson's disease: an empirical comparison with the phenomenology of the disease in man', *J Neural Transm (Vienna),* 103 (8-9), 987-1041.
Giladi, N. (2001), 'Freezing of gait. Clinical overview', *Adv Neurol,* 87, 191-7.
Gilbertson, T., et al. (2005), 'Existing motor state is favored at the expense of new movement during 13-35 Hz oscillatory synchrony in the human corticospinal system', *J Neurosci,* 25 (34), 7771-9.
Gillies, M. J., et al. (2017), 'The Cognitive Role of the Globus Pallidus interna; Insights from Disease States', *Exp Brain Res,* 235 (5), 1455-65.
Gjerstad, M. D., et al. (2007), 'Insomnia in Parkinson's disease: frequency and progression over time', *J Neurol Neurosurg Psychiatry,* 78 (5), 476-9.
Gjerstad, M. D., et al. (2006), 'Excessive daytime sleepiness in Parkinson disease: is it the drugs or the disease?', *Neurology,* 67 (5), 853-8.
Gloor, P. (1985), 'Neuronal generators and the problem of localization in electroencephalography: application of volume conductor theory to electroencephalography', *J Clin Neurophysiol,* 2 (4), 327-54.
Goetz, C. G., et al. (1987), 'Relationships among pain, depression, and sleep alterations in Parkinson's disease', *Adv Neurol,* 45, 345-7.
Goetz, C. G., et al. (1986), 'Pain in Parkinson's disease', *Mov Disord,* 1 (1), 45-9.
Goldberg, J. A., et al. (2004), 'Spike synchronization in the cortex/basal-ganglia networks of Parkinsonian primates reflects global dynamics of the local field potentials', *J Neurosci,* 24 (26), 6003-10.
Gotham, A. M., Brown, R. G., and Marsden, C. D. (1988), "Frontal' cognitive function in patients with Parkinson's disease 'on' and 'off' levodopa', *Brain,* 111 (Pt 2), 299-321.

Goto, Y. and O'Donnell, P. (2001), 'Network synchrony in the nucleus accumbens in vivo', *J Neurosci,* 21 (12), 4498-504.
Gradinaru, V., et al. (2009), 'Optical deconstruction of parkinsonian neural circuitry', *Science,* 324 (5925), 354-9.
Graybiel, A. M. (1984), 'Correspondence between the dopamine islands and striosomes of the mammalian striatum', *Neuroscience,* 13 (4), 1157-87.
Graybiel, A. M. and Ragsdale, C. W., Jr. (1978), 'Histochemically distinct compartments in the striatum of human, monkeys, and cat demonstrated by acetylthiocholinesterase staining', *Proc Natl Acad Sci U S A,* 75 (11), 5723-6.
Greenamyre, J. T. and Hastings, T. G. (2004), 'Biomedicine. Parkinson's--divergent causes, convergent mechanisms', *Science,* 304 (5674), 1120-2.
Grillner, S., Robertson, B., and Stephenson-Jones, M. (2013), 'The evolutionary origin of the vertebrate basal ganglia and its role in action selection', *J Physiol,* 591 (22), 5425-31.
Grion, N., et al. (2016), 'Coherence between Rat Sensorimotor System and Hippocampus Is Enhanced during Tactile Discrimination', *PLoS Biol,* 14 (2), e1002384.
Guntekin, B. and Basar, E. (2015), 'Review of evoked and event-related delta responses in the human brain', *Int J Psychophysiol*.
Hammond, C. and Yelnik, J. (1983), 'Intracellular labelling of rat subthalamic neurones with horseradish peroxidase: computer analysis of dendrites and characterization of axon arborization', *Neuroscience,* 8 (4), 781-90.
Hammond, C., Bergman, H., and Brown, P. (2007), 'Pathological synchronization in Parkinson's disease: networks, models and treatments', *Trends Neurosci,* 30 (7), 357-64.
Hampshire, A. and Owen, A. M. (2006), 'Fractionating attentional control using event-related fMRI', *Cereb Cortex,* 16 (12), 1679-89.
Hayden, B. Y., et al. (2011), 'Surprise signals in anterior cingulate cortex: neuronal encoding of unsigned reward prediction errors driving adjustment in behavior', *J Neurosci,* 31 (11), 4178-87.
Hazrati, L. N. and Parent, A. (1991a), 'Contralateral pallidothalamic and pallidotegmental projections in primates: an anterograde and retrograde labeling study', *Brain Res,* 567 (2), 212-23.
--- (1991b), 'Projection from the external pallidum to the reticular thalamic nucleus in the squirrel monkey', *Brain Res,* 550 (1), 142-6.
Head, D., Bolton, D., and Hymas, N. (1989), 'Deficit in cognitive shifting ability in patients with obsessive-compulsive disorder', *Biol Psychiatry,* 25 (7), 929-37.
Heilbronner, S. R. and Hayden, B. Y. (2016), 'Dorsal Anterior Cingulate Cortex: A Bottom-Up View', *Annu Rev Neurosci,* 39, 149-70.
Hely, M. A., et al. (2005), 'Sydney Multicenter Study of Parkinson's disease: non-L-dopa-responsive problems dominate at 15 years', *Mov Disord,* 20 (2), 190-9.
Herkenham, M. (1979), 'The afferent and efferent connections of the ventromedial thalamic nucleus in the rat', *J Comp Neurol,* 183 (3), 487-517.
Hernandez-Gonzalez, S., et al. (2017), 'A Cognition-Related Neural Oscillation Pattern, Generated in the Prelimbic Cortex, Can Control Operant Learning in Rats', *J Neurosci,* 37 (24), 5923-35.
Herrojo Ruiz, M., et al. (2014), 'Involvement of human internal globus pallidus in the early modulation of cortical error-related activity', *Cereb Cortex,* 24 (6), 1502-17.
Hirschmann, J., et al. (2011), 'Distinct oscillatory STN-cortical loops revealed by simultaneous MEG and local field potential recordings in patients with Parkinson's disease', *Neuroimage,* 55 (3), 1159-68.

Holgado, A. J., Terry, J. R., and Bogacz, R. (2010), 'Conditions for the generation of beta oscillations in the subthalamic nucleus-globus pallidus network', *J Neurosci*, 30 (37), 12340-52.
Holroyd, C. B. and Coles, M. G. H. (2002), 'The neural basis of human error processing: reinforcement learning, dopamine, and the error-related negativity', *Psychol Rev*, 109 (4), 679-709.
Horvitz, J. C. (2000), 'Mesolimbocortical and nigrostriatal dopamine responses to salient non-reward events', *Neuroscience*, 96 (4), 651-6.
Huebl, J., et al. (2016), 'Processing of emotional stimuli is reflected by modulations of beta band activity in the subgenual anterior cingulate cortex in patients with treatment resistant depression', *Soc Cogn Affect Neurosci*, 11 (8), 1290-8.
Hutchison, W. D., et al. (1999), 'Pain-related neurons in the human cingulate cortex', *Nature Neuroscience*, 2 (5), 403-05.
Hyman, J. M., et al. (2013), 'Action and outcome activity state patterns in the anterior cingulate cortex', *Cereb Cortex*, 23 (6), 1257-68.
Ito, K., et al. (2013), 'Automatic extraction of the cingulum bundle in diffusion tensor tract-specific analysis: feasibility study in Parkinson's disease with and without dementia', *Magn Reson Med Sci*, 12 (3), 201-13.
Ito, S., et al. (2003), 'Performance monitoring by the anterior cingulate cortex during saccade countermanding', *Science*, 302 (5642), 120-2.
Iversen, J. R., Repp, B. H., and Patel, A. D. (2009), 'Top-down control of rhythm perception modulates early auditory responses', *Ann N Y Acad Sci*, 1169, 58-73.
Jahanshahi, M., Rowe, J., and Fuller, R. (2003), 'Cognitive executive function in dystonia', *Mov Disord*, 18 (12), 1470-81.
Jahanshahi, M., et al. (2015), 'A fronto-striato-subthalamic-pallidal network for goal-directed and habitual inhibition', *Nat Rev Neurosci*, 16 (12), 719-32.
Jankovic, J. (2008), 'Parkinson's disease: clinical features and diagnosis', *J Neurol Neurosurg Psychiatry*, 79 (4), 368-76.
Jenkinson, N. and Brown, P. (2011), 'New insights into the relationship between dopamine, beta oscillations and motor function', *Trends Neurosci*, 34 (12), 611-8.
Jenkinson, N., Kuhn, A. A., and Brown, P. (2013), 'gamma oscillations in the human basal ganglia', *Exp Neurol*, 245, 72-6.
Jensen, O. and Tesche, C. D. (2002), 'Frontal theta activity in humans increases with memory load in a working memory task', *Eur J Neurosci*, 15 (8), 1395-9.
Jensen, O. and Lisman, J. E. (2005), 'Hippocampal sequence-encoding driven by a cortical multi-item working memory buffer', *Trends Neurosci*, 28 (2), 67-72.
Joel, D. and Weiner, I. (1997), 'The connections of the primate subthalamic nucleus: indirect pathways and the open-interconnected scheme of basal ganglia-thalamocortical circuitry', *Brain Res Brain Res Rev*, 23 (1-2), 62-78.
Johansen, J. P., Fields, H. L., and Manning, B. H. (2001), 'The affective component of pain in rodents: direct evidence for a contribution of the anterior cingulate cortex', *Proc Natl Acad Sci U S A*, 98 (14), 8077-82.
Kawaguchi, Y., Wilson, C. J., and Emson, P. C. (1989), 'Intracellular recording of identified neostriatal patch and matrix spiny cells in a slice preparation preserving cortical inputs', *J Neurophysiol*, 62 (5), 1052-68.
Keeler, J. F. and Robbins, T. W. (2011), 'Translating cognition from animals to humans', *Biochem Pharmacol*, 81 (12), 1356-66.
Kehagia, A. A., Barker, R. A., and Robbins, T. W. (2010), 'Neuropsychological and clinical heterogeneity of cognitive impairment and dementia in patients with Parkinson's disease', *Lancet Neurol*, 9 (12), 1200-13.

Kennerley, S. W. and Walton, M. E. (2011), 'Decision making and reward in frontal cortex: complementary evidence from neurophysiological and neuropsychological studies', *Behav Neurosci,* 125 (3), 297-317.
Kennerley, S. W., Behrens, T. E., and Wallis, J. D. (2011), 'Double dissociation of value computations in orbitofrontal and anterior cingulate neurons', *Nat Neurosci,* 14 (12), 1581-9.
Kim, J. Y., et al. (2015), 'Spinal dopaminergic projections control the transition to pathological pain plasticity via a D1/D5-mediated mechanism', *J Neurosci,* 35 (16), 6307-17.
Klamer, S., et al. (2015), 'Differences between MEG and high-density EEG source localizations using a distributed source model in comparison to fMRI', *Brain Topogr,* 28 (1), 87-94.
Klausberger, T. and Somogyi, P. (2008), 'Neuronal diversity and temporal dynamics: the unity of hippocampal circuit operations', *Science,* 321 (5885), 53-7.
Klimesch, W. (1996), 'Memory processes, brain oscillations and EEG synchronization', *Int J Psychophysiol,* 24 (1-2), 61-100.
--- (1999), 'EEG alpha and theta oscillations reflect cognitive and memory performance: a review and analysis', *Brain Res Brain Res Rev,* 29 (2-3), 169-95.
Klimesch, W., Schimke, H., and Pfurtscheller, G. (1993), 'Alpha frequency, cognitive load and memory performance', *Brain Topogr,* 5 (3), 241-51.
Klimesch, W., et al. (1997), 'Brain oscillations and human memory: EEG correlates in the upper alpha and theta band', *Neurosci Lett,* 238 (1-2), 9-12.
Klockgether, T., et al. (1986), 'The rat ventromedial thalamic nucleus and motor control: role of N-methyl-D-aspartate-mediated excitation, GABAergic inhibition, and muscarinic transmission', *J Neurosci,* 6 (6), 1702-11.
Klostermann, F., et al. (2007), 'Task-related differential dynamics of EEG alpha- and beta-band synchronization in cortico-basal motor structures', *Eur J Neurosci,* 25 (5), 1604-15.
Knyazev, G. G. (2007), 'Motivation, emotion, and their inhibitory control mirrored in brain oscillations', *Neurosci Biobehav Rev,* 31 (3), 377-95.
Knyazev, G. G., Savostyanov, A. N., and Levin, E. A. (2006), 'Alpha synchronization and anxiety: implications for inhibition vs. alertness hypotheses', *Int J Psychophysiol,* 59 (2), 151-8.
Kolling, N., et al. (2016), 'Value, search, persistence and model updating in anterior cingulate cortex', *Nat Neurosci,* 19 (10), 1280-5.
Konishi, S., et al. (1998), 'No-go dominant brain activity in human inferior prefrontal cortex revealed by functional magnetic resonance imaging', *Eur J Neurosci,* 10 (3), 1209-13.
Kopell, N., et al. (2000), 'Gamma rhythms and beta rhythms have different synchronization properties', *Proc Natl Acad Sci U S A,* 97 (4), 1867-72.
Koski, L. and Paus, T. (2000), 'Functional connectivity of the anterior cingulate cortex within the human frontal lobe: a brain-mapping meta-analysis', *Exp Brain Res,* 133 (1), 55-65.
Kozelj, S. and Baker, S. N. (2014), 'Different phase delays of peripheral input to primate motor cortex and spinal cord promote cancellation at physiological tremor frequencies', *J Neurophysiol,* 111 (10), 2001-16.
Kringelbach, M. L., et al. (2007), 'Translational principles of deep brain stimulation', *Nat Rev Neurosci,* 8 (8), 623-35.
Kudlicka, A., Clare, L., and Hindle, J. V. (2011), 'Executive functions in Parkinson's disease: systematic review and meta-analysis', *Mov Disord,* 26 (13), 2305-15.

Kuhn, A. A., et al. (2006), 'Reduction in subthalamic 8-35 Hz oscillatory activity correlates with clinical improvement in Parkinson's disease', *Eur J Neurosci,* 23 (7), 1956-60.
Kuhn, A. A., et al. (2005), 'The relationship between local field potential and neuronal discharge in the subthalamic nucleus of patients with Parkinson's disease', *Exp Neurol,* 194 (1), 212-20.
Kuhn, A. A., et al. (2004), 'Event-related beta desynchronization in human subthalamic nucleus correlates with motor performance', *Brain,* 127 (Pt 4), 735-46.
Kuhn, A. A., et al. (2008a), 'Increased beta activity in dystonia patients after drug-induced dopamine deficiency', *Exp Neurol,* 214 (1), 140-3.
Kuhn, A. A., et al. (2008b), 'High-frequency stimulation of the subthalamic nucleus suppresses oscillatory beta activity in patients with Parkinson's disease in parallel with improvement in motor performance', *J Neurosci,* 28 (24), 6165-73.
Kuramoto, E., et al. (2009), 'Two types of thalamocortical projections from the motor thalamic nuclei of the rat: a single neuron-tracing study using viral vectors', *Cereb Cortex,* 19 (9), 2065-77.
Kuramoto, E., et al. (2011), 'Complementary distribution of glutamatergic cerebellar and GABAergic basal ganglia afferents to the rat motor thalamic nuclei', *Eur J Neurosci,* 33 (1), 95-109.
Kuramoto, E., et al. (2015), 'Ventral medial nucleus neurons send thalamocortical afferents more widely and more preferentially to layer 1 than neurons of the ventral anterior-ventral lateral nuclear complex in the rat', *Cereb Cortex,* 25 (1), 221-35.
Lalo, E., et al. (2008), 'Patterns of bidirectional communication between cortex and basal ganglia during movement in patients with Parkinson disease', *J Neurosci,* 28 (12), 3008-16.
Lanciego, J. L., Luquin, N., and Obeso, J. A. (2012), 'Functional neuroanatomy of the basal ganglia', *Cold Spring Harb Perspect Med,* 2 (12), a009621.
Laufs, H., et al. (2003), 'Electroencephalographic signatures of attentional and cognitive default modes in spontaneous brain activity fluctuations at rest', *Proc Natl Acad Sci U S A,* 100 (19), 11053-8.
Le Cavorzin, P., et al. (2003), 'A computer model of rigidity and related motor dysfunction in Parkinson's disease', *Mov Disord,* 18 (11), 1257-65.
Lee, S. and Jones, S. R. (2013), 'Distinguishing mechanisms of gamma frequency oscillations in human current source signals using a computational model of a laminar neocortical network', *Front Hum Neurosci,* 7, 869.
Lees, A. J. and Smith, E. (1983), 'Cognitive deficits in the early stages of Parkinson's disease', *Brain,* 106 (Pt 2), 257-70.
Lega, B. C., et al. (2011), 'Neuronal and oscillatory activity during reward processing in the human ventral striatum', *Neuroreport,* 22 (16), 795-800.
Lempka, S. F. and McIntyre, C. C. (2013), 'Theoretical analysis of the local field potential in deep brain stimulation applications', *PLoS One,* 8 (3), e59839.
Leopold, D. A. and Logothetis, N. K. (2003), 'Spatial patterns of spontaneous local field activity in the monkey visual cortex', *Rev Neurosci,* 14 (1-2), 195-205.
Leventhal, D. K., et al. (2012), 'Basal ganglia beta oscillations accompany cue utilization', *Neuron,* 73 (3), 523-36.
Levy, R., et al. (2002), 'Dependence of subthalamic nucleus oscillations on movement and dopamine in Parkinson's disease', *Brain,* 125 (Pt 6), 1196-209.
Levy, R., et al. (1997), 'Re-evaluation of the functional anatomy of the basal ganglia in normal and Parkinsonian states', *Neuroscience,* 76 (2), 335-43.

Lima, D. and Coimbra, A. (1990), 'Structural types of marginal (lamina I) neurons projecting to the dorsal reticular nucleus of the medulla oblongata', *Neuroscience,* 34 (3), 591-606.
Limousin, P., et al. (1995), 'Effect of parkinsonian signs and symptoms of bilateral subthalamic nucleus stimulation', *Lancet,* 345 (8942), 91-5.
Lindsen, J. P., et al. (2010), 'Neural components underlying subjective preferential decision making', *Neuroimage,* 50 (4), 1626-32.
Lipsman, N., et al. (2014), 'Beta coherence within human ventromedial prefrontal cortex precedes affective value choices', *Neuroimage,* 2, 769-78.
Logothetis, N. K., et al. (2001), 'Neurophysiological investigation of the basis of the fMRI signal', *Nature,* 412 (6843), 150-7.
Lorenz, J., Minoshima, S., and Casey, K. L. (2003), 'Keeping pain out of mind: the role of the dorsolateral prefrontal cortex in pain modulation', *Brain,* 126, 1079-91.
Lutcke, H. and Frahm, J. (2008), 'Lateralized anterior cingulate function during error processing and conflict monitoring as revealed by high-resolution fMRI', *Cereb Cortex,* 18 (3), 508-15.
Magill, P. J., et al. (2004), 'Synchronous unit activity and local field potentials evoked in the subthalamic nucleus by cortical stimulation', *J Neurophysiol,* 92 (2), 700-14.
Makeig, S. (1993), 'Auditory event-related dynamics of the EEG spectrum and effects of exposure to tones', *Electroencephalogr Clin Neurophysiol,* 86 (4), 283-93.
Malekmohammadi, M., Elias, W. J., and Pouratian, N. (2015), 'Human thalamus regulates cortical activity via spatially specific and structurally constrained phase-amplitude coupling', *Cereb Cortex,* 25 (6), 1618-28.
Marsden, J. F., et al. (2001), 'Subthalamic nucleus, sensorimotor cortex and muscle interrelationships in Parkinson's disease', *Brain,* 124 (Pt 2), 378-88.
Martinez-Fernandez, R., Castrioto, A., and Krack, P. (2014), 'Prefrontal--STN projections, the highway for emotion and cognition control', *Mov Disord,* 29 (3), 305.
Martinez-Martin, P. (2011), 'The importance of non-motor disturbances to quality of life in Parkinson's disease', *J Neurol Sci,* 310 (1-2), 12-6.
Marzullo, G.J. Gage; H. Parikh; T.C. (2008), 'The Cingulate Cortex Does Everything', *Annals of Improbable Research,* 14 (3), 12-15.
Maurer, C., et al. (2003), 'Effect of chronic bilateral subthalamic nucleus (STN) stimulation on postural control in Parkinson's disease', *Brain,* 126 (Pt 5), 1146-63.
Mayberg, H. S., et al. (2005), 'Deep brain stimulation for treatment-resistant depression', *Neuron,* 45 (5), 651-60.
McKinlay, A., et al. (2010), 'Characteristics of executive function impairment in Parkinson's disease patients without dementia', *J Int Neuropsychol Soc,* 16 (2), 268-77.
Mehler, W. R., Feferman, M. E., and Nauta, W. J. (1960), 'Ascending axon degeneration following anterolateral cordotomy. An experimental study in the monkey', *Brain,* 83, 718-50.
Menon, V., et al. (2001), 'Error-related brain activation during a Go/NoGo response inhibition task', *Hum Brain Mapp,* 12 (3), 131-43.
Merkl, A., et al. (2016), 'Modulation of Beta-Band Activity in the Subgenual Anterior Cingulate Cortex during Emotional Empathy in Treatment-Resistant Depression', *Cereb Cortex,* 26 (6), 2626-38.
Meyer-Lindenberg, A., et al. (2005), 'Midbrain dopamine and prefrontal function in humans: interaction and modulation by COMT genotype', *Nat Neurosci,* 8 (5), 594-6.
Miller, E. K. and Cohen, J. D. (2001), 'An integrative theory of prefrontal cortex function', *Annu Rev Neurosci,* 24, 167-202.

Mitzdorf, U. (1985), 'Current source-density method and application in cat cerebral cortex: investigation of evoked potentials and EEG phenomena', *Physiol Rev*, 65 (1), 37-100.
Mohseni, H. R., et al. (2012), 'MEG can map short and long-term changes in brain activity following deep brain stimulation for chronic pain', *PLoS One*, 7 (6).
Moore, R. Y., et al. (2003), 'Monoamine neuron innervation of the normal human brain: an 18F-DOPA PET study', *Brain Res*, 982 (2), 137-45.
Morecraft, R. J. and Van Hoesen, G. W. (1998), 'Convergence of limbic input to the cingulate motor cortex in the rhesus monkey', *Brain Res Bull*, 45 (2), 209-32.
Muslimovic, D., et al. (2005), 'Cognitive profile of patients with newly diagnosed Parkinson disease', *Neurology*, 65 (8), 1239-45.
Mylius, V., et al. (2009), 'Pain sensitivity and descending inhibition of pain in Parkinson's disease', *Journal of Neurology Neurosurgery and Psychiatry*, 80 (1), 24-28.
Nakamura, K., Roesch, M. R., and Olson, C. R. (2005), 'Neuronal activity in macaque SEF and ACC during performance of tasks involving conflict', *J Neurophysiol*, 93 (2), 884-908.
Nambu, A., Tokuno, H., and Takada, M. (2002), 'Functional significance of the cortico-subthalamo-pallidal 'hyperdirect' pathway', *Neurosci Res*, 43 (2), 111-7.
Nambu, A., et al. (1997), 'Corticosubthalamic input zones from forelimb representations of the dorsal and ventral divisions of the premotor cortex in the macaque monkey: comparison with the input zones from the primary motor cortex and the supplementary motor area', *Neurosci Lett*, 239 (1), 13-6.
Negre-Pages, L., et al. (2008), 'Chronic pain in Parkinson's disease: The cross-sectional French DoPaMiP survey', *Movement Disorders*, 23 (10), 1361-69.
Neubert, F. X., et al. (2015), 'Connectivity reveals relationship of brain areas for reward-guided learning and decision making in human and monkey frontal cortex', *Proc Natl Acad Sci U S A*, 112 (20), E2695-704.
Neuper, C. and Pfurtscheller, G. (2001), 'Event-related dynamics of cortical rhythms: frequency-specific features and functional correlates', *Int J Psychophysiol*, 43 (1), 41-58.
Nussbaum, R. L. and Ellis, C. E. (2003), 'Alzheimer's disease and Parkinson's disease', *N Engl J Med*, 348 (14), 1356-64.
O'Reilly, J. X., et al. (2013), 'Dissociable effects of surprise and model update in parietal and anterior cingulate cortex', *Proc Natl Acad Sci U S A*, 110 (38), E3660-9.
Okazaki, M., et al. (2008), 'Perceptual change in response to a bistable picture increases neuromagnetic beta-band activities', *Neurosci Res*, 61 (3), 319-28.
Olsson, M., et al. (1995), 'Forelimb akinesia in the rat Parkinson model: differential effects of dopamine agonists and nigral transplants as assessed by a new stepping test', *J Neurosci*, 15 (5 Pt 2), 3863-75.
Ongur, D. and Price, J. L. (2000), 'The organization of networks within the orbital and medial prefrontal cortex of rats, monkeys and humans', *Cereb Cortex*, 10 (3), 206-19.
Ongur, D., Ferry, A. T., and Price, J. L. (2003), 'Architectonic subdivision of the human orbital and medial prefrontal cortex', *J Comp Neurol*, 460 (3), 425-49.
Osaka, M. (1984), 'Peak alpha frequency of EEG during a mental task: task difficulty and hemispheric differences', *Psychophysiology*, 21 (1), 101-5.
Oswal, A., Brown, P., and Litvak, V. (2013), 'Synchronized neural oscillations and the pathophysiology of Parkinson's disease', *Curr Opin Neurol*, 26 (6), 662-70.
Owen, A. M. (2004), 'Cognitive dysfunction in Parkinson's disease: the role of frontostriatal circuitry', *Neuroscientist*, 10 (6), 525-37.
Owen, A. M., et al. (1993), 'Contrasting mechanisms of impaired attentional set-shifting in patients with frontal lobe damage or Parkinson's disease', *Brain*, 116 (Pt 5), 1159-75.

Palmigiano, A., et al. (2017), 'Flexible information routing by transient synchrony', *Nat Neurosci*, 20 (7), 1014-22.
Palva, S. and Palva, J. M. (2007), 'New vistas for alpha-frequency band oscillations', *Trends Neurosci*, 30 (4), 150-8.
Pandya, M., et al. (2012), 'Where in the brain is depression?', *Curr Psychiatry Rep*, 14 (6), 634-42.
Parent, A., et al. (2000), 'Organization of the basal ganglia: the importance of axonal collateralization', *Trends Neurosci*, 23 (10 Suppl), S20-7.
Parkinson, J. (1817), 'An essay on the shaking palsy. 1817', *J Neuropsychiatry Clin Neurosci*, 14 (2), 223-36; discussion 22.
Parr-Brownlie, L. C., et al. (2007), 'Dopamine lesion-induced changes in subthalamic nucleus activity are not associated with alterations in firing rate or pattern in layer V neurons of the anterior cingulate cortex in anesthetized rats', *Eur J Neurosci*, 26 (7), 1925-39.
Parra, L. C., et al. (2005), 'Recipes for the linear analysis of EEG', *Neuroimage*, 28 (2), 326-41.
Passingham, R. E. and Wise, Steven P. (2012), *The neurobiology of the prefrontal cortex : anatomy, evolution, and the origin of insight* (1st edn., Oxford psychology series; Oxford, United Kingdom: Oxford University Press) xxii, 399 p.
Paus, T. (2001), 'Primate anterior cingulate cortex: where motor control, drive and cognition interface', *Nat Rev Neurosci*, 2 (6), 417-24.
Penny, G. R., Wilson, C. J., and Kitai, S. T. (1988), 'Relationship of the axonal and dendritic geometry of spiny projection neurons to the compartmental organization of the neostriatum', *J Comp Neurol*, 269 (2), 275-89.
Pereira, E. A. and Aziz, T. Z. (2014), 'Neuropathic pain and deep brain stimulation', *Neurotherapeutics*, 11 (3), 496-507.
Pesaran, B., Nelson, M. J., and Andersen, R. A. (2008), 'Free choice activates a decision circuit between frontal and parietal cortex', *Nature*, 453 (7193), 406-9.
Pfurtscheller, G. and Aranibar, A. (1977), 'Event-related cortical desynchronization detected by power measurements of scalp EEG', *Electroencephalogr Clin Neurophysiol*, 42 (6), 817-26.
Pfurtscheller, G., Stancak, A., Jr., and Neuper, C. (1996), 'Post-movement beta synchronization. A correlate of an idling motor area?', *Electroencephalogr Clin Neurophysiol*, 98 (4), 281-93.
Pogosyan, A., et al. (2009), 'Boosting cortical activity at Beta-band frequencies slows movement in humans', *Curr Biol*, 19 (19), 1637-41.
Polli, F. E., et al. (2005), 'Rostral and dorsal anterior cingulate cortex make dissociable contributions during antisaccade error commission', *Proc Natl Acad Sci U S A*, 102 (43), 15700-5.
Ponsen, M. M., et al. (2004), 'Idiopathic hyposmia as a preclinical sign of Parkinson's disease', *Ann Neurol*, 56 (2), 173-81.
Price, D. D. (2000), 'Psychological and neural mechanisms of the affective dimension of pain', *Science*, 288 (5472), 1769-72.
Priori, A., et al. (2004), 'Rhythm-specific pharmacological modulation of subthalamic activity in Parkinson's disease', *Exp Neurol*, 189 (2), 369-79.
Pritchard, W. S. (1992), 'The brain in fractal time: 1/f-like power spectrum scaling of the human electroencephalogram', *Int J Neurosci*, 66 (1-2), 119-29.
Procyk, E., et al. (2016), 'Midcingulate Motor Map and Feedback Detection: Converging Data from Humans and Monkeys', *Cereb Cortex*, 26 (2), 467-76.
Puig, M. V., Antzoulatos, E. G., and Miller, E. K. (2014a), 'Prefrontal dopamine in associative learning and memory', *Neuroscience*, 282, 217-29.

Puig, M. V., et al. (2014b), 'Dopamine modulation of learning and memory in the prefrontal cortex: insights from studies in primates, rodents, and birds', *Front Neural Circuits,* 8, 93.
Ramadan, W., Eschenko, O., and Sara, S. J. (2009), 'Hippocampal sharp wave/ripples during sleep for consolidation of associative memory', *PLoS One,* 4 (8), e6697.
Rascol, O., Brefel-Courbon, C., and Blin, O. (1998), '[Clinical pharmacology of dyskinesias induced by L-dopa in Parkinsonian patients]', *Therapie,* 53 (1), 43-8.
Ravina, B., et al. (2009), 'A longitudinal program for biomarker development in Parkinson's disease: a feasibility study', *Mov Disord,* 24 (14), 2081-90.
Rivlin-Etzion, M., et al. (2006), 'Basal ganglia oscillations and pathophysiology of movement disorders', *Curr Opin Neurobiol,* 16 (6), 629-37.
Robinson, D. L. and Wightman, R. M. (2007), 'Rapid Dopamine Release in Freely Moving Rats', in A. C. Michael and L. M. Borland (eds.), *Electrochemical Methods for Neuroscience* (Boca Raton (FL)).
Rodriguez-Oroz, M. C., et al. (2011), 'Involvement of the subthalamic nucleus in impulse control disorders associated with Parkinson's disease', *Brain,* 134 (Pt 1), 36-49.
Rommelfanger, K. S. and Wichmann, T. (2010), 'Extrastriatal dopaminergic circuits of the Basal Ganglia', *Front Neuroanat,* 4, 139.
Rosenberg, J. R., et al. (1989), 'The Fourier approach to the identification of functional coupling between neuronal spike trains', *Prog Biophys Mol Biol,* 53 (1), 1-31.
Rosin, Boris, et al. (2007), 'Physiology and pathophysiology of the basal ganglia—thalamo—cortical networks', *Parkinsonism & Related Disorders,* 13, S437-S39.
Rubia, K., et al. (2001), 'Mapping motor inhibition: conjunctive brain activations across different versions of go/no-go and stop tasks', *Neuroimage,* 13 (2), 250-61.
Ruiz, M. H., et al. (2011), 'EEG oscillatory patterns are associated with error prediction during music performance and are altered in musician's dystonia', *Neuroimage,* 55 (4), 1791-803.
Rushworth, M. F., et al. (2011), 'Frontal cortex and reward-guided learning and decision-making', *Neuron,* 70 (6), 1054-69.
Sage, J. R., et al. (2003), 'Analysis of probabilistic classification learning in patients with Parkinson's disease before and after pallidotomy surgery', *Learn Mem,* 10 (3), 226-36.
Salazar, R. F., et al. (2012), 'Content-specific fronto-parietal synchronization during visual working memory', *Science,* 338 (6110), 1097-100.
Saleh, M., et al. (2010), 'Fast and slow oscillations in human primary motor cortex predict oncoming behaviorally relevant cues', *Neuron,* 65 (4), 461-71.
Sallet, J., et al. (2007), 'Expectations, gains, and losses in the anterior cingulate cortex', *Cogn Affect Behav Neurosci,* 7 (4), 327-36.
Sanes, J. N. and Donoghue, J. P. (1993), 'Oscillations in local field potentials of the primate motor cortex during voluntary movement', *Proc Natl Acad Sci U S A,* 90 (10), 4470-4.
Sano, I., et al. (1959), 'Distribution of catechol compounds in human brain', *Biochim Biophys Acta,* 32, 586-7.
Sawada, Y., et al. (2012), 'Attentional set-shifting deficit in Parkinson's disease is associated with prefrontal dysfunction: an FDG-PET study', *PLoS One,* 7 (6), e38498.
Schaeffer, E. and Berg, D. (2017), 'Dopaminergic Therapies for Non-motor Symptoms in Parkinson's Disease', *CNS Drugs*.
Schall, J. D., Stuphorn, V., and Brown, J. W. (2002), 'Monitoring and control of action by the frontal lobes', *Neuron,* 36 (2), 309-22.
Schapira, A. H. (2013), 'Recent developments in biomarkers in Parkinson disease', *Curr Opin Neurol,* 26 (4), 395-400.

Schapira, A. H., et al. (2014), 'Slowing of neurodegeneration in Parkinson's disease and Huntington's disease: future therapeutic perspectives', *Lancet,* 384 (9942), 545-55.
Schapira, A. H. V., Chaudhuri, K. R., and Jenner, P. (2017), 'Non-motor features of Parkinson disease', *Nat Rev Neurosci,* 18 (8), 509.
Scheggia, D., et al. (2014), 'The ultimate intra-/extra-dimensional attentional set-shifting task for mice', *Biol Psychiatry,* 75 (8), 660-70.
Scherder, E., et al. (2005), 'Pain in Parkinson's disease and multiple sclerosis: Its relation to the medial and lateral pain systems', *Neuroscience and Biobehavioral Reviews,* 29 (7), 1047-56.
Schrag, A., Sauerbier, A., and Chaudhuri, K. R. (2015), 'New clinical trials for nonmotor manifestations of Parkinson's disease', *Mov Disord,* 30 (11), 1490-504.
Schroder, K. F., et al. (1975), '[Morphometrical-statistical structure analysis of human striatum, pallidum and subthalamic nucleus]', *J Hirnforsch,* 16 (4), 333-50.
Schroeder, C. E., et al. (2008), 'Neuronal oscillations and visual amplification of speech', *Trends Cogn Sci,* 12 (3), 106-13.
Schultz, W. (1997), 'Dopamine neurons and their role in reward mechanisms', *Curr Opin Neurobiol,* 7 (2), 191-7.
--- (2010), 'Multiple functions of dopamine neurons', *F1000 Biol Rep,* 2.
Schultz, W., Dayan, P., and Montague, P. R. (1997), 'A neural substrate of prediction and reward', *Science,* 275 (5306), 1593-9.
Schwarting, R. K. and Huston, J. P. (1996), 'The unilateral 6-hydroxydopamine lesion model in behavioral brain research. Analysis of functional deficits, recovery and treatments', *Prog Neurobiol,* 50 (2-3), 275-331.
Schweimer, J. and Hauber, W. (2006), 'Dopamine D1 receptors in the anterior cingulate cortex regulate effort-based decision making', *Learn Mem,* 13 (6), 777-82.
Scott, R. B., et al. (2003), 'Executive cognitive deficits in primary dystonia', *Mov Disord,* 18 (5), 539-50.
Seeley, W. W., et al. (2007), 'Dissociable intrinsic connectivity networks for salience processing and executive control', *J Neurosci,* 27 (9), 2349-56.
Senard, J. M., et al. (1997), 'Prevalence of orthostatic hypotension in Parkinson's disease', *J Neurol Neurosurg Psychiatry,* 63 (5), 584-9.
Shahed, J. and Jankovic, J. (2007), 'Motor symptoms in Parkinson's disease', *Handb Clin Neurol,* 83, 329-42.
Shenhav, A., Botvinick, M. M., and Cohen, J. D. (2013), 'The expected value of control: an integrative theory of anterior cingulate cortex function', *Neuron,* 79 (2), 217-40.
Shenhav, A., Cohen, J. D., and Botvinick, M. M. (2016), 'Dorsal anterior cingulate cortex and the value of control', *Nat Neurosci,* 19 (10), 1286-91.
Sheth, S. A., et al. (2012), 'Human dorsal anterior cingulate cortex neurons mediate ongoing behavioural adaptation', *Nature,* 488 (7410), 218-21.
Silvetti, M., et al. (2014), 'From conflict management to reward-based decision making: actors and critics in primate medial frontal cortex', *Neuroscience and biobehavioral reviews,* 1, 44-57.
Smith, Y., et al. (1998), 'Microcircuitry of the direct and indirect pathways of the basal ganglia', *Neuroscience,* 86 (2), 353-87.
Snider, S. R., et al. (1976), 'Primary sensory symptoms in parkinsonism', *Neurology,* 26 (5), 423-9.
Solari, N., et al. (2013), 'Understanding cognitive deficits in Parkinson's disease: lessons from preclinical animal models', *Learn Mem,* 20 (10), 592-600.
Solomon, E. A., et al. (2017), 'Widespread theta synchrony and high-frequency desynchronization underlies enhanced cognition', *Nat Commun,* 8 (1), 1704.

Starr, P. A., et al. (2005), 'Spontaneous pallidal neuronal activity in human dystonia: comparison with Parkinson's disease and normal macaque', *J Neurophysiol,* 93 (6), 3165-76.
Steriade, M., McCormick, D. A., and Sejnowski, T. J. (1993), 'Thalamocortical oscillations in the sleeping and aroused brain', *Science,* 262 (5134), 679-85.
Stern, M. B., et al. (1994), 'Olfactory function in Parkinson's disease subtypes', *Neurology,* 44 (2), 266-8.
Sugimoto, T. and Hattori, T. (1983), 'Confirmation of thalamosubthalamic projections by electron microscopic autoradiography', *Brain Res,* 267 (2), 335-9.
Sugimoto, T., et al. (1983), 'Direct projections from the centre median-parafascicular complex to the subthalamic nucleus in the cat and rat', *J Comp Neurol,* 214 (2), 209-16.
Swann, N. C., et al. (2016), 'Gamma Oscillations in the Hyperkinetic State Detected with Chronic Human Brain Recordings in Parkinson's Disease', *J Neurosci,* 36 (24), 6445-58.
Swinn, L., et al. (2003), 'Sweating dysfunction in Parkinson's disease', *Mov Disord,* 18 (12), 1459-63.
Tagliati, M. (2012), 'Turning tables: should GPi become the preferred DBS target for Parkinson disease?', *Neurology,* 79 (1), 19-20.
Tamaru, F. (1997), 'Disturbances in higher function in Parkinson's disease', *Eur Neurol,* 38 Suppl 2, 33-6.
Tan, H., Jenkinson, N., and Brown, P. (2014), 'Dynamic neural correlates of motor error monitoring and adaptation during trial-to-trial learning', *J Neurosci,* 34 (16), 5678-88.
Taylor, S. F., et al. (2006), 'Medial frontal cortex activity and loss-related responses to errors', *J Neurosci,* 26 (15), 4063-70.
Tinazzi, M., et al. (2006), 'Pain and motor complications in Parkinson's disease', *J Neurol Neurosurg Psychiatry,* 77 (7), 822-5.
Tononi, G., Edelman, G. M., and Sporns, O. (1998), 'Complexity and coherency: integrating information in the brain', *Trends Cogn Sci,* 2 (12), 474-84.
Traub, R. D., et al. (1996), 'A mechanism for generation of long-range synchronous fast oscillations in the cortex', *Nature,* 383 (6601), 621-4.
Traub, R. D., et al. (2002), 'Axonal gap junctions between principal neurons: a novel source of network oscillations, and perhaps epileptogenesis', *Rev Neurosci,* 13 (1), 1-30.
Turner, J. G., et al. (2005), 'Hearing in laboratory animals: strain differences and nonauditory effects of noise', *Comp Med,* 55 (1), 12-23.
Turner, R. S. and Anderson, M. E. (2005), 'Context-dependent modulation of movement-related discharge in the primate globus pallidus', *J Neurosci,* 25 (11), 2965-76.
Turner, R. S. and Desmurget, M. (2010), 'Basal ganglia contributions to motor control: a vigorous tutor', *Curr Opin Neurobiol,* 20 (6), 704-16.
Tzagarakis, C., et al. (2010), 'Beta-band activity during motor planning reflects response uncertainty', *J Neurosci,* 30 (34), 11270-7.
Uhlhaas, P. J. and Singer, W. (2006), 'Neural synchrony in brain disorders: relevance for cognitive dysfunctions and pathophysiology', *Neuron,* 52 (1), 155-68.
Ungerstedt, U. (1968), '6-Hydroxy-dopamine induced degeneration of central monoamine neurons', *Eur J Pharmacol,* 5 (1), 107-10.
van Driel, J., Ridderinkhof, K. R., and Cohen, M. X. (2012), 'Not all errors are alike: theta and alpha EEG dynamics relate to differences in error-processing dynamics', *J Neurosci,* 32 (47), 16795-806.
Varela, F., et al. (2001), 'The brainweb: phase synchronization and large-scale integration', *Nat Rev Neurosci,* 2 (4), 229-39.

Villanueva, L., Bernard, J. F., and Le Bars, D. (1995), 'Distribution of spinal cord projections from the medullary subnucleus reticularis dorsalis and the adjacent cuneate nucleus: a Phaseolus vulgaris-leucoagglutinin study in the rat', *J Comp Neurol,* 352 (1), 11-32.
Villanueva, L., Bouhassira, D., and Le Bars, D. (1996), 'The medullary subnucleus reticularis dorsalis (SRD) as a key link in both the transmission and modulation of pain signals', *Pain,* 67 (2-3), 231-40.
Villanueva, L., et al. (1988), 'Convergence of heterotopic nociceptive information onto subnucleus reticularis dorsalis neurons in the rat medulla', *J Neurophysiol,* 60 (3), 980-1009.
Villanueva, L., et al. (1989), 'Encoding of electrical, thermal, and mechanical noxious stimuli by subnucleus reticularis dorsalis neurons in the rat medulla', *J Neurophysiol,* 61 (2), 391-402.
Vingerhoets, F. J., et al. (1997), 'Which clinical sign of Parkinson's disease best reflects the nigrostriatal lesion?', *Ann Neurol,* 41 (1), 58-64.
Vitek, J. L. (2008), 'Deep brain stimulation: how does it work?', *Cleve Clin J Med,* 75 Suppl 2, S59-65.
Vogt, B. A. and Pandya, D. N. (1987), 'Cingulate cortex of the rhesus monkey: II. Cortical afferents', *J Comp Neurol,* 262 (2), 271-89.
Vogt, B. A., Pandya, D. N., and Rosene, D. L. (1987), 'Cingulate cortex of the rhesus monkey: I. Cytoarchitecture and thalamic afferents', *J Comp Neurol,* 262 (2), 256-70.
Waldert, S., et al. (2008), 'Hand movement direction decoded from MEG and EEG', *J Neurosci,* 28 (4), 1000-8.
Walton, M. E., et al. (2003), 'Functional specialization within medial frontal cortex of the anterior cingulate for evaluating effort-related decisions', *J Neurosci,* 23 (16), 6475-9.
Warren, J. M., Akert, K., and Pennsylvania State University. (1964), *The frontal granular cortex and behavior* (New York,: McGraw-Hill) x, 492 p.
Watson, B. O., Ding, M., and Buzsaki, G. (2017), 'Temporal coupling of field potentials and action potentials in the neocortex', *Eur J Neurosci*.
Weinberger, M., et al. (2012), 'Oscillatory activity in the globus pallidus internus: comparison between Parkinson's disease and dystonia', *Clin Neurophysiol,* 123 (2), 358-68.
Weinberger, M., et al. (2006), 'Beta oscillatory activity in the subthalamic nucleus and its relation to dopaminergic response in Parkinson's disease', *J Neurophysiol,* 96 (6), 3248-56.
Welker, C. (1971), 'Microelectrode delineation of fine grain somatotopic organization of (SmI) cerebral neocortex in albino rat', *Brain Res,* 26 (2), 259-75.
Wen, H. and Liu, Z. (2016), 'Broadband Electrophysiological Dynamics Contribute to Global Resting-State fMRI Signal', *J Neurosci,* 36 (22), 6030-40.
Williams, D., et al. (2003), 'Behavioural cues are associated with modulations of synchronous oscillations in the human subthalamic nucleus', *Brain,* 126 (Pt 9), 1975-85.
Williams, D., et al. (2005), 'The relationship between oscillatory activity and motor reaction time in the parkinsonian subthalamic nucleus', *Eur J Neurosci,* 21 (1), 249-58.
Willis, W. D. and Westlund, K. N. (1997), 'Neuroanatomy of the pain system and of the pathways that modulate pain', *Journal of Clinical Neurophysiology,* 14 (1), 2-31.
Witjas, T., et al. (2002), 'Nonmotor fluctuations in Parkinson's disease: frequent and disabling', *Neurology,* 59 (3), 408-13.
Womelsdorf, T. and Fries, P. (2006), 'Neuronal coherence during selective attentional processing and sensory-motor integration', *J Physiol Paris,* 100 (4), 182-93.
--- (2007), 'The role of neuronal synchronization in selective attention', *Curr Opin Neurobiol,* 17 (2), 154-60.

Womelsdorf, T., et al. (2010), 'Theta-activity in anterior cingulate cortex predicts task rules and their adjustments following errors', *Proc Natl Acad Sci U S A*, 107 (11), 5248-53.
Yahr, M. D., et al. (1969), 'Treatment of parkinsonism with levodopa', *Arch Neurol*, 21 (4), 343-54.
Yener, G. G. and Basar, E. (2010), 'Sensory evoked and event related oscillations in Alzheimer's disease: a short review', *Cogn Neurodyn*, 4 (4), 263-74.
Yeung, N., Botvinick, M. M., and Cohen, J. D. (2004), 'The neural basis of error detection: conflict monitoring and the error-related negativity', *Psychol Rev*, 111 (4), 931-59.
Yianni, J., Green, A. L., and Aziz, T. Z. (2011), 'Surgical treatment of dystonia', *Int Rev Neurobiol*, 98, 573-89.
Yuan, H., et al. (2005), 'Histological, behavioural and neurochemical evaluation of medial forebrain bundle and striatal 6-OHDA lesions as rat models of Parkinson's disease', *J Neurosci Methods*, 144 (1), 35-45.
Zaghloul, K. A., et al. (2009), 'Human substantia nigra neurons encode unexpected financial rewards', *Science*, 323 (5920), 1496-9.
Zavala, B., et al. (2016), 'Human subthalamic nucleus-medial frontal cortex theta phase coherence is involved in conflict and error related cortical monitoring', *Neuroimage*, 137, 178-87.
Zavala, B., et al. (2013), 'Subthalamic nucleus local field potential activity during the Eriksen flanker task reveals a novel role for theta phase during conflict monitoring', *J Neurosci*, 33 (37), 14758-66.
Zesiewicz, T. A., Sullivan, K. L., and Hauser, R. A. (2006), 'Nonmotor symptoms of Parkinson's disease', *Expert Rev Neurother*, 6 (12), 1811-22.
Zgaljardic, D. J., Foldi, N. S., and Borod, J. C. (2004), 'Cognitive and behavioral dysfunction in Parkinson's disease: neurochemical and clinicopathological contributions', *J Neural Transm (Vienna)*, 111 (10-11), 1287-301.
Zgaljardic, D. J., et al. (2003), 'A review of the cognitive and behavioral sequelae of Parkinson's disease: relationship to frontostriatal circuitry', *Cogn Behav Neurol*, 16 (4), 193-210.
Zgaljardic, D. J., et al. (2006), 'An examination of executive dysfunction associated with frontostriatal circuitry in Parkinson's disease', *J Clin Exp Neuropsychol*, 28 (7), 1127-44.
Zhang, K., et al. (2007), 'Dopamine-mushroom body circuit regulates saliency-based decision-making in Drosophila', *Science*, 316 (5833), 1901-4.
Zhang, Q., et al. (2014), 'Decreased response of interneurons in the medial prefrontal cortex to 5-HT(1)A receptor activation in the rat 6-hydroxydopamine Parkinson model', *Neurol Sci*, 35 (8), 1181-7.